Foundations and Trends® in Networking
Vol. 9, No. 2 (2014) 107–215

DOI: 10.1561/1300000048

now
the essence of knowledge

Wireless Network Optimization by Perron-Frobenius Theory

Chee Wei Tan
City University of Hong Kong
cheewtan@cityu.edu.hk

Contents

Abstract

A basic question in wireless networking is how to optimize the wireless network resource allocation for utility maximization and interference management. How can we overcome interference to efficiently optimize fair wireless resource allocation, under various stochastic constraints on quality of service demands? Network designs are traditionally divided into layers. How does fairness permeate through layers? Can physical layer innovation be jointly optimized with network layer routing control? How should large complex wireless networks be analyzed and designed with clearly-defined fairness using beamforming?

This monograph provides a comprehensive survey of the models, algorithms, analysis, and methodologies using a Perron-Frobenius theoretic framework to solve wireless utility maximization problems. This approach overcomes the notorious non-convexity barriers in these problems, and the optimal value and solution of the optimization problems can be analytically characterized by the spectral property of matrices induced by nonlinear positive mappings. It also provides a systematic way to derive distributed and fast-convergent algorithms and to evaluate the fairness of resource allocation. This approach can even solve several previously open problems in the wireless networking literature.

More generally, this approach links fundamental results in nonnegative matrix theory and (linear and nonlinear) Perron-Frobenius theory with the solvability of non-convex problems. In particular, it can solve a particular class of max-min problems optimally; for truly nonconvex problems, e.g., the sum rate maximization problem, it can even be used to identify polynomial-time solvable special cases or to enable convex relaxation for global optimization. We highlight the key aspects of the nonlinear Perron-Frobenius theoretic framework through several practical examples in MIMO wireless cellular, heterogeneous small-cell and cognitive radio networks.

C. W. Tan. *Wireless Network Optimization by Perron-Frobenius Theory*. Foundations and Trends® in Networking, vol. 9, no. 2, pp. 107–215, 2014.
DOI: 10.1561/1300000048.

1

Wireless Network Optimization

1.1 Introduction

The demand for broadband mobile data services has grown significantly and rapidly in wireless networks. As such, many new wireless devices are increasingly operating in the wireless spectrum that are meant to be shared among many different users. Yet, the sharing of the spectrum is far from perfect. Due to the broadcast nature of the wireless medium, interference has become a major source of performance impairment. Current systems suffer from deteriorating quality due to a fixed resource allocation that does not adequately take interference into account.

As wireless networks become more heterogeneous and ubiquitous in our life, they also become more difficult to design and optimize. How should these large complex wireless networks be analyzed and designed with clearly-defined fairness and optimality in mind? In this regard, wireless network optimization has become an important tool to design resource allocation algorithms that can realize the untapped benefits of co-sharing wireless resources and to manage interference in wireless networks [56, 36, 69, 19, 23]. Without appropriate resource coordination, the wireless network may become unstable or may operate in a highly inefficient and unfair manner.

In wireless network optimization, the performance objective of a wireless transmission can be modeled by a nonlinear utility function that takes into account important wireless link metrics. Examples of these wireless metrics are the Signal-to-Interference-and-Noise Ratio (SINR), the Mean Square Error (MSE) or the transmission outage probability. The total utility function is then maximized over the joint solution space of all possible operating points in the wireless network. These operating points are realized in terms of the powers and interference at the physical link layer.

As such, wireless network optimization can be used to address engineering issues such as how to design wireless network algorithms or analyzing the tradeoffs between individual link performance and overall system performance. It can even be useful for understanding cross-layer optimization, for example, how these algorithms interact between different network layers, such as the physical and medium access control layers, in order to achieve provable efficiency for the overall system. It also sheds insights on how fairness permeates through the network layers when interference is dominant. This can open up new opportunities to jointly optimize physical layer innovation and other networking control mechanism that lead to more robust and reliable wireless network protocols.

1.2 Related Work

Due to the need to share limited wireless resources, fairness is an important consideration in wireless networks. Fairness is affected by the choice of the nonlinear utility functions of the wireless link metrics [56, 19, 21, 12]. In addition, fairness experienced by each user in the wireless networks is also affected by the channel conditions, multiuser interference, and other factors such as the wireless quality-of-service requirements. An example of such a requirement is the interference temperature constraints in cognitive radio networks that are essentially constraints imposed on the received interference for some users [40, 96, 70]. Another example is outage probability specification constraints in heterogeneous networks [45, 52]. As such, fairness can be

provisioned by choosing an optimal operating point that is fair in some sense to all the users by an appropriate formulation of a wireless utility maximization. The main challenges in solving these wireless utility maximization problems come from the nonlinear and coupling dependency of link metrics on channel conditions and powers, as well as the interference among the users. In addition, these are nonconvex problems that are notoriously difficult to solve optimally. Moreover, designing scalable and distributed algorithms with low-complexity to solve these nonconvex problems is even harder.

In fact, there are several important considerations to algorithm design in wireless networks. First, algorithms have to adapt the wireless resources such as the transmit power and to overcome interference based on locally available information. This means that the algorithms have to be as distributed as possible. Second, the algorithms are practical to deploy in a decentralized manner, i.e., the algorithms have minimal or, preferably, no parameter tuning by a controller. Third, the algorithms have good convergence performance. This is especially important since wireless users can arrive and depart in a dynamic setting. Henceforth, wireless resources need to be adapted fast enough to converge to a new optimal operating point whenever the network conditions change. This can be particularly challenging for some kinds of wireless networks such as wireless cognitive radio networks due to the tight coupling in the transmit powers and the interference temperature constraints between the primary users and the secondary users [40, 96, 70]. Whatever the algorithms may be, the algorithm design methodology is intrinsically driven by the theoretical approach used in analyzing the optimization problems. Finding an appropriate theoretical approach to study wireless network optimization is thus important.

There are several work in the literature on tackling the nonconvexity hurdles in wireless network optimization. The authors in [20, 19, 23, 45] applied geometric programming to solve a certain class of nonconvex wireless utility maximization problems that can be transformed into convex ones. The authors in [12] studied the use of Gibbs sampling techniques to solve nonconvex utility maximization problems, but the optimality of the solutions cannot be guaranteed. The authors in

[21, 39, 54] tackled deterministic wireless utility maximization problems that involved rates and powers, but the proposed techniques could not handle stochastic constraints. In [77, 76, 72, 74, 16, 18, 97, 100, 99], the authors studied the max-min utility fairness problem in wireless networks using a particular form of nonlinear Perron-Frobenius theory [50], [55]. These works demonstrated that the optimal solution to various widely-studied max-min optimization problems, e.g., the max-min SINR and max-min rate problems, can be characterized analytically and, more importantly, can be efficiently computed by iterative algorithms that can be made distributed. We introduce and present some of these work using the nonlinear Perron-Frobenius theory approach in this monograph.

1.3 Why is the Perron-Frobenius Theory useful?

The Perron-Frobenius theory introduced in this monograph is a new theoretical framework for analyzing a class of nonconvex optimization problems for resource allocation in wireless networks. Essentially, this framework provides a convenient suite of theories and algorithms to solve a broad class of wireless network optimization problems optimally by leveraging on the recent developments of the nonlinear Perron-Frobenius theory in mathematics. When combined with optimization-theoretic approaches such as convex reformulation and convex relaxation, this nonlinear Perron-Frobenius theory framework enables the design of efficient algorithms with low complexity that are applicable to a wide range of wireless network applications. Let us first discuss a special case of this nonlinear Perron-Frobenius theory in the following.

In nonnegative matrix theory, the classical *linear Perron-Frobenius theorem* is an important result that concerns the eigenvalue problem of nonnegative matrices, and has many engineering applications [63, 35, 68, 64, 30]. Notably, the linear Perron-Frobenius Theorem has consistently proven to be a useful tool in wireless network resource allocation problems. Its application to power control in wireless networks has been widely recognized (see, e.g., [67, 80, 22]), and can be traced back to earlier work in [1, 60] on balancing the signal to interference

ratio in satellite communication that was later adopted for wireless cellular networks in [2, 94, 31, 87, 92, 83, 66, 90, 10, 11] and wireless ad hoc networks [28]. In particular, it has been used in a total power minimization problem studied in [31, 92, 83, 66, 28], in which the Perron-Frobenius Theorem is used to ascertain the problem feasibility and the stability of power control algorithms proposed in [31, 83, 66, 28].

In the seminal work in [1] that first formulated and analyzed the signal to interference ratio balancing problem, the linear Perron-Frobenius theorem was used to derive the optimal solution analytically for this nonconvex problem. Subsequently, the same problem formulation was adopted in [60, 2, 94, 87] for designing power control algorithms for both satellite and wireless cellular communication networks that converge to the solution established in [1]. That the Perron-Frobenius theorem is fundamental is due to two facts. First, the problem parameters and optimization variables in wireless network optimization problems are mostly *nonnegative*. Second, it captures succinctly the unique feature of *competition* for limited resources among users, namely, *increasing the share of one decreases the shares of others* as well as *who is competing with whom*.

Another popular approach to tackle the nonconvexity hurdles in these wireless network optimization problems has been the use of geometric programming (see [27, 15, 20, 14] for an introduction) and its successive convex approximation as used by the authors in [45, 19, 23, 20]. The idea of the geometric programming approach is to reformulate the nonconvex problems as suitable classes of convex optimization problems (geometric programs) through a logarithmic change-of-variable trick. This leverages the inherent nonnegativity property. The geometric programs are then typically solved numerically by the interior-point method in a centralized fashion. In fact, geometric programming is closely related to the Perron-Frobenius theorem. For example, it can be used to establish the log-convexity property of the Perron-Frobenius eigenvalue [46, 61] (also see [15]).

The use of the linear Perron-Frobenius theorem in earlier work however has several limitations. They cannot address the general case (such as when we consider the thermal noise or general power constraints). In

addition, the Perron-Frobenius theorem has not been used to systematically solve other broader nonconvex wireless network optimization problems beyond the power control optimization problems studied in [1, 60, 2, 94, 87, 31, 92, 83, 66, 28]. In fact, to overcome the specific challenges due to nonconvexity, it is imperative to consider more general (i.e., nonlinear) version of the Perron-Frobenius theory that can spawn new approaches to characterize optimality and analyze the equilibrium as well as designing distributed algorithms for wireless networks.

There are various mathematical advances in extending the linear Perron-Frobenius theorem to nonlinear ones. These include works that extend the Perron-Frobenius theorem for positive matrices to nonsmooth and nonlinear functions in the 1960s (e.g., see Chapter 16 in [5], [55]) for studying the dynamics of cone-preserving operators. The nonlinear Perron-Frobenius theory is now emerging as a rigorous and practically useful mathematical tool to solve a wide range of important engineering problems and applications [49, 50, 9, 3, 55]. In this monograph, we will introduce and illustrate how the nonlinear Perron-Frobenius theory can tackle several key challenging wireless network optimization problems following the work in [76, 79, 78, 72, 77, 16, 18, 17, 43, 97, 100, 99, 98, 53, 42, 73, 74]. Whenever applicable, we also highlight the connection to previous works that rely on the linear Perron-Frobenius theorem as special cases.

The following notation is used in this monograph. Boldface uppercase letters denote matrices, boldface lowercase letters denote column vectors, and $\mathbf{u} \geq \mathbf{v}$ denotes componentwise inequality between vectors $\mathbf{u}$ and $\mathbf{v}$. We also let $(\mathbf{By})_l$ denote the lth element of $\mathbf{By}$. Let $\mathbf{x} \circ \mathbf{y}$ denote the Schur product of the vectors $\mathbf{x}$ and $\mathbf{y}$, i.e., $\mathbf{x} \circ \mathbf{y} = [x_1 y_1, \ldots, x_L y_L]^\top$. Let $\|\mathbf{w}\|_\infty^{\mathbf{x}}$ be the weighted maximum norm of the vector $\mathbf{w}$ with respect to the weight $\mathbf{x}$, i.e., $\|\mathbf{w}\|_\infty^{\mathbf{x}} = \max_l w_l/x_l$, $\mathbf{x} > \mathbf{0}$. We write $\mathbf{B} \geq \mathbf{F}$ if $B_{ij} \geq F_{ij}$ for all i, j. The Perron-Frobenius eigenvalue of a nonnegative matrix $\mathbf{F}$ is denoted as $\rho(\mathbf{F})$, and the Perron right and left eigenvector of $\mathbf{F}$ associated with $\rho(\mathbf{F})$ are denoted by $\mathbf{x}(\mathbf{F}) \geq \mathbf{0}$ and $\mathbf{y}(\mathbf{F}) \geq \mathbf{0}$ (or simply $\mathbf{x}$ and $\mathbf{y}$ when the context is clear), respectively. The superscript $(\cdot)^\top$ denotes transpose. We denote $\mathbf{e}_l$ as the lth unit coordinate vector and $\mathbf{I}$ as the identity matrix.

1.4 System Model

In this section, we introduce the system models for the wireless network utility maximization problems considered in the monograph. There are primarily two different kinds of system models - one that considers a static transmission channel (i.e., frequency-flat fading) and one that considers stochastic channel fading. Whenever applicable, we will emphasize the system model to avoid confusion.

Let us first introduce the static transmission channel for modeling a wireless network by the Gaussian interference channel [24]. There are altogether L links or users (equivalently, transceiver pairs) that want to communicate with its desired receiver. Due to mutual interfering channels, each user treats the multiuser interference as noise, i.e., no interference cancellation. This is a commonly used model (in, e.g., [19, 23, 22]) to model many wireless networks such as the radio cellular networks and ad-hoc networks. Let us denote the transmit power for the lth user as p_l for all l. Assuming that a linear single-user receiver (e.g., a matched-filter) is used, the Signal-to-Interference-and-Noise-Ratio (SINR) for the lth user can be given by

$$\mathsf{SINR}_l(\mathbf{p}) = \frac{G_{ll}p_l}{\sum_{j\neq l} G_{lj}p_j + n_l}, \tag{1.1}$$

where G_{lj} are the channel gains from the transmitter j to the receiver l and n_l is the additive white Gaussian noise (AWGN) power for the lth receiver. For brevity, we collect the channel gains in the channel gain matrix $\mathbf{G}$, and the channel gains take into account propagation loss, spreading loss and other transmission modulation factors. Notice that the SINR is a function in terms of the transmit powers and, furthermore, it is always nonnegative since all the quantities involved in (1.1) are nonnegative. There are many other important wireless performance metrics that are also directly dependent on the achieved SINR. For example, assuming a fixed bit error rate at the receiver, the Shannon capacity formula can be used to deduce the achievable data rate of the lth link as [24]:

$$\log\left(1 + \mathsf{SINR}_l(\mathbf{p})\right) \quad \text{nats/symbol.} \tag{1.2}$$

Let us define a nonnegative square matrix $\mathbf{F}$ with the entries given by:

$$F_{lj} = \begin{cases} 0, & \text{if } l = j \\ \frac{G_{lj}}{G_{ll}}, & \text{if } l = j \end{cases} \tag{1.3}$$

and a vector

$$\mathbf{v} = \left(\frac{n_1}{G_{11}}, \frac{n_2}{G_{22}}, \ldots, \frac{n_L}{G_{LL}} \right)^\top. \tag{1.4}$$

Observe that $\mathbf{F}$ and $\mathbf{v}$ capture the normalized values of the cross-channel gain parameters and the background noise power respectively. They are regarded as given constant problem parameters and are useful for notations represented in a compact manner in this monograph.

Let us next introduce the system model with stochastic channel fading that builds on top of the static transmission channel model by taking into account more realistic wireless transmission features. One important feature is the stochastic channel fading that is typically modeled by a Rayleigh, a Ricean or a Nakagami distribution depending on the wireless environment [80, 47]. For example, Rayleigh fading is relevant to in-building coverage model and urban environments (where small cells are mostly deployed in a heterogeneous network).

Under stochastic channel fading, the power received from the jth transmitter at lth receiver is given by $G_{lj}R_{lj}p_j$ where G_{lj} models a constant nonnegative path gain and R_{lj} is a random variable to model the stochastic channel fading between the jth transmitter and the lth receiver. In particular, we assume that R_{lj} is independently distributed with unit mean. For example, under Rayleigh fading, the distribution of the received power from the jth transmitter at the lth receiver is exponential with a mean value $\mathsf{E}[G_{lj}R_{lj}p_j] = G_{lj}p_j$.

When there is stochastic channel fading, the Signal-to-Interference-Noise Ratio (SINR) at the lth receiver can be expressed as the following by using the above notations [45, 22]:

$$\mathsf{SINR}_l(\mathbf{p}) = \frac{R_{ll}p_l}{\sum_{j \neq l} F_{lj}R_{lj}p_j + v_l}. \tag{1.5}$$

Notice that (1.5) is a random variable that depends on the stochastic channel fading realization. In particular, this random variable in

(1.5) is also a function of the transmit powers (and should not be confused with (1.1) which has no direct physical meaning in the context of stochastic channel fading).

Now, the transmission from the lth transmitter to its receiver is successful if $\mathsf{SINR}_l(\mathbf{p}) \geq \beta_l$ (no outage), where β_l is a given threshold for reliable communication. An outage occurs at the lth receiver whenever $\mathsf{SINR}_l(\mathbf{p}) < \beta_l$. We express this outage probability of the lth user by

$$P(\mathsf{SINR}_l(\mathbf{p}) < \beta_l). \tag{1.6}$$

Notice that the transmit powers are typically coupled together through the various wireless performance metric functions for any particular user. For example, the transmit powers of different users are coupled in (1.1) and (1.6) when the channel has frequency-flat fading and stochastic fading respectively. Adapting the transmit powers directly influences the wireless performance metrics. As such, in the wireless network optimization problems studied in this monograph, the transmit power vector $(p_1, \ldots, p_L)^\top$ is the main optimization variable of interest.

In addition, the transmit powers in wireless networks are typically constrained. This is modeled by a power constraint set $\mathcal{P}$ that can be due to resource budget consideration [80]. For example, in a cellular uplink system, we often have individual power constraints, i.e.,

$$\mathcal{P} = \{\mathbf{p} \mid \mathbf{p} \geq \mathbf{0}, p_l \leq \bar{p} \quad l\}. \tag{1.7}$$

Power constraints can also be used for interference management. Let us give an example of interference management in wireless heterogeneous networks. Say, in a wireless heterogeneous network, there are two different user type - the small cell users and the macrocell users. A basic premise imposed on small cells in wireless heterogeneous networks is that the following two conditions are satisfied [52]:

1. A small cell user receives adequate levels of transmission quality within the small cell.

2. The small cell users do not cause unacceptable levels of interference to the macrocell users.

To satisfy the second condition above, a possibility is to explicitly impose power constraints on the small cell users. Let us illustrate using an example of a single macrocell user and multiple small cells in [52]. Assume that there is no fading between this single macrocell receiver and all the small cell users. This assumption holds only in this paragraph for illustration purpose. Let us denote this macrocell user by the index 0 and the small cell users by indices $1, \ldots, L$. The macrocell user transmits with a fixed power P_0, where $P_0 \geq \gamma_0 v_0$, i.e., the macrocell user can satisfy the SINR threshold γ_0 even when there is no interference from the small cells. In the presence of small cells' interference, the SINR of this macrocell user has to satisfy $\frac{P_0}{\sum_{j=1}^{L} F_{0j} p_j + v_0} \geq \gamma_0$, which can be rewritten as a single power constraint to yield

$$\mathcal{P} = \left\{ \mathbf{p} \mid \mathbf{p} \geq \mathbf{0}, \sum_{j=1}^{L} F_{0j} p_j \leq (P_0/\gamma_0 - v_0) \right\} \tag{1.8}$$

that must be satisfied by the transmit powers of all the small cell users. Note that (1.8) is feasible when $P_0 \geq \gamma_0 v_0$. In general, a feasible power constraint of the form $\mathbf{a}^{\top} \mathbf{p} \leq 1$ for some positive constant vector $\mathbf{a}$ can be used to model interference management requirements. Notice that this example of an interference management constraint is also applicable to other wireless applications such as the cognitive radio networks with the primary user and secondary user types [40, 96, 70].

Now, there are many different possible ways to satisfy the first condition above on the adequate levels of transmission quality. In this monograph, we examine some of these different ways that in fact also relate to how this monograph is organized in the following.

We first begin with the mathematical preliminaries on the Perron-Frobenius theorem and the nonlinear Perron-Frobenius theory in Chapter 2, and then introduce how these theories are used to solve various optimization problems in subsequent chapters. In the first part of Chapter 3, we study the optimization of the *max-min weighted SINR* using (1.1) for a static channel model. In the second part of Chapter 3, we study the optimization of the *worst-case outage probability* using (1.6), i.e., minimizing the maximum outage probability when there is stochastic channel fading, to provision a minimum adequate level of fairness for

all the users. These two problems only involve simple power constraints such as that given in (1.8). In Chapter 4, we study more general utility functions to capture the satisfaction level of transmission quality in different kinds of wireless networks, and also to consider a broader class of nontrivial power constraint sets to model resource constraints and interference management requirements. The Perron-Frobenius theory suggests that the unique equilibrium that results from the competition for resources in the optimization problems in Chapters 3 and 4 is a meaningful one. In Chapter 5, we study more general nonconvex optimization problems involving the achievable data rate using (1.2) and show how the Perron-Frobenius theory can be a useful mathematical tool to tackle nonconvexity. We also highlight the open issues in these various wireless network optimization problems and finally conclude the monograph in Chapter 6.

2

Mathematical Preliminaries

In this chapter, we state the classical linear Perron-Frobenius theorem and its various nonlinear extensions. We also review several results found in the nonnegative matrix theory literature that are related to the linear Perron-Frobenius theorem. In particular, we will describe fundamental inequalities, the log-convexity property of the Perron-Frobenius eigenvalue and the inverse eigenvalue problem in nonnegative matrix theory. To facilitate reading, we will highlight the application of these mathematical tools whenever they are used in the various wireless network optimization problems encountered in the subsequent chapters of this monograph.

2.1 Perron-Frobenius Theorem

The classical linear Perron-Frobenius theorem states that the spectral radius of a square nonnegative matrix is in the spectrum of the matrix [63, 35, 7, 68].

Theorem 2.1. Let $\mathbf{A} \quad \mathsf{R}_{+}^{L\times L}$ be an irreducible[1] nonnegative matrix. Then, the following statements hold:

[1] A nonnegative matrix $\mathbf{F}$ is said to be irreducible if there exists a positive integer m such that the matrix $\mathbf{F}^m$ has all entries positive.

1. The spectral radius of $\mathbf{A}$, $\rho(\mathbf{A})$, is a positive eigenvalue of $\mathbf{A}$.

2. $\rho(\mathbf{A})$ is an algebraically simple eigenvalue of A

3. All other eigenvalues λ of $\mathbf{A}$ satisfy the inequality $\lambda \leq \rho(\mathbf{A})$ if and only if $\mathbf{A}$ is primitive, i.e. $\mathbf{A}^k > \mathbf{0}$ for some integer $k \geq 1$.

Let us call this spectral radius (eigenvalue with the largest absolute value) of an irreducible nonnegative matrix $\mathbf{F}$ as the Perron-Frobenius eigenvalue of $\mathbf{F}$ denoted by $\rho(\mathbf{F})$. The Perron-Frobenius right and left eigenvector of $\mathbf{F}$ associated with $\rho(\mathbf{F})$ are denoted by $\mathbf{x}(\mathbf{F}) \geq \mathbf{0}$ and $\mathbf{y}(\mathbf{F}) \geq \mathbf{0}$ respectively. Furthermore, from Theorem 2.1 above, $\rho(\mathbf{F})$ is simple and positive, and $\mathbf{x}(\mathbf{F}), \mathbf{y}(\mathbf{F}) > \mathbf{0}$ (cf. [63, 35, 68] and Proposition 6.6 in [8]).

In addition, there is a widely-known numerical method in linear algebra that can be used to compute the Perron-Frobenius eigenvectors of the matrix $\mathbf{A}$ in Theorem 2.1. This is the *power method* that is an iterative fixed-point algorithm (see, e.g., [84, 5, 82, 8]). Taking the matrix $\mathbf{A}$ as an input and letting k be the iteration index, the *power method* is described by

$$\mathbf{z}(k+1) = \frac{\mathbf{A}\mathbf{z}(k)}{\|\mathbf{A}\mathbf{z}(k)\|}$$

for some positive norm $\|\cdot\|$ that computes the Perron-Frobenius right eigenvector of the matrix $\mathbf{A}$. Here, starting from any positive vector $\mathbf{z}(0)$, the vector $\mathbf{z}(k)$ is multiplied with $\mathbf{A}$ and then normalized at the kth iteration. This iteration converges asymptotically to the Perron-Frobenius right eigenvector of the matrix $\mathbf{A}$ in Theorem 2.1 up to a positive scaling factor. On the other hand, by using $\mathbf{A}^\top$ as the input, one can use this power method to numerically compute the Perron-Frobenius left eigenvector of the matrix $\mathbf{A}$ in Theorem 2.1.

This celebrated result has numerous applications in pure and applied mathematics as well as a diverse range of engineering applications. We refer the reader to [7, 6, 68, 64, 30] for more details.

2.2 Key Inequalities

In this section, we state some fundamental results and inequalities in nonnegative matrix theory that are related to the Perron-Frobenius Theorem (Theorem 2.1). Of particular importance is the so-called *Friedland-Karlin inequalities* established in [34]. We also give several extensions and applications of the Friedland-Karlin inequalities in conjunction with the linear Perron-Frobenius theorem.

The first inequality that is fairly well-known in nonnegative matrix theory is the arithmetic-geometric mean inequality [68] (also see [27] for its generalized version). The arithmetic-geometric mean inequality states that

$$\sum_l \alpha_l v_l \geq \prod_l v_l^{\alpha_l}, \tag{2.1}$$

where $\mathbf{v} > \mathbf{0}$ and $\boldsymbol{\alpha} \geq \mathbf{0}$, $\mathbf{1}^\top \boldsymbol{\alpha} = 1$. Equality is achieved in (2.1) if and only if $v_1 = v_2 = \cdots = v_L$. In fact, the arithmetic-geometric mean inequality is a fundamental inequality of geometric programming in convex optimization theory [27, 15, 14, 20].

2.2.1 Collatz-Wielandt Theorem

A well-known result in nonnegative matrix theory is the max-min characterization of the Perron-Frobenius eigenvalue of an irreducible nonnegative matrix $\mathbf{A}$. This result is known as the Collatz-Wielandt Theorem in nonnegative matrix theory, e.g., see [7, 34]. In particular, the max-min characterization of $\rho(\mathbf{A})$ is given by:

$$\max_{\mathbf{z}>\mathbf{0}} \min_l \frac{(\mathbf{A}\mathbf{z})_l}{z_l} = \min_{\mathbf{z}>\mathbf{0}} \max_l \frac{(\mathbf{A}\mathbf{z})_l}{z_l} = \rho(\mathbf{A}), \tag{2.2}$$

The Collatz-Wielandt Theorem given in (2.2) provides an interesting optimality characterization of the Perron-Frobenius eigenvalue as the optimal value to both a max-min optimization problem and a min-max optimization problem (, in fact, both are nonconvex), and, in addition, the corresponding Perron-Frobenius right eigenvector as the corresponding optimal solution. The Collatz-Wielandt Theorem is well-known in standard linear algebra. This optimality characterization

of the Perron-Frobenius eigenvalue leads to the following Subinvariance Theorem in nonnegative matrix theory [68].

2.2.2 Subinvariance Theorem

We state the following result from [68].

Theorem 2.2 (Theorem 1.6, [68]). Let $\mathbf{A}$ be an irreducible nonnegative matrix, s a positive number, and $\mathbf{z} \geq \mathbf{0}$, a vector satisfying $\mathbf{Az} \leq s\mathbf{z}$. Then, (i) $\mathbf{z} > \mathbf{0}$; (ii) $s \geq \rho(\mathbf{A})$. Moreover, $s = \rho(\mathbf{A})$ if and only if $\mathbf{Az} = s\mathbf{z}$.

From the min-max optimization problem in (2.2) of the Collatz-Wielandt Theorem, we see that the Subinvariance Theorem further characterizes the optimality condition related to this problem. In particular, the optimal solution is unique and can be obtained by solving a fixed-point equation $\mathbf{Az} = s\mathbf{z}$ where the solution to $\mathbf{z}$ is simply the Perron-Frobenius right eigenvector of $\mathbf{A}$.

Now, another equally important mathematical tool in nonnegative matrix theory is the Friedland-Karlin inequalities established in [34]. The Friedland-Karlin inequalities are useful in the sense that they can be used to deduce the Collatz-Wielandt Theorem and the Subinvariance Theorem in the above.

2.2.3 Friedland-Karlin Inequalities

We state several important results on the Friedland-Karlin inequalities as given in [34]:

Theorem 2.3 (Theorem 3.1 [34]). Let $\mathbf{A} \quad \mathsf{R}_{+}^{L\times L}$ be an irreducible nonnegative matrix. Assume that $\mathbf{x}(\mathbf{A}) = (x_1(\mathbf{A}), \ldots, x_L(\mathbf{A}))^{\top}, \mathbf{y}(\mathbf{A}) = (y_1(\mathbf{A}), \ldots, y_L(\mathbf{A}))^{\top} > \mathbf{0}$ are the right and left Perron-Frobenius eigenvectors of $\mathbf{A}$, normalized such that $\mathbf{x}(\mathbf{A}) \circ \mathbf{y}(\mathbf{A})$ is a probability vector. Suppose $\boldsymbol{\gamma}$ is a nonnegative vector. Then,

$$\rho(\mathbf{A}) \prod_{l=1}^{L} \gamma_l^{(\mathbf{x}(\mathbf{A})\circ\mathbf{y}(\mathbf{A}))_l} \leq \rho(\mathrm{diag}(\boldsymbol{\gamma})\mathbf{A}). \tag{2.3}$$

If $\boldsymbol{\gamma}$ is a positive vector then equality holds if and only if all γ_l are equal. Furthermore, for any positive vector $\mathbf{z} = (z_1, \ldots, z_L)^\top$, the following inequality holds:

$$\rho(\mathbf{A}) \leq \prod_{l=1}^{L} \left(\frac{(\mathbf{A}\mathbf{z})_l}{z_l} \right)^{(\mathbf{x}(\mathbf{A}) \circ \mathbf{y}(\mathbf{A}))_l}. \tag{2.4}$$

If $\mathbf{A}$ is an irreducible nonnegative matrix with positive diagonal elements, then equality holds in (2.4) if and only if $\mathbf{z} = t\mathbf{x}(\mathbf{A})$ for some positive t.

We state below some convexity results related to the Perron-Frobenius eigenvalue that are of direct consequences of the Friedland-Karlin inequalities [32, 33].

2.2.4 Convexity Property of the Perron-Frobenius Eigenvalue

By using the arithmetic-geometic mean inequality in (2.1) along with the Friedland-Karlin inequality in (2.4), we have the following result.

$$\max_{\boldsymbol{\lambda} \geq \mathbf{0}, \mathbf{1}^\top \boldsymbol{\lambda} = 1} \min_{\mathbf{p} \geq \mathbf{0}} \sum_l \lambda_l \frac{(\mathbf{A}\mathbf{p})_l}{p_l} = \min_{\mathbf{p} \geq \mathbf{0}} \max_{\boldsymbol{\lambda} \geq \mathbf{0}, \mathbf{1}^\top \boldsymbol{\lambda} = 1} \sum_l \lambda_l \frac{(\mathbf{A}\mathbf{p})_l}{p_l} \tag{2.5}$$

It is interesting to note that Friedland in [32, 33] established Theorem 2.3 by using the Donsker-Varadhan's variational principle as given in (2.5) and also the linear Perron-Frobenius theorem (Theorem 2.1) [29, 32, 33]. In other words, (2.5) offers a characterization of the Perron-Frobenius eigenvalue via the Donsker-Varadhan's variational principle (cf. Theorem 3.2 in [32]).

As an important application of the Friedland-Karlin inequalities, (2.5) can be used to show that, given a nonnegative matrix $\mathbf{B}$, the function

$$\log \rho(\mathrm{diag}(e^{\boldsymbol{\eta}})\mathbf{B}) \tag{2.6}$$

is convex. Furthermore, it is strictly convex if $\mathbf{B}$ is irreducible [29, 32, 33]. In fact, this makes use of the log-convexity property of the Perron-Frobenius eigenvalue. This convexity result will be used in the following.

2.3 Inverse Eigenvalue Problem

In this section, we introduce an application of the Friedland-Karlin inequalities and the linear Perron-Frobenius theorem to solve an inverse eigenvalue problem in nonnegative matrix theory. An interesting by-product is a convex optimization problem with the Perron-Frobenius eigenvalue as its constraint sets. We will outline how this convex optimization problem can be solved analytically by leveraging the log-convexity property of the Perron-Frobenius eigenvalue. Consider the following inverse eigenvalue problem.

Problem Let $\mathbf{B} \quad R_+^{L\times L}, \mathbf{m} \quad R_+^L$ be a given irreducible nonnegative matrix and a positive probability vector, respectively. There are two key questions related to this.

First, when does there exist $\boldsymbol{\eta} \quad R^L$ such that $\mathbf{x}(\mathrm{diag}(e^{\boldsymbol{\eta}})\mathbf{B}) \circ \mathbf{y}(\mathrm{diag}(e^{\boldsymbol{\eta}})\mathbf{B}) = \mathbf{m}$?

Second, if such $\boldsymbol{\eta}$ exists, when is it unique up to an addition $t\mathbf{1}$?

To solve this inverse eigenvalue problem, let us recall Theorem 3.2 in [34] (a consequence of Theorem 2.3 in the above, i.e., Theorem 3.1 in [34]) that is reproduced in the following.

Theorem 2.4 (Theorem 3.2 [34]). Let $\mathbf{A} \quad R_+^{L\times L}, \mathbf{u}, \mathbf{v} \quad R_+^L$ be given, where $\mathbf{A}$ is irreducible with positive diagonal elements and $\mathbf{u}, \mathbf{v}$ are positive. Then, there exists $\mathbf{D}_1, \mathbf{D}_2 \quad R_+^{L\times L}$ such that

$$\mathbf{D}_1\mathbf{A}\mathbf{D}_2\mathbf{u} = \mathbf{u},\ \mathbf{v}^\top\mathbf{D}_1\mathbf{A}\mathbf{D}_2 = \mathbf{v}^\top,\ \mathbf{D}_1 = \mathrm{diag}(\mathbf{f}),\ \mathbf{D}_2 = \mathrm{diag}(\mathbf{g}), \quad (2.7)$$

where $\mathbf{f}, \mathbf{g} > \mathbf{0}$.

The pair $(\mathbf{D}_1, \mathbf{D}_2)$ is unique to the change $(t\mathbf{D}_1, t^{-1}\mathbf{D}_2)$ for any $t > 0$. There exist $\boldsymbol{\eta} \quad R^L$ such that $\mathbf{x}(\mathrm{diag}(e^{\boldsymbol{\eta}}\mathbf{B})) \circ \mathbf{y}(\mathrm{diag}(e^{\boldsymbol{\eta}}\mathbf{B})) = \mathbf{m}$. Furthermore, $\boldsymbol{\eta}$ is unique up to an addition $t\mathbf{1}$.

In brief, Theorem 2.4 proves the existence of the solution to Problem 2.3, and this solution can be efficiently obtained by a numerical method as given in the following result.

Corollary 2.5 (Corollary A.6 [78]). Let $\mathbf{B} \quad R_+^{L\times L}, \mathbf{m} \quad R_+^L$ be a given irreducible nonnegative matrix with positive diagonal elements and a positive probability vector, respectively. Then, there exists $\boldsymbol{\eta} \quad R^L$ such

that $\mathbf{x}(\mathrm{diag}(e^{\boldsymbol{\eta}})\mathbf{B}) \circ \mathbf{y}(\mathrm{diag}(e^{\boldsymbol{\eta}})\mathbf{B}) = \mathbf{m}$. Furthermore, $\boldsymbol{\eta}$ is unique up to an addition of $t\mathbf{1}$. In particular, this $\boldsymbol{\eta}$ can be computed by solving the following convex optimization problem:

$$\begin{array}{ll} \text{maximize} & \mathbf{m}^{\top}\boldsymbol{\eta} \\ \text{subject to} & \log \rho(\mathrm{diag}(e^{\boldsymbol{\eta}})\mathbf{B}) \leq 0, \\ \text{variables:} & \boldsymbol{\eta} = (\eta_1, \ldots, \eta_L)^{\top} \quad R^L. \end{array} \tag{2.8}$$

Observe that (2.8) has a linear objective function and a constraint set expressed by the Perron-Frobenius eigenvalue function of a nonnegative matrix. A unique feature of this Perron-Frobenius eigenvalue characterization is the log-convexity property of the Perron-Frobenius eigenvalue [46, 61]. In other words, the constraint set in (2.8) is convex and hence (2.8) is a convex optimization problem. This can be solved numerically using an interior-point solver (see, for example, the `cvx` convex optimization software package [38]). We give a software implementation in the appendix to numerically handle the Perron-Frobenius eigenvalue function in (2.8) as part of the `cvx` software package in modeling and numerical evaluation of the Perron-Frobenius eigenvalue function whenever it appears in the objective function or in the constraint functions in an optimization problem formulation.

In summary, even though some of these optimization problems encountered in nonnegative matrix theory, e.g., (2.2) and (2.5), are nonconvex, they can be converted into equivalent convex ones (similar in form as (2.8)) by a logarithmic change-of-variable trick and be solved efficiently. More interestingly, the optimal solutions and optimal value can be obtained analytically often in terms of the Perron-Frobenius eigenvalue and its eigenvectors (in fact, the same can be said for its optimal Lagrange dual solution, namely, the optimal dual solution of (2.8) is the Schur product of the Perron-Frobenius right and left eigenvectors). We refer the reader to the details and additional results on the inverse eigenvalue problem in [78].

2.3.1 Quasi-invertibility

We describe here a notion of *quasi-invertibility* of a nonnegative matrix introduced by Wong in [88]. This *quasi-inverse* notion was analyzed

using nonnegative matrix theory tools in [88], and finds useful applications in analyzing linear economic model equilibrium problems in [88] and the nonconvex optimization problems studied in Chapter 5 of this monograph. This quasi-inverse of a nonnegative matrix is defined as follows [88]:

Definition 2.1 (Quasi-invertibility)**.** A square nonnegative matrix $\mathbf{A}$ is a quasi-inverse of a square nonnegative matrix $\mathbf{B}$ if $\mathbf{A} - \mathbf{B} = \mathbf{AB} = \mathbf{BA}$. Furthermore, $(\mathbf{I} - \mathbf{B})^{-1} = \mathbf{I} + \mathbf{A}$.

In other words, for a given square nonnegative matrix $\mathbf{A}$, we first compute either $\mathbf{A}(\mathbf{I} + \mathbf{A})^{-1}$ or $(\mathbf{I} + \mathbf{A})^{-1}\mathbf{A}$. If this computed matrix is nonnegative, we denote this computed matrix $\mathbf{B} \geq \mathbf{0}$ and say that the quasi-inverse of $\mathbf{B}$ exists (which is $\mathbf{A}$ by Definition 2.1).

In general, a nonnegative matrix may have a quasi-inverse or it may not have. When a nonnegative matrix has a quasi-inverse, the Perron-Frobenius theorem can be used to relate the spectrum of this nonnegative matrix to that of its quasi-inverse. There are special cases of the quasi-inverses that can be analytically characterized. For example, a strictly positive matrix with zero diagonal elements is not a quasi-inverse of any nonnegative matrix. The dyadic product of two nonnegative vectors having the same dimension always has a quasi-inverse that is a dyadic product [77, 76]. This quasi-inverse notion is used together with optimization reformulation techniques in Chapter 5 to derive convex relaxations and to identify special cases of nonconvex problems that can be solved optimally in polynomial time.

2.4 Nonlinear Perron-Frobenius Theory

We now turn our attention to the extension and generalization of the Perron-Frobenius theorem (Theorem 2.1). The classical linear Perron-Frobenius theorem for the positive operator, Theorem 2.1 as expounded in [63, 35], has been significantly extended and generalized in mathematics since the 1960s (e.g., see Chapter 16 in [5], [55]). There have been various characterization of the nonlinear Perron-Frobenius theory that can be found in the mathematics literature [4, 59, 49, 50, 9, 3, 55].

In the following, we describe some extensions to the linear Perron-Frobenius theorem, and highlight those version of the nonlinear Perron-Frobenius theory in [50] that will be useful to the wireless network optimization problems considered in the monograph.

First, the following result extends the Perron-Frobenius theorem to a linear matrix pencil version.

Lemma 2.6 ([4, 59]). Let $\mathbf{A}, \mathbf{B} \quad R^{L \times L}$ with $\mathbf{B} - \mathbf{A}$ nonsingular, and $(\mathbf{B} - \mathbf{A})^{-1}\mathbf{A}$ (entrywise) nonnegative and irreducible. Then there exists $\lambda \quad (0, 1)$ and a positive vector $\mathbf{z}$ satisfying $\mathbf{A}\mathbf{z} = \lambda \mathbf{B}\mathbf{z}$. The eigenvalue λ associated with the nonnegative eigenvector is the maximum real eigenvalue in $(0, 1)$, and is given by

$$\lambda = \frac{\rho((\mathbf{B} - \mathbf{A})^{-1}\mathbf{A})}{(1 + \rho((\mathbf{B} - \mathbf{A})^{-1}\mathbf{A}))}.$$

It is easy to see that Lemma 2.6 particularizes to the linear Perron-Frobenius theorem, i.e., Theorem 2.1, whenever $\mathbf{B}$ is an identity matrix, i.e., $\mathbf{B} = \mathbf{I}$, and $\mathbf{A}$ is an irreducible and nonnegative matrix.

Next, we introduce in the following a nonlinear Perron-Frobenius theory due to Krause in his work [49, 50, 51].

We begin with the definition of a *concave self-mapping* given in [50] as follows.

Definition 2.2 (Concave Self-mapping [50]). A mapping $\mathbf{f} : K \to K$ is concave if

$$\mathbf{f}(a\mathbf{c} + (1 - a)\mathbf{z}) \geq a\mathbf{f}(\mathbf{c}) + (1 - a)\mathbf{f}(\mathbf{z}) \quad \mathbf{c}, \mathbf{z} \quad K, \ a \quad [0, 1],$$

and monotone if $\mathbf{0} \leq \mathbf{c} \leq \mathbf{z}$ implies $\mathbf{0} \leq \mathbf{f}(\mathbf{c}) \leq \mathbf{f}(\mathbf{z})$.

Let $\cdot$ be a norm on R^L that is monotone, i.e., $\mathbf{c} \leq \mathbf{z}$. A concave self-mapping of K is monotone on K and continuous on the interior of K with respect to $\cdot$ [50].

Note that any concave self-mapping of K is in $\mathcal{K}$ and it is monotone and continuous [51].

Now, the following result, as established by Krause in his work [49, 50, 51], extends the Perron-Frobenius theorem (Theorem 2.1) to a positive concave self-mapping version.

Theorem 2.7 (Krause's theorem [50]). Let $\|\cdot\|$ be a monotone norm on R^L. For a concave mapping $f : \mathsf{R}_+^L \to \mathsf{R}_+^L$ with $f(\mathbf{z}) > 0$ for $\mathbf{z} \geq \mathbf{0}$, the following statements hold. The conditional eigenvalue problem $f(\mathbf{z}) = \lambda\mathbf{z}, \lambda \in \mathsf{R}, \mathbf{z} \geq \mathbf{0}, \|\mathbf{z}\| = 1$ has a unique solution $(\lambda^*, \mathbf{z}^*)$, where $\lambda^* > 0$, $\mathbf{z}^* > \mathbf{0}$. Furthermore, $\lim_{k\to\infty} \tilde{f}(\mathbf{z}(k))$ converges geometrically fast[2] to $\mathbf{z}^*$, where $\tilde{f}(\mathbf{z}) = f(\mathbf{z})/\|f(\mathbf{z})\|$.

Naturally, a notable special case of Theorem 2.7 is when $f(\mathbf{z}) = \mathbf{F}\mathbf{z}$ where $\mathbf{F}$ is an irreducible nonnegative square matrix. This special case is, of course, the linear Perron-Frobenius theorem, i.e., Theorem 2.1.

Another special case of Theorem 2.7 is the following result:

Lemma 2.8 (Conditional eigenvalue [9], Corollary 13). Let $\mathbf{A}$ be a nonnegative matrix and $\mathbf{b}$ be a nonnegative vector. If $\rho(\mathbf{A} + \mathbf{b}\mathbf{1}^\top) > \rho(\mathbf{A})$, then the conditional eigenvalue problem $\lambda\mathbf{s} = \mathbf{A}\mathbf{s} + \mathbf{b}, \lambda \in \mathsf{R}, \mathbf{s} \geq \mathbf{0}, \sum_l s_l = 1$, has a unique solution given by $\lambda = \rho(\mathbf{A} + \mathbf{b}\mathbf{1}^\top)$ and $\mathbf{s}$ being the unique normalized Perron eigenvector of $\mathbf{A} + \mathbf{b}\mathbf{1}^\top$.

We now state the following result in [72, 74] that is derived by combining the above conditional eigenvalue result, i.e., Lemma 2.8, and the Friedland-Karlin inequality result in [34, 32] (see Theorem 2.3).

Lemma 2.9. Let $\mathbf{A} \in \mathsf{R}^{L\times L}$ be an irreducible nonnegative matrix, $\mathbf{b} \in \mathsf{R}^{L\times 1}$ a nonnegative vector and $\|\cdot\|$ a norm on R^L with a corresponding dual norm $\|\cdot\|_D$. Then,

$$\begin{aligned}
\log\rho(\mathbf{A} + \mathbf{b}\mathbf{c}_*^\top) &= \max_{\|\mathbf{c}\|_D=1} \log\rho(\mathbf{A} + \mathbf{b}\mathbf{c}^\top) \\
&= \max_{\boldsymbol{\lambda}\geq\mathbf{0}, \mathbf{1}^\top\boldsymbol{\lambda}=1} \min_{\|\mathbf{p}\|=1} \sum_{l=1}^{L} \lambda_l \log\frac{(\mathbf{A}\mathbf{p} + \mathbf{b})_l}{p_l} \qquad (2.9) \\
&= \min_{\|\mathbf{p}\|=1} \max_{\boldsymbol{\lambda}\geq\mathbf{0}, \mathbf{1}^\top\boldsymbol{\lambda}=1} \sum_{l=1}^{L} \lambda_l \log\frac{(\mathbf{A}\mathbf{p} + \mathbf{b})_l}{p_l}, \qquad (2.10)
\end{aligned}$$

where the optimal $\mathbf{p}$ in (2.9) and (2.10) are both given by $\mathbf{x}(\mathbf{A} + \mathbf{b}\mathbf{c}_*^\top)$,

[2] Let $\|\cdot\|$ be an arbitrary vector norm. A sequence $\{\mathbf{p}(k)\}$ is said to converge geometrically fast to a fixed point $\mathbf{p}'$ if and only if $\|\mathbf{p}(k) - \mathbf{p}'\|$ converges to zero geometrically fast, i.e., there exists constants $A \geq 0$ and $\eta \in [0, 1)$ such that $\|\mathbf{p}(k) - \mathbf{p}'\| \leq A\eta^k$ for all k [8].

and the optimal $\boldsymbol{\lambda}$ in (2.9) and (2.10) are both given by $\mathbf{x}(\mathbf{A}+\mathbf{b}\mathbf{c}_*^\top)\circ \mathbf{y}(\mathbf{A}+\mathbf{b}\mathbf{c}_*^\top)$.

Furthermore, $\mathbf{p} = \mathbf{x}(\mathbf{A}+\mathbf{b}\mathbf{c}_*^\top)$ is the dual of $\mathbf{c}_*$ with respect to $\cdot\ _D$.[3]

Lemma 2.9 is a general version of the Friedland-Karlin spectral radius minimax characterization in [34, 32]. In particular, if $\mathbf{b} = \mathbf{0}$, we obtain (2.5), i.e., the Perron-Frobenius eigenvalue characterization via the Donsker-Varadhan's variational principle (cf. Theorem 3.2 in [32]). Lemma 2.9 also characterizes an interesting duality relationship of the Perron-Frobenius eigenvalue and its eigenvectors in the sense of Lagrange duality.

Theorem 2.7 and its generalization (e.g., see Theorem 4.4 in Chapter 4) are extremely useful for solving the wireless network optimization problems in this monograph. The generalization to nonlinear positive monotone self-mappings and connecting them to mathematical tools in nonnegative matrix theory can potentially provide new analytical insights to solving problems in many other engineering applications.

[3] A pair $(\mathbf{x},\mathbf{y})$ of vectors of R^L is said to be a dual pair with respect to $\cdot$ if $\mathbf{y}\ _D\ \mathbf{x} = \mathbf{y}^\top \mathbf{x} = 1$.

3

Max-min Fairness Optimization

In this chapter, we describe how the nonlinear Perron-Frobenius theory can be used to solve two representative problems: the max-min SINR problem under the static transmission channel model in [1, 58, 76, 79, 78, 72, 77, 97] and the min-max outage probability problem under the stochastic channel fading model in [45, 72, 74].

3.1 Max-min SINR Fairness

The first and most basic version of the max-min SINR problem under the static transmission channel model was formulated as an application for power control in satellite communication networks by Aein in 1973 [1]. However, only the interference-limited case was completely solved by Aein in [1]. Since then, the max-min SINR problem finds many applications in different wireless networks (such as wireless cellular and cognitive radio networks) and involves various optimization extensions related to transmission strategy requirements such as transmit beamforming or transmission scheduling.

We first consider a general formulation of the max-min SINR problem with a single power constraint before discussing its other extensions and special cases. Let $\boldsymbol{\beta}$ be a given positive vector, where the lth entry

β_l is assigned to the lth link to reflect some priority relative to the other users. A bigger β_l value means a higher priority.

Suppose that there are L users in the wireless network. Consider the following max-min weighted SINR problem [90, 58, 77, 76]:

$$\begin{array}{rl} \text{maximize} & \min\limits_{l} \ \dfrac{\mathsf{SINR}_l(\mathbf{p})}{\beta_l} \\ \text{subject to} & \mathbf{a}^{\top}\mathbf{p} \leq \bar{P},\ \mathbf{p} \geq \mathbf{0}, \\ \text{variables:} & \mathbf{p}. \end{array} \tag{3.1}$$

Even though (3.1) is nonconvex, we describe how it can be solved optimally and analytically. We shall use the notations introduced in Chapter 1 and assume that $\mathbf{F}$ in (1.3) is irreducible. This assumption can be easily satisfied by a sufficient condition that $F_{lj} > 0$ for all $l = j$, i.e., all the users can interfere with one another. Let us define the following nonnegative matrix

$$\mathbf{B} = \mathbf{F} + (1/\bar{P})\mathbf{v}\mathbf{a}^{\top}. \tag{3.2}$$

We now show that the spectra of the product of a diagonal nonnegative matrix and $\mathbf{B}$ in (3.2), i.e., $\mathrm{diag}(\boldsymbol{\beta})\mathbf{B}$, (particularly, its Perron-Frobenius eigenvalue and eigenvectors) will be useful to obtain the analytical solution to (3.1) as well as for analyzing a computational algorithm to solve (3.1) numerically in the following.

3.1.1 Optimal solution and algorithm

A closed form solution to (3.1) can be obtained by exploiting a connection between the Perron-Frobenius theory and the algebraic structure of (3.1).

Lemma 3.1. The optimal value and solution of (3.1) is given by

$$1/\rho(\mathrm{diag}(\boldsymbol{\beta})\mathbf{B})$$

and

$$(\bar{P}/\mathbf{a}^{\top}\mathbf{x}(\mathrm{diag}(\boldsymbol{\beta})\mathbf{B}))\ \mathbf{x}(\mathrm{diag}(\boldsymbol{\beta})\mathbf{B})$$

respectively.

Note that the optimal power in Lemma 3.1 can also be expressed as

$$\mathbf{p} = (\rho(\mathrm{diag}(\boldsymbol{\beta})\mathbf{B})\mathbf{I} - \mathbf{F})^{-1}\,\mathbf{v}. \tag{3.3}$$

The following algorithm computes the solution given in Lemma 3.1. We let k index discrete time slots.

Algorithm 1 Max-min Weighted SINR

1. Update power $\mathbf{p}(k+1)$:

$$p_l(k+1) = \left(\frac{\beta_l}{\mathsf{SINR}_l(\mathbf{p}(k))}\right) p_l(k) \qquad l. \tag{3.4}$$

2. Normalize $\mathbf{p}(k+1)$:

$$\mathbf{p}(k+1) \leftarrow \mathbf{p}(k+1) \cdot \bar{P}/\mathbf{a}^{\top}\mathbf{p}(k+1). \tag{3.5}$$

Corollary 3.2. Starting from any initial point $\mathbf{p}(0)$, $\mathbf{p}(k)$ in Algorithm 1 converges geometrically fast to the optimal solution of (3.1), $(\bar{P}/\mathbf{a}^{\top}\mathbf{x}(\mathrm{diag}(\boldsymbol{\beta})\mathbf{B}))\mathbf{x}(\mathrm{diag}(\boldsymbol{\beta})\mathbf{B})$.

3.1.2 Proof

There can be several approaches to proving Lemma 3.1. Let the optimal solution and the optimal value in (3.1) be $\mathbf{p}^*$ and τ^* respectively. A key observation is that the weighted SINR values for all the users are equal at optimality. This implies, at optimality of (3.1),

$$\frac{p_l^*}{\sum_{j\neq l} F_{lj}p_j^* + v_l} = \beta_l\tau^* \tag{3.6}$$

for all l. In matrix form, (3.6) can be rewritten as

$$(1/\tau^*)\mathbf{p}^* = \mathrm{diag}(\boldsymbol{\beta})\mathbf{F}\mathbf{p}^* + \mathrm{diag}(\boldsymbol{\beta})\mathbf{v}(\mathbf{a}^{\top}\mathbf{p}^*/\bar{P}), \tag{3.7}$$

where we also use the fact that $\sum_l a_l p_l^* = \bar{P}$ at optimality. By the linear Perron-Frobenius theorem, this shows that $\mathbf{p}^* = \mathbf{x}(\mathrm{diag}(\boldsymbol{\beta})(\mathbf{F} +$

$(1/\bar{P})\mathbf{v}\mathbf{a}^\top))$ (unique up to a scaling constant) is a fixed point of (3.7). Other approaches to construct a proof for Lemma 3.1 include the nonlinear Perron-Frobenius theory in [9, 50] (e.g., see [75, 76] in using Lemma 2.8 in Chapter 2), the Lagrange duality of geometric programming in [75] and the optimal value characterization in [58].

Remark 3.1. Let us address an open issue in [52]. A special case of (3.1) is when $\boldsymbol{\beta} = \mathbf{1}$ and when $\boldsymbol{P}$ in (3.1) is given by (1.8), which corresponds to a max-min SINR problem for a macro-small cell network studied in [52]. In particular, (1.8), written in a general form as $\mathbf{a}^\top\mathbf{p} \leq 1$ for some positive $\mathbf{a}$, can be associated with a weighted ℓ-1 monotone norm $(\ \mathrm{diag}(\mathbf{a}) \cdot\ _1)$, and this permits the use of Theorem 2.7 (cf. [75, 76] and also Table 3.1). Its analytical closed-form solution is given by $\mathbf{p} = \mathbf{x}(\mathbf{F} + \mathbf{v}\mathbf{a}^\top)$ (up to a scaling constant). In addition, the fixed-point iteration (essentially Algorithm 1) given by

$$\mathbf{p}(k+1) = \frac{\mathbf{F}\mathbf{p}(k) + \mathbf{v}}{\mathbf{a}^\top(\mathbf{F}\mathbf{p}(k) + \mathbf{v})} \tag{3.8}$$

converges geometrically fast to the optimal solution of the macro-small cell problem in [52], thereby resolving an open issue in [52].

Another interesting perspective to solving (3.1) is a reformulation technique that rewrites (3.1) to another optimization problem that determines the optimal achieved SINR values of all the different users. Essentially, this reformulates (3.1) as solving an inverse eigenvalue problem as described in Chapter 2. Once these optimal SINR values are determined, they are then used to recover the optimal power solution. In particular, this reformulation technique turns (3.1) to solving the following convex optimization problem:

$$\begin{array}{rl} \text{maximize} & \mathbf{w}^\top\boldsymbol{\eta} \\ \text{subject to} & \log\rho(\mathrm{diag}(e^{\boldsymbol{\eta}})\mathbf{B}) \leq 0, \\ \text{variables:} & \boldsymbol{\eta}, \end{array} \tag{3.9}$$

where $\mathbf{w}$ is intentionally chosen to be $\mathbf{x}(\mathrm{diag}(\boldsymbol{\beta})\mathbf{B}) \circ \mathbf{y}(\mathrm{diag}(\boldsymbol{\beta})\mathbf{B})$ in (3.9). After we have obtained the optimal $\boldsymbol{\eta}$ by solving (3.9), the optimal power solution is then given by

$$\mathbf{p} = (\mathbf{I} - \mathrm{diag}(e^{\boldsymbol{\eta}})\mathbf{F})^{-1}\,\mathrm{diag}(e^{\boldsymbol{\eta}})\mathbf{v}. \tag{3.10}$$

or, simply,

$$\mathbf{p} = \mathbf{x}(\mathrm{diag}(\boldsymbol{\beta})\mathbf{B}) \tag{3.11}$$

as it should be.

3.1.3 Interference-limited Case

Let us consider the special case of interference-limited scenario, i.e., no thermal noise and no power constraint. In fact, this interference-limited special case is the very first version of the max-min SINR problem formulated in 1973 by Aein in [1] to balance the signal-to-interference ratio of multibeam satellite systems[1] (see [1, 2, 60]), and then subsequently being adopted in wireless cellular networks [94, 87, 37, 48, 67, 58].

Consider the interference-limited special case problem:

$$\begin{array}{rl} \text{maximize} & \min\limits_{l} \dfrac{G_{ll}p_l}{\sum\limits_{j\neq l} G_{lj}p_j} \\ \text{subject to} & \mathbf{p} \geq \mathbf{0}, \\ \text{variables:} & \mathbf{p}. \end{array} \tag{3.12}$$

It is immediate, notably using the Collatz-Wielandt Theorem as has been shown in [1], that the optimal value and the optimal solution to (3.12) can be analytically given by $1/\rho(\mathbf{F})$ and the Perron-Frobenius right eigenvector $\mathbf{x}(\mathbf{F})$ respectively. Furthermore, the optimal solution can be computed using the *power method* in linear algebra. Indeed, the power control work in [1, 2, 60, 94, 87, 37, 67] proposed iterative power control algorithms that are inspired by the *power method* in linear algebra. Let us briefly review these algorithms in the following.

Now, the power control algorithm proposed in [94] (called the distributed balancing algorithm), when written in vector form, is Algorithm 2 with the matrix $\mathbf{A}$ in (3.13) being a square matrix with unit diagonal entries and off-diagonal elements given by $G_{ij}/G_{ii} < 1$, $i = j$ (with a Perron-Frobenius eigenvalue strictly greater than one). A particular choice to update the scalar coefficient is given in [94, 67]

[1] In these earlier literature on satellite systems for space communications, the signal-to-interference ratio is more commonly known as the carrier-power-to-interference ratio. This problem is thus known as balancing the carrier-power-to-interference ratio or signal to interference ratio [1, 2, 60, 94, 87, 37, 67].

Algorithm 2 Signal-to-Interference Ratio Balancing

1. Update power $\mathbf{p}(k+1)$:

$$\mathbf{p}(k+1) = c(k) \cdot \mathbf{A}\mathbf{p}(k). \tag{3.13}$$

2. Update the positive scalar coefficient $c(k+1)$ appropriately.

as $c(k) = 1/\max_{l=1,\ldots,L} p_l(k)$. On the other hand, consider an alternative choice of the matrix $\mathbf{A}$ in (3.13) given by $\mathbf{F}$ and $c(k) = 1/\max_{l=1,\ldots,L} p_l(k)$ in [60, 37, 67], then the convergence performance of this algorithm (called the distributed power control algorithm in [37]) to $\mathbf{x}(\mathbf{F})$ can be greatly enhanced. In particular, different choices of $\mathbf{A}$ in (3.13) lead to different spectrum, each of which differs in the ratio of the absolute values of the largest and the second largest eigenvalues that governs the convergence rate of the power method (hence Algorithm 2). Different choices of updating $c(k+1)$ also affects the overall convergence behavior. We refer the reader to [37, 87, 48, 67] for more details on the algorithms and their performance comparisons.

3.1.4 Transmit Beamforming by Extended Matrix Approach

Let us consider a special case of (3.1) with $\mathbf{a} = \mathbf{1}$ (a single total power constraint) and $\boldsymbol{\beta} = \mathbf{1}$. This special case is typically used to model the *downlink problem* in a wireless cellular network. A downlink transmission means that data information is transmitted from the base station and received at the mobile users. By the same token, it is also valid to consider the *uplink problem* when the transmission direction is reversed, i.e., information is transmitted from the mobile users and received at the base station. It is often assumed that the channel gain parameters for the uplink problem are symmetrical to the downlink problem. The downlink problem typically considers jointly optimizing both the transmit powers and the transmit antenna beamformers.

The solvability of both the uplink and downlink problems by the nonlinear Perron-Frobenius theory were studied in [76, 77, 97]. Prior to

the nonlinear Perron-Frobenius theory approach in [76, 77, 97], the authors in [90] proposed the *extended matrix* approach to solve the downlink problem in (3.1). We outline below this approach in [90] to solve (3.1) that is mainly centralized. On the other hand, Algorithm 1 exploits an algorithm in [31] (cf. Step 1 of Algorithm 1) and is distributed. The extended matrix approach first introduced in [90] was later used in [10, 11] for designing downlink beamforming algorithms. We refer the reader to Chapter 7.3 in [22] for these related discussions. We now describe how this extended matrix approach in [90] can be connected to the nonlinear Perron-Frobenius theory approach for this special case.

The idea in [90] is to construct an *extended matrix* (see $\mathbf{E}$ below) such that the problem in (3.1) has an optimal value and an optimal power vector $\mathbf{p}^\star$, respectively, given by $1/\rho(\mathbf{E})$ and the vector that contains the first L elements of the eigenvector $\mathbf{x}(\mathbf{E})$ (with $(\mathbf{x}(\mathbf{E}))_{L+1} = 1$). This extended matrix is given by:

$$\mathbf{E} = \begin{bmatrix} \mathbf{F} & \mathbf{v} \\ (1/\bar{P})\mathbf{1}^\top\mathbf{F} & (1/\bar{P})\mathbf{1}^\top\mathbf{v} \end{bmatrix}. \tag{3.14}$$

In particular, observe that $\mathbf{E}$ can be decomposed as

$$\mathbf{E} = \begin{bmatrix} \mathbf{I} & \mathbf{0} \\ (1/\bar{P})\mathbf{1}^\top & 1 \end{bmatrix} \begin{bmatrix} \mathbf{F} + (1/\bar{P})\mathbf{v}\mathbf{1}^\top & \mathbf{0} \\ \mathbf{0}^\top & 0 \end{bmatrix} \begin{bmatrix} \mathbf{I} & \mathbf{0} \\ (1/\bar{P})\mathbf{1}^\top & 1 \end{bmatrix}^{-1} \tag{3.15}$$

whose characteristic equation is therefore

$$\det\left(\begin{bmatrix} \mathbf{F} + (1/\bar{P})\mathbf{v}\mathbf{1}^\top & \mathbf{0} \\ \mathbf{0}^\top & 0 \end{bmatrix} \right) = 0. \tag{3.16}$$

This thereby implies that the spectrum of $\mathbf{E}$ is identical to that of $\mathbf{B}$ in addition to a zero eigenvalue. Hence, we deduce that

$$\rho(\mathbf{E}) = \rho(\mathbf{B}) \tag{3.17}$$

and

$$\mathbf{x}(\mathbf{E}) = \begin{bmatrix} \mathbf{x}(\mathbf{B}) \\ 1 \end{bmatrix}, \tag{3.18}$$

where $\mathbf{1}^\top\mathbf{x}(\mathbf{B}) = \bar{P}$.

Now, using the fact that the optimal max-min SINR value is unique (and $\rho(\mathbf{B}) = \rho(\mathbf{E})$) and the above requirement in [90] that $[\mathbf{p}^\star \ 1]^\top = \mathbf{x}(\mathbf{E})$, we have

$$\rho(\mathbf{B}) = \frac{1}{\bar{P}}\mathbf{1}^\top \mathbf{F}\mathbf{p}^\star + \frac{1}{\bar{P}}\mathbf{1}^\top \mathbf{v}. \tag{3.19}$$

From an algorithm design perspective, it was shown in [10] that the uplink-downlink duality can be combined with the *extended matrix* approach in [90] to solve the downlink problem in (3.1). Briefly speaking, the uplink-downlink duality theory states that, under a same total power constraint for all the users, the achievable SINR region for a downlink transmission with joint transmit beamforming and power control optimization is equivalent to that of a reciprocal uplink transmission with joint receive beamforming and power control optimization. In particular, the optimal receive beamformers in the uplink are the optimal transmit beamformers in the downlink and, in fact, take the form of linear minimum mean-square error (LMMSE) filters. The uplink problem does not have the beamformer coupling difficulty associated with the downlink (hence easier to solve), and is first solved for the LMMSE beamformers. The optimal downlink transmit power is then computed by keeping these LMMSE beamformers fixed. In other words, another extended matrix is constructed for the uplink problem given by:

$$\hat{\mathbf{E}} = \begin{bmatrix} \mathbf{F}^\top & \mathbf{v} \\ (1/\bar{P})\mathbf{1}^\top \mathbf{F}^\top & (1/\bar{P})\mathbf{1}^\top \mathbf{v} \end{bmatrix}, \tag{3.20}$$

where the authors in [10] showed that the first L elements of the eigenvector $\mathbf{x}(\hat{\mathbf{E}})$ (with $(\mathbf{x}(\hat{\mathbf{E}}))_{L+1} = 1$) yields the uplink power vector (denote that by $\mathbf{q}$) that can be used to compute the LMMSE beamformers iteratively (see Table I in [10]).

For the general MIMO case, the max-min SINR problem with transmit beamforming has been studied in [86] by a conic programming approach that in general requires a centralized algorithm (interior-point method) to solve the conic programs. Using the uplink-downlink duality, the authors in [86] also proposed a distributed heuristic algorithm (to update the uplink power $\mathbf{q}$) whose convergence proof was later established using the nonlinear Perron-Frobenius theory in [16, 17] for the MISO special case. Other related work with joint optimization can

be found in [26, 41, 62, 43] for a beamforming communication system and in [89] for a time-reversal communication system.

3.1.5 Uplink and Downlink Duality by Nonlinear Perron-Frobenius Theory

Continuing on the discussion of solving the total-power constrained problem for the MISO case, we highlight how the uplink-downlink duality that connects both the downlink and uplink problems can be established using the Friedland-Karlin inequalities in Chapter 2. This fact can be exploited to shed further insights to these max-min problems and for designing distributed algorithms.

Let us consider Lemma 2.9 in Chapter 2. In particular, let $\mathbf{A} = \text{diag}(\boldsymbol{\beta})\mathbf{F}$, $\mathbf{b} = (1/\bar{P})\text{diag}(\boldsymbol{\beta})\mathbf{v}$ and $\mathbf{c}_* = \mathbf{1}$ in Lemma 2.9 to deduce that the optimal SINR allocation in (3.1) is a weighted geometric mean of the optimal SINR, where the weights are the normalized Schur product of the uplink power and the downlink power (i.e., the Perron-Frobenius right and left eigenvectors of $\text{diag}(\boldsymbol{\beta})\mathbf{B}$, respectively):[2]

$$\prod_{l=1}^{L}(\mathsf{SINR}_l(\mathbf{p})/\beta_l)^{p_l q_l/(\beta_l v_l)} = 1/\rho(\text{diag}(\boldsymbol{\beta})\mathbf{B}). \tag{3.21}$$

Furthermore, both the optimal uplink and the downlink power form dual pairs with the vector $(1/\bar{P})\mathbf{1}$, i.e., $(\mathbf{p}, (1/\bar{P})\mathbf{1})$ and $(\mathbf{q}, (1/\bar{P})\mathbf{1})$ are dual pairs with respect to $\|\cdot\|_1$. Finally, we summarize in Fig. 3.1 the analytical relationship between this uplink-downlink duality with the nonlinear Perron-Frobenius theorem and the Friedland-Karlin minimax characterization given in Section 3.1.5. We refer the reader to [90, 76, 10, 16, 41, 97] for more discussions on the uplink-downlink duality for wireless max-min fairness optimization problems.

In summary, there are several insights from this nonlinear Perron-Frobenius theory approach: The spectrum of an *appropriately-constructed nonnegative matrix* or an appropriately-identified positive

[2] The normalization of the Schur product is done such that $\sum_l p_l q_l/(\beta_l v_l) = 1$. The uplink and the downlink powers can be obtained from a normalized sub-vector of the Perron-Frobenius right and left eigenvectors of a $(L+1) \times (L+1)$ extended matrix in [90, 10] or from that of the $L \times L$ matrix $\text{diag}(\boldsymbol{\beta})\mathbf{B}$ in (3.2).

Uplink-downlink Duality Correspondence

Downlink		Uplink
$\mathbf{p} = \mathbf{x}(\mathrm{diag}(\boldsymbol{\beta})\mathbf{B})$	$\leftrightarrow$	$\mathbf{q} = \mathbf{x}(\mathrm{diag}(\boldsymbol{\beta})\mathbf{B}^\top)$ $= \mathrm{diag}(\boldsymbol{\beta})\mathbf{y}(\mathrm{diag}(\boldsymbol{\beta})\mathbf{B})$
$\frac{\mathsf{SINR}_l(\mathbf{p})}{\beta_l} = \frac{1}{\rho(\mathrm{diag}(\boldsymbol{\beta})\mathbf{B})}$	$\leftrightarrow$	$\frac{\hat{\mathsf{SINR}}_l(\mathbf{q})}{\beta_l} = \frac{1}{\rho(\mathrm{diag}(\boldsymbol{\beta})\mathbf{B}^\top)}$
$\boldsymbol{\lambda} = \mathbf{p} \circ \mathrm{diag}(\boldsymbol{\beta})^{-1}\mathbf{q}$	$\leftrightarrow$	$\boldsymbol{\lambda} = \mathbf{q} \circ \mathrm{diag}(\boldsymbol{\beta})^{-1}\mathbf{p}$
$(\mathbf{p}, \mathbf{c}_* = (1/\bar{P})\mathbf{1})$	$\leftrightarrow$	$(\mathbf{q}, \mathbf{c}_* = (1/\bar{P})\mathbf{1})$
LMMSE Transmit	$\leftrightarrow$	LMMSE Receive

Figure 3.1: The uplink-downlink duality characterized through the nonlinear Perron-Frobenius theorem and the Friedland-Karlin spectral radius minimax theorem. The equality notation used in the equations denotes equality up to a scaling constant.

function can provide an analytical characterization of the optimality to these nonconvex max-min problems. Furthermore, it also provides a systematic framework to design efficient distributed algorithms (i.e., iterative algorithms that resemble the *power method* in linear algebra). In addition, the overall performance of these distributed algorithms can be rigorously evaluated. There are also various deep insights of this nonlinear Perron-Frobenius theory approach such as its connection to duality in optimization theory. Let us demonstrate this using another fairness optimization problem in the following.

3.2 Min-max Outage Probability Fairness

3.2.1 Worst Outage Probability Minimization

Consider the stochastic channel fading model. The problem of minimizing the worst outage probability can be formulated as

$$\begin{array}{lll} \text{minimize} & \max\limits_{l=1,\ldots,L} & P(\mathsf{SINR}_l(\mathbf{p}) < \beta_l) \\ \text{subject to} & \mathbf{p} \quad P, & \\ \text{variables:} & \mathbf{p}. & \end{array} \tag{3.22}$$

Let us denote the optimal worst outage probability, i.e., the optimal

value of (3.22), by $O^\star$.

Assuming independent Rayleigh fading at all the signals, the outage probability of the lth user can be given analytically by [45]:[3]

$$P(\mathsf{SINR}_l(\mathbf{p}) < \beta_l) = 1 - e^{\frac{-v_l\beta_l}{p_l}} \prod_{j=1}^{L} \left(1 + \frac{\beta_l F_{lj} p_j}{p_l}\right)^{-1}. \tag{3.23}$$

Observe that the probability of successful transmission, i.e., the complement of (3.23), is simply the product of two factors, namely, $e^{-v_l\beta_l/p_l}$ and $\prod_{j=1}^{L}\left(1 + \frac{\beta_l F_{lj} p_j}{p_l}\right)^{-1}$, which are the probability of successful transmission in a noise-limited Rayleigh-fading channel (i.e., no interference) and an interference-limited Rayleigh-fading channel (i.e., no additive white Gaussian noise) respectively.

By using (3.23) and defining a deterministic function:

$$\phi_l(\mathbf{p}) = 1 - e^{\frac{-v_l\beta_l}{p_l}} \prod_{j=1}^{L} \left(1 + \frac{\beta_l F_{lj} p_j}{p_l}\right)^{-1} \qquad l, \tag{3.24}$$

then the stochastic program in (3.22) simplifies to a deterministic problem:

$$\begin{array}{ll} \text{minimize} & \max\limits_{l=1,\ldots,L} \ \phi_l(\mathbf{p}) \\ \text{subject to} & \mathbf{p} \quad P. \end{array} \tag{3.25}$$

Note that (3.25) is always feasible as long as the given power budget constraints in (1.7) and (1.8) are feasible, and its optimal solution is strictly positive. Previous work in the literature, e.g., [45], only considered (3.25) for the interference-limited case, i.e., $\mathbf{v} = 0$ and *without any power constraint*. In this special case, [45] showed that (3.25) can be reformulated as a geometric program (a special class of convex optimization [27, 15]), and then solved numerically by the interior point method [15].

In the following, we give a reformulation of (3.25) as a convex optimization problem (not a geometric program but reduces to one in the

[3] A closed form expression was first derived in [91], but we use this another equivalent form derived in [45].

interference-limited special case). By exploiting the nonlinear Perron-Frobenius theory, the authors in [72, 74] proposed a fast algorithm[4] (no parameter tuning whatsoever and orders of magnitude faster than standard convex optimization algorithms such as the interior point method) to solve (3.25) optimally. As a by-product, it resolves an open problem on the convergence of a previously proposed heuristic algorithm in [45]. Furthermore, we characterize analytically the optimal value and solution of (3.25) in terms of a Perron-Frobenius eigenvalue and eigenvector of a specially constructed nonnegative matrix respectively.

Let us introduce an auxiliary variable τ and write (3.25) in the epigraph form (augmenting the constraint set with additional L constraints):

$$\begin{array}{ll} \text{minimize} & \tau \\ \text{subject to} & 1 - e^{\frac{-v_l\beta_l}{p_l}} \prod_{j=1}^{L} \left(1 + \frac{\beta_l F_{lj} p_j}{p_l}\right)^{-1} \leq \tau \quad l, \\ & \mathbf{p} \quad P, \\ \text{variables:} & \mathbf{p},\ \tau. \end{array} \tag{3.26}$$

Let us introduce a new variable

$$\alpha = -\log(1 - \tau), \tag{3.27}$$

and then, by rewriting the L augmented constraints in (3.26), (3.26) is equivalent to the following problem:

$$\begin{array}{ll} \text{minimize} & \alpha \\ \text{subject to} & \frac{v_l\beta_l}{p_l} + \sum_{j=1}^{L} \log\left(1 + \frac{\beta_l F_{lj} p_j}{p_l}\right) \leq \alpha \quad l, \\ & \mathbf{p} \quad P, \\ \text{variables:} & \mathbf{p},\ \alpha. \end{array} \tag{3.28}$$

We call the first L constraints of (3.28) the *outage constraints*, and denote the optimal solution to (3.28) by $(\mathbf{p}^\star, \alpha^\star)$. Note that $\mathbf{p}^\star$ is also the optimal solution to (3.25).

[4] Some key computational considerations are the extremely fast signal processing requirement at the transceiver chip and the decentralized environment.

Now, (3.28) is nonconvex in $(\mathbf{p}, \alpha)$. However, by making a logarithmic change of variable in $\mathbf{p}$, i.e., $\tilde{p}_l = \log p_l$ for all l, (3.28) can be converted into the following convex optimization problem in $(\tilde{\mathbf{p}}, \alpha)$:[5]

$$\begin{array}{lll} \text{minimize} & \alpha & \\ \text{subject to} & v_l \beta_l e^{-\tilde{p}_l} + \displaystyle\sum_{j=1}^{L} \log\left(1 + \beta_l F_{lj} e^{\tilde{p}_j - \tilde{p}_l}\right) \leq \alpha & l, \\ & e^{\tilde{\mathbf{p}}} \quad \mathcal{P}, & \\ \text{variables:} & \tilde{\mathbf{p}},\ \alpha. & \end{array} \tag{3.29}$$

Though solving the nonconvex problem in (3.28) is equivalent to solving the convex problem[6] in (3.29), we shall use a nonlinear Perron-Frobenius theory-based approach to solve (3.28) optimally. Using nonnegative matrix theory, we then connect (3.28) to the Lagrange duality of (3.29) (cf. Lemma 2.9 later) to shed further insights to the solution.

Lemma 3.3. At optimality of (3.28), the outage constraints in (3.28) are tight:

$$\frac{v_l \beta_l}{p_l^\star} + \sum_{j=1}^{L} \log\left(1 + \frac{\beta_l F_{lj} p_j^\star}{p_l^\star}\right) = \alpha^\star \quad l. \tag{3.30}$$

Furthermore, if $\mathcal{P} = \{\mathbf{p} \mid \mathbf{a}^\top \mathbf{p} \leq \bar{P}\}$, we have $\mathbf{a}^\top \mathbf{p}^\star = \bar{P}$, and if $\mathcal{P} = \{\mathbf{p} \mid p_l \leq \bar{p} \quad l\}$, we have $p_i^\star = \bar{p}$ for some i.

Proof. First, we note that it has been pointed out in [45] that all the outage constraints are tight for the interference-limited case, i.e., $\mathbf{v} = \mathbf{0}$. We prove the first part of Lemma 3.3 for the general case here. Clearly, the function on the lefthand side of the lth outage constraint in (3.28) is monotone increasing in p_j, $j = l$, and monotone decreasing in p_l. Suppose the lth constraint is not tight at optimality, i.e., $v_l \beta_l / p_l^\star +$

[5] Note that (3.28) cannot be rewritten as a geometric programming formulation, as has been done in [45]. Nevertheless, after a logarithmic change of variables, a convex form can still be obtained as shown here.

[6] The optimization problem in (3.29) is convex, because the objective function is linear and the constraint set is convex. In particular, the function $\sum_{j=1}^{L} \log\left(1 + \beta_l F_{lj} e^{\tilde{p}_j - \tilde{p}_l}\right)$ is convex because the log-sum-exp function is convex [15]. Thus, the constraint set in (3.29) that consists of exponentials and log-sum-exp functions is a convex one.

$\sum_{j=1}^{L} \log\left(1+\frac{\beta_l F_{lj} p_j^\star}{p_l^\star}\right) < \alpha^\star$. Then, we choose a feasible power $p_l < p_l^\star$ such that the evaluated value of $v_l\beta_l/p_l + \sum_{j=1}^{L} \log\left(1+\frac{\beta_l F_{lj} p_j^\star}{p_l}\right)$ is still less than $\alpha^\star$. Now, $v_j\beta_j/p_j^\star + \sum_{k\neq l} \log\left(1+\frac{\beta_j F_{jk} p_k^\star}{p_j^\star}\right) + \log\left(1+\frac{\beta_j F_{jl} p_l}{p_j^\star}\right)$ for all $j = l$. This implies that the value of α can be further decreased, i.e., $\alpha < \alpha^\star$, which contradicts the assumption. Hence, the lth constraint must be tight at optimality for all l.

We next prove the second part for $\mathcal{P} = \{\mathbf{p} \mid p_l \leq \bar{p} \quad l\}$. Suppose $p_l^\star < \bar{p}$ at optimality for all l. Let a positive scalar $a = \min_{l=1,\ldots,L} \bar{p}/p_l^\star > 1$, and choose a feasible power $\mathbf{p} = a\mathbf{p}^\star$, which evaluates the outage constraints as $v_l\beta_l/p_l + \sum_j \log\left(1+\frac{\beta_l F_{lj} p_j}{p_l}\right) = v_l\beta_l/ap_l^\star + \sum_{j=1}^{L} \log\left(1+\frac{\beta_l F_{lj} p_j^\star}{p_l^\star}\right) < v_l\beta_l/p_l^\star + \sum_{j=1}^{L} \log\left(1+\frac{\beta_l F_{lj} p_j^\star}{p_l^\star}\right) = \alpha^\star$ for all l. This implies that α can be further decreased, i.e., $\alpha < \alpha^\star$, which contradicts the assumption. Hence, $p_i^\star = \bar{p}$ for some i. A similar proof can be given when $\mathcal{P} = \{\mathbf{p} \mid \mathbf{a}^\top \mathbf{p} \leq \bar{P}\}$ and is omitted. □

Hence, by using Lemma 3.3, we have the optimal worst outage probability

$$O^\star = \phi_l(\mathbf{p}^\star) \qquad l, \tag{3.31}$$

and also $O^\star = 1 - e^{-\alpha^\star}$.

Remark 3.2. Now, finding the fixed-point solution in (3.30) in Lemma 3.3 may seem nontrivial. However, by exploiting a connection between the nonlinear Perron-Frobenius theory in [9, 50] (that includes unveiling a hidden convexity in (3.30)), we give an analytical solution to (3.30) and, equivalently, the optimal value and the optimal solution of (3.25) in Section 3.3 (see Table 3.1 later). Interestingly, $\alpha^\star$ in (3.28) (equivalently the optimal value of (3.25)) and the optimal solution $\mathbf{p}^\star$ can be viewed as a *nonlinear Perron-Frobenius eigenvalue* and its *nonlinear eigenvector*.[7]

[7] In summary, the intuition of using the nonlinear Perron-Frobenius theory to solve nonconvex optimization problem such as that in (3.25) lies in examining the fixed-point equations corresponding to the set of primal constraints that are tight at optimality. In particular, the fixed-point equations exhibit special properties such as nonnegativity, monotonicity and convexity.

The authors in [72, 74] proposed the following algorithm (with geometric convergence rate and no parameter tuning whatsoever) that computes the optimal solution of (3.28). We let k index discrete time slots.

Algorithm 3 Worst Outage Probability Minimization

1. Update power $\mathbf{p}(k+1)$:

$$p_l(k+1) = -\log\left(1 - \phi_l(\mathbf{p}(k))\right) p_l(k) \qquad l. \tag{3.32}$$

2. Normalize $\mathbf{p}(k+1)$:

$$\mathbf{p}(k+1) \leftarrow \frac{\mathbf{p}(k+1)\cdot \bar{P}}{\mathbf{a}^\top \mathbf{p}(k+1)} \text{ if } P = \{\mathbf{p} \mid \mathbf{a}^\top \mathbf{p} \le \bar{P}\}. \tag{3.33}$$

$$\mathbf{p}(k+1) \leftarrow \frac{\mathbf{p}(k+1)\cdot \bar{p}}{\max\limits_{j=1,\ldots,L} p_j(k+1)} \text{ if } P = \{\mathbf{p} \mid p_l \le \bar{p} \quad l\}. \tag{3.34}$$

Theorem 3.4. Starting from any initial point $\mathbf{p}(0)$, $\mathbf{p}(k)$ in Algorithm 3 converges geometrically fast to the optimal solution of (3.25).

Proof. Let us write the left-hand side of the lth outage constraint in (3.28) as $\frac{f_l(\mathbf{p})}{p_l} \le \alpha$, where

$$f_l(\mathbf{p}) = v_l\beta_l + \sum_{j=1}^{L} p_l \log\left(1 + \frac{\beta_l F_{lj} p_j}{p_l}\right). \tag{3.35}$$

In the following, we show that

$$\mathbf{f}(\mathbf{p}) = \left[f_1(\mathbf{p}),\ f_2(\mathbf{p}), \ldots,\ f_L(\mathbf{p})\right]^\top \tag{3.36}$$

is a positive *concave self-mapping* on the standard cone $K = \mathsf{R}_+^L$.

We first show that $\mathbf{f}(\mathbf{p}) = \left[f_1(\mathbf{p}),\ f_2(\mathbf{p}), \ldots,\ f_L(\mathbf{p})\right]^\top$ is a *cone mapping*[8] with respect to the interior of K. Taking the derivative of

[8] Recall the definition of concave self-mapping in Chapter 2. A self-mapping $\mathbf{f}$ of a

$f_l(\mathbf{p})$ with respect to p_l, the jth entry of the first derivative $\nabla f_l(\mathbf{p})$ is given by:

$$(\nabla f_l(\mathbf{p}))_j = \begin{cases} \sum_{k=1}^{L} \left(\log\left(1 + \frac{\beta_l F_{lk} p_k}{p_l}\right) - \frac{\beta_l F_{lk} p_k}{p_l + \beta_l F_{lk} p_k} \right), & \text{if } j = l \\ \frac{\beta_l F_{lj} p_l}{p_l + \beta_l F_{lj} p_j}, & \text{if } j = l. \end{cases} \tag{3.37}$$

Since $z/(1+z) \leq \log(1+z)$ for $z \geq 0$, $(\nabla f_l(\mathbf{p}))_l \geq 0$. Thus, $(\nabla f_l(\mathbf{p}))_j \geq 0$ for all j, i.e., $f_l(\mathbf{p})$ increases monotonically in $\mathbf{p}$. Now, we state the following result [51].

Theorem 3.5 (Proposition 3.2 in [51]). Let K be the set of cone mappings with respect to the interior of the positive standard cone. Suppose $\mathbf{f} : K \to K$ is differentiable and the following inequalities hold for the component mappings: $f_l : K \to \mathbb{R}_+$ for all l: $\sum_j p_j \mid (\nabla f_l(\mathbf{p}))_j \mid \leq f_l(\mathbf{p})$ on K. Then $\mathbf{f}$ K.

Now, we have

$$\begin{aligned} \sum_{j=1}^{L} p_j \mid (\nabla f_l(\mathbf{p}))_j \mid &= \textstyle\sum_{j=1}^{L} p_j (\nabla f_l(\mathbf{p}))_j \\ &= \sum_{k=1}^{L} \left(p_l \log\left(1 + \frac{\beta_l F_{lk} p_k}{p_l}\right) - \frac{\beta_l F_{lk} p_k p_l}{p_l + \beta_l F_{lk} p_k} \right) \\ &\quad + \sum_{j \neq l} \frac{\beta_l F_{lj} p_l p_j}{p_l + \beta_l F_{lj} p_j} \\ &= \sum_{k=1}^{L} p_l \log\left(1 + \frac{\beta_l F_{lk} p_k}{p_l}\right) \\ &\leq f_l(\mathbf{p}). \end{aligned} \tag{3.38}$$

Hence, by Theorem 3.5, $f_l(\mathbf{p})$ is a strictly positive and monotone cone mapping on K.

---

cone K is called a *cone mapping* if for every $\mathbf{c}, \mathbf{z}$ K and $1 \leq \lambda$ from $\lambda^{-1}\mathbf{c} \leq \mathbf{z} \leq \lambda\mathbf{c}$, it follows that $\lambda^{-1}\mathbf{f}(\mathbf{c}) \leq \mathbf{f}(\mathbf{z}) \leq \lambda\mathbf{f}(\mathbf{c})$, that is a cone mapping $\mathbf{f}$ maps any interval $[\lambda^{-1}\mathbf{z}, \lambda\mathbf{z}]$ into $[\lambda^{-1}\mathbf{f}(\mathbf{z}), \lambda\mathbf{f}(\mathbf{z})]$.

We next show that $\mathbf{f}(\mathbf{p}) = [f_1(\mathbf{p}),\ f_2(\mathbf{p}), \ldots,\ f_L(\mathbf{p})]^\top$ is a concave self-mapping. Taking the second derivative, we obtain the Hessian $\mathsf{O}^2 f_l(\mathbf{p})$ with entries given by:

$$(\mathsf{O}^2 f_l(\mathbf{p}))_{jk} = \begin{cases} -\dfrac{(\beta_l F_{lj})^2 p_j}{(p_l + \beta_l F_{lj} p_j)^2}, & \text{if } j = k, k = l \\ \dfrac{(\beta_l F_{lj})^2 p_j}{(p_l + \beta_l F_{lj} p_j)^2}, & \text{if } j = k, \text{ either } k \text{ or } j = l \\ -\displaystyle\sum_{m=1}^{L} \dfrac{(\beta_l F_{lm})^2 p_m^2 / p_l}{(p_l + \beta_l F_{lm} p_m)^2}, & \text{if } j = k = l \\ 0, & \text{otherwise.} \end{cases} \tag{3.39}$$

Now, the Hessian $\mathsf{O}^2 f_l(\mathbf{p})$ is indeed negative definite: for all real vectors $\mathbf{z}$, we have

$$\begin{aligned} \mathbf{z}^\top \mathsf{O}^2 f_l(\mathbf{p}) \mathbf{z} &= -\frac{1}{p_l} \sum_{k=1}^{L} \frac{(\beta_l F_{lk})^2 (p_l z_k - p_k z_l)^2}{(p_l + \beta_l F_{lk} p_k)^2} \\ &< 0. \end{aligned} \tag{3.40}$$

Another proof is to observe that $t \log(1 + x/t)$ is strictly concave in (x, t) for strictly positive t, as it is the perspective function of the strictly concave function $\log(1+x)$ [15]. Hence, $f_l(\mathbf{p})$ is a sum of strictly concave perspective function, and therefore $\mathbf{f}(\mathbf{p})$ is strictly concave in $\mathbf{p}$.

Also, observe that $f_l(\mathbf{p})$ is monotone increasing in $\mathbf{p}$ as has been shown earlier. We are now ready to apply the nonlinear Perron-Frobenius theorem given in Theorem 2.7 in Chapter 2. Note that the weighted sum and individual power constraints in (1.7) are the monotone weighted ℓ_1 norm constraint $\|\mathrm{diag}(\mathbf{a})\mathbf{p}\|_1 = \bar{P}$ and the ℓ_∞ norm constraint $\|\mathbf{p}\|_\infty = \bar{p}$ respectively. By Theorem 2.7, the convergence of the iteration

$$\mathbf{p}(k+1) = \frac{\mathbf{f}(\mathbf{p}(k))}{\|\mathbf{f}(\mathbf{p}(k))\|} \tag{3.41}$$

to the *unique* fixed point $\mathbf{p} = \mathbf{f}(\mathbf{p})/\|\mathbf{f}(\mathbf{p})\|$ is geometrically fast, regardless of the initial point. □

Remark 3.3. We remark that Algorithm 1 is a purely deterministic algorithm, and, upon convergence, all the users will transmit at the optimal power solution *keeping the power fixed regardless of the Rayleigh-fading random realization over time*. This means that no channel realization, e.g., the random variable R_{lj} for all l, j, is required in the update at each iteration. What is needed is only the additive white Gaussian noise power and the channel gains G_{lj} for all l, j which is assumed to be fairly static and does not vary at the Rayleigh fading timescale. The update in (3.32) is obtained by applying the nonlinear Perron-Frobenius theory to (3.30) of Lemma 3.3, which is then rewritten using the notation given in (3.24). To compute $\phi_l(\mathbf{p}(k))$ in (3.32), the lth user measures separately the received interfering power $\{F_{lj}p_j(k)\}, j = l$. The normalization at Step 2 can be made distributed using gossip algorithms to compute either $\max_{l=1,\ldots,L} p_l(k+1)$ or $\mathbf{a}^\top \mathbf{p}(k+1)$ [13].

In the following, we first derive useful bounds to $O^\star$ given in terms of the problem parameters of (3.25). Then, we solve (3.25) analytically in the interference-limited special case without any power constraint, and then extend the analysis to the general case with power constraints.

3.2.2 Worst Outage Probability Bounds

We now develop lower and upper bounds for the worst outage probability $O^\star$ using a certainty-equivalent margin (CEM) problem[9] as proxy. In particular, the CEM problem replaces the stochastic variation in the desired signal and the interference of (1.5) by their respective mean values, i.e., replace the random variables in (1.5) by the unit mean. This yields a purely deterministic function of powers. We shall refrain from calling it a deterministic SINR since it has no physical context meaning in the fading system model considered here. Mathematically, this yields the first optimization problem we have considered in Section 3.1. Let

[9] The certainty-equivalent margin (CEM) problem, in its simplified case where $v_l = 0$ for all l and without power constraint, was first used in the seminal work [45] to relate to the worst outage probability problem in the interference-limited special case (i.e., assuming no additive white Gaussian noise and no power constraint). We retain the CEM terminology here to be consistent with [45].

us write down the following problem:

$$\begin{array}{ll} \text{maximize} & \min\limits_{l=1,\ldots,L} \ \dfrac{1}{\beta_l} \dfrac{p_l}{\sum\limits_{j \neq l} F_{lj} p_j + v_l} \\ \text{subject to} & \mathbf{p} \quad P, \ \mathbf{p} \geq \mathbf{0}. \end{array} \tag{3.42}$$

Now, the optimal value and solution of (3.42) can be obtained analytically (as has already been shown in Section 3.1), and this allows us to deduce the following bounds using the CEM analytical optimal value (also in terms of the constant problem parameters of (3.28)).

Corollary 3.6. If $P = \{\mathbf{p} \mid p_l \leq \bar{p} \quad l\}$, the worst outage probability $O^\star$ satisfies

$$\begin{array}{ll} \frac{\rho(\mathrm{diag}(\boldsymbol{\beta})(\mathbf{F}+(1/\bar{p})\mathbf{v}\mathbf{e}_i^\top))}{1+\rho(\mathrm{diag}(\boldsymbol{\beta})(\mathbf{F}+(1/\bar{p})\mathbf{v}\mathbf{e}_i^\top))} & \leq O^\star = 1 - e^{-\alpha^\star} \\ & \leq 1 - e^{-\rho(\mathrm{diag}(\boldsymbol{\beta})(\mathbf{F}+(1/\bar{p})\mathbf{v}\mathbf{e}_i^\top))}, \end{array} \tag{3.43}$$

$$\text{where} \ \ i = \arg \max_{l=1,\ldots,L} \rho(\mathrm{diag}(\boldsymbol{\beta})(\mathbf{F} + (1/\bar{p})\mathbf{v}\mathbf{e}_l^\top)) \tag{3.44}$$

and $\alpha^\star$ is the optimal value to (3.28).

Proof. Using the inequalities $1 + \sum_{l=1}^{L} z_l \leq \prod_{l=1}^{L}(1+z_l) \leq e^{\sum_{l=1}^{L} z_l}$ for nonnegative $\mathbf{z}$ (cf. [45]), a lower and upper bound on $\alpha^\star$ can be given by $1/(1+\mathsf{cem}) \leq \alpha^\star \leq 1 - e^{-1/\mathsf{cem}}$, where cem is the optimal value of (3.42) and is analytically given by $1/\rho(\mathrm{diag}(\boldsymbol{\beta})(\mathbf{F} + (1/\bar{p})\mathbf{v}\mathbf{e}_i^\top))$, where i is given by (3.44) [75]. The bounds on $O^\star = 1 - e^{-\alpha^\star}$ can thus be obtained, hence proving Corollary 3.6. □

Remark 3.4. Note that the lower bound in Corollary 3.6 is not necessarily the tightest, but the bounds in Corollary 3.6 illustrate that the CEM problem, i.e., the spectral information of a concave self-mapping $\mathbf{f}(\mathbf{p}) = \mathrm{diag}(\boldsymbol{\beta})(\mathbf{F}\mathbf{p} + \mathbf{v})$ (cf. [75]) can provide useful quick bounds to the worst outage probability. Corollary 3.6 reduces to a result in [45] in the interference-limited case. Results similar to Corollary 3.6 can also be obtained for the case when $P = \{\mathbf{p} \mid \mathbf{a}^\top \mathbf{p} \leq \bar{P}\}$, but is omitted here.

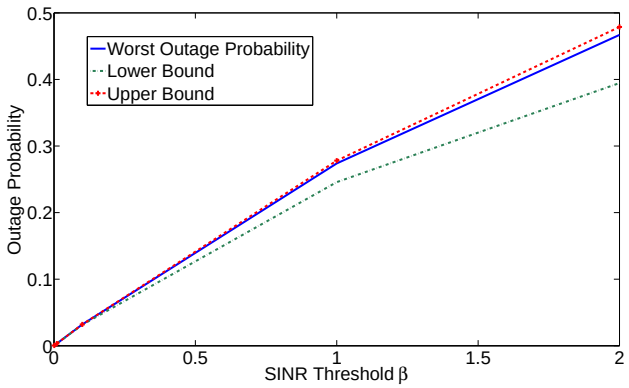

Figure 3.2: The worst outage probability versus the SINR threshold β for a system with 20 small cell users, where each user has a common SINR threshold β. The corresponding lower and upper bounds in Corollary 3.6 are also illustrated.

Example 3.1. Figure 3.2 plots the worst outage probability and the bounds for a system with 20 small cell users with individual power constraints using parameters in [93], where each user has a common SINR threshold β. We make several observations. First, the worst outage probability value and its bounds are concave in β. Second, the worst outage probability is very close to its upper bound. In fact, one observes that the optimal power $\mathbf{p}^\star$ is also close in value to the optimal solution of (3.42), i.e., $\mathbf{x}(\mathrm{diag}(\boldsymbol{\beta})(\mathbf{F} + (1/\bar{p})\mathbf{v}\mathbf{e}_i^\top))$, where i is given by (3.44) (cf. [75]). Further, for small β, the upper and lower bounds are very close to each other. This suggests that, in low-powered networks, the CEM solution can give sufficiently good approximation to the worst outage probability.

3.2.3 Interference-limited Case

We now turn to solve (3.25) analytically for the interference-limited case, i.e., $\mathbf{v} = \mathbf{0}$.[10] In this case, (3.35) is in addition a *primitive positive*

[10] The geometric programming approach in [45] to this interference-limited special case is to first rewrite (3.26) as a standard geometric program and then solve it numerically using the interior point method [15].

homogeneous function of degree one. Next, we define the nonnegative matrix $\mathbf{B}$ with the entries (that are functions of $\mathbf{p}$):

$$B_{lj} = \begin{cases} 0, & \text{if } l = j \\ \frac{p_l}{\beta_l p_j} \log\left(1 + \frac{\beta_l F_{lj} p_j}{p_l}\right), & \text{if } l = j. \end{cases} \tag{3.45}$$

Note that $\mathbf{B}(\mathbf{p})$ is irreducible whenever $\mathbf{F}$ is. Using (3.45), as shown in [45], we can write the optimal value $\alpha^\star$ and optimal solution $\mathbf{p}^\star$ of (3.28) in the interference-limited special case as

$$\alpha^\star = \rho(\text{diag}(\boldsymbol{\beta})\mathbf{B}(\mathbf{p}^\star)) \tag{3.46}$$

$$\text{and } \mathbf{p}^\star = \mathbf{x}(\text{diag}(\boldsymbol{\beta})\mathbf{B}(\mathbf{p}^\star)) \text{ (up to a scaling constant)} \tag{3.47}$$

respectively. Thus, $\mathbf{p}^\star$ is a fixed point of

$$\mathbf{p} = \frac{1}{\rho(\text{diag}(\boldsymbol{\beta})\mathbf{B}(\mathbf{p}))}\text{diag}(\boldsymbol{\beta})\mathbf{B}(\mathbf{p})\mathbf{p}. \tag{3.48}$$

Further, it is interesting to note the following result of $\mathbf{p}^\star$.

Corollary 3.7. In the interference-limited case, the optimal power of (3.28), $\mathbf{p}^\star$, satisfies

$$\mathbf{p}^\star = \arg\max_{\mathbf{p}>\mathbf{0}} \rho(\text{diag}(\boldsymbol{\beta})\mathbf{B}(\mathbf{p})). \tag{3.49}$$

Proof. Using (3.45), we can rewrite the outage constraints in (3.28) in matrix form as

$$\text{diag}(\boldsymbol{\beta})\mathbf{B}(\mathbf{p})\mathbf{p} \leq \alpha\mathbf{p}. \tag{3.50}$$

Next, we need the Subinvariance Theorem 2.2 stated in Chapter 2 to (3.50) (let $\mathbf{A} = \text{diag}(\boldsymbol{\beta})\mathbf{B}(\mathbf{p})$, $\mathbf{z}$ be a feasible $\mathbf{p}$ and $s = \alpha$), we have $\rho(\text{diag}(\boldsymbol{\beta})\mathbf{B}(\mathbf{p})) \leq \alpha$ for any feasible $\mathbf{p}$ and α. But $\alpha^\star = \rho(\text{diag}(\boldsymbol{\beta})\mathbf{B}(\mathbf{p}^\star))$. Hence, $\rho(\text{diag}(\boldsymbol{\beta})\mathbf{B}(\mathbf{p})) \leq \rho(\text{diag}(\boldsymbol{\beta})\mathbf{B}(\mathbf{p}^\star))$. This proves Corollary 3.7. □

The following method was first proposed in [45] to compute the optimal solution for the interference-limited case without any power constraint:

$$\mathbf{p}(k+1) = \frac{1}{\rho(\text{diag}(\boldsymbol{\beta})\mathbf{B}(\mathbf{p}(k)))}\text{diag}(\boldsymbol{\beta})\mathbf{B}(\mathbf{p}(k))\mathbf{p}(k). \tag{3.51}$$

The authors in [45] observed that this iteration converges numerically to an acceptable accuracy with a fixed initial vector $\mathbf{p}(0) = \mathbf{x}(\mathrm{diag}(\boldsymbol{\beta})\mathbf{F})$ (optimal solution of (3.42) without power constraints and noise power). The issues of convergence and existence of a fixed point were however left open in [45].

Now, Algorithm 3 in fact reduces to an update similar to (3.51) when $\mathbf{v} = \mathbf{0}$, and computes a solution that is equal to the fixed point of (3.48) up to a scaling constant. The scaling factor in (3.51) tends to $\rho(\mathrm{diag}(\boldsymbol{\beta})\mathbf{B}(\mathbf{p}^\star))$ with increasing k. From Theorem 3.4, this means that (3.51) converges from *any initial point* to the fixed point in (3.48) geometrically fast, thus resolving the open issues of convergence and fixed-point existence in [45].

3.3 Duality by Lagrange and Perron-Frobenius

We now show that the optimal value $\alpha^\star$ and optimal solution $\mathbf{p}^\star$ of (3.28) can be derived analytically from the spectral information of a specially constructed rank-one perturbation of $\mathrm{diag}(\boldsymbol{\beta})\mathbf{B}$, where $\mathbf{B}$ is given in (3.45). The following result is obtained based on Lemma 2.9 in Chapter 2 using the nonlinear Perron-Frobenius theory in [9] and the Friedland-Karlin inequality result in Theorem 2.3 given in Chapter 2.

Lemma 3.8. The optimal solution $(\mathbf{p}^\star, \alpha^\star)$ of (3.28) satisfies

$$\begin{aligned}
\log \alpha^\star &= \log \rho(\mathrm{diag}(\boldsymbol{\beta})(\mathbf{B}(\mathbf{p}^\star) + \mathbf{v}\mathbf{c}_*^\top)) \\
&= \max_{\|\mathbf{c}\|_D=1} \log \rho(\mathrm{diag}(\boldsymbol{\beta})(\mathbf{B}(\mathbf{p}^\star) + \mathbf{v}\mathbf{c}^\top)) \\
&= \max_{\boldsymbol{\lambda}\geq \mathbf{0}, \mathbf{1}^\top\boldsymbol{\lambda}=1} \min_{\mathbf{p}\in\mathcal{P}} \sum_{l=1}^{L} \lambda_l \log \frac{\beta_l(\mathbf{B}(\mathbf{p})\mathbf{p} + \mathbf{v})_l}{p_l} \qquad (3.52) \\
&= \min_{\mathbf{p}\in\mathcal{P}} \max_{\boldsymbol{\lambda}\geq \mathbf{0}, \mathbf{1}^\top\boldsymbol{\lambda}=1} \sum_{l=1}^{L} \lambda_l \log \frac{\beta_l(\mathbf{B}(\mathbf{p})\mathbf{p} + \mathbf{v})_l}{p_l}, \qquad (3.53)
\end{aligned}$$

where the optimal $\mathbf{p}$ in (3.52) and (3.53) are both given by $\mathbf{x}(\mathrm{diag}(\boldsymbol{\beta})(\mathbf{B}(\mathbf{p}^\star)+\mathbf{v}\mathbf{c}_*^\top))$ (which is equal to $\mathbf{p}^\star$ up to a scaling constant), and the optimal $\boldsymbol{\lambda}$ in (3.52) and (3.53) are both given by the Hadamard product of $\mathbf{x}(\mathrm{diag}(\boldsymbol{\beta})(\mathbf{B}(\mathbf{p}^\star) + \mathbf{b}\mathbf{c}_*^\top))$ and $\mathbf{y}(\mathrm{diag}(\boldsymbol{\beta})(\mathbf{B}(\mathbf{p}^\star) + \mathbf{b}\mathbf{c}_*^\top))$.

Furthermore, $\mathbf{p} = \mathbf{x}(\mathrm{diag}(\boldsymbol{\beta})(\mathbf{B}(\mathbf{p}^\star) + \mathbf{v}\mathbf{c}_*^\top))$ is the dual of $\mathbf{c}_*$ with respect to $\|\cdot\|_D$.[11]

Proof. The proof outline of Lemma 3.8 is to first consider the Lagrange duality of (3.29) and then apply Lemma 2.9 in Chapter 2.

First, we express the outage constraints in (3.29) using the matrix $\mathbf{B}$ and rewrite (3.29) as the following equivalent problem (let $\tilde{\alpha} = \log \alpha$):

$$\begin{array}{rll} \text{minimize} & \tilde{\alpha} & \\ \text{subject to} & \log\left(\frac{\beta_l(v_l+\mathbf{B}(e^{\tilde{\mathbf{p}}})e^{\tilde{\mathbf{p}}})_l}{e^{\tilde{p}_l}}\right) \le \tilde{\alpha} & l, \\ & e^{\tilde{\mathbf{p}}} \quad \mathcal{P}, & \\ \text{variables:} & \tilde{\mathbf{p}},\ \tilde{\alpha}. & \end{array} \tag{3.54}$$

Next, by augmenting only the outage constraints, the partial Lagrangian function of (3.54) is given by

$$\begin{aligned} L(\tilde{\alpha}, \tilde{\mathbf{p}}, \boldsymbol{\lambda}) &= \left(1 - \sum_{l=1}^{L} \lambda_l\right) \tilde{\alpha} + \\ &\quad \sum_{l=1}^{L} \lambda_l \log\left(\frac{\beta_l(v_l + \mathbf{B}(e^{\tilde{\mathbf{p}}})e^{\tilde{\mathbf{p}}})_l}{e^{\tilde{p}_l}}\right). \end{aligned} \tag{3.55}$$

Now, the Lagrange dual function of (3.54) is finite only if $\sum_{l=1}^{L} \lambda_l = 1$ for all feasible $\boldsymbol{\lambda}$. Hence, the Lagrange dual function is given by

$$\min_{\tilde{\alpha}, e^{\tilde{\mathbf{p}}} \in \mathcal{P}} L(\tilde{\alpha}, \tilde{\mathbf{p}}, \boldsymbol{\lambda}) = \sum_{l=1}^{L} \lambda_l \log\left(\frac{\beta_l(v_l + \mathbf{B}(e^{\tilde{\mathbf{p}}^\star})e^{\tilde{\mathbf{p}}^\star})_l}{e^{\tilde{p}_l^\star}}\right), \tag{3.56}$$

where $\tilde{\mathbf{p}}^\star$ is the optimal solution to (3.54).

Now, we are ready to apply Lemma 2.9 to (3.56). In particular, we can compute $\mathbf{c}_*$ explicitly depending on the choice of $\mathcal{P}$. For the case when $\mathcal{P} = \{\mathbf{p} | \mathbf{a}^\top \mathbf{p} \le \bar{P}\}$, let $\mathbf{A} = \mathrm{diag}(\boldsymbol{\beta})\mathbf{B}(\mathbf{p}^\star)$, $\mathbf{b} = \mathrm{diag}(\boldsymbol{\beta})\mathbf{v}$ and $\mathbf{c}_* = (1/\bar{P})\mathbf{a}$ in Lemma 2.9. For the case when $\mathcal{P} = \{\mathbf{p} | p_l \le \bar{p}_l\}$, let $\mathbf{A} = \mathrm{diag}(\boldsymbol{\beta})\mathbf{B}(\mathbf{p}^\star)$, $\mathbf{b} = \mathrm{diag}(\boldsymbol{\beta})\mathbf{v}$ and $\mathbf{c}_* = (1/\bar{p})\mathbf{e}_i$, where $i = \arg\max_{l=1,\ldots,L} \rho(\mathrm{diag}(\boldsymbol{\beta})(\mathbf{B}(\mathbf{p}^\star) + \mathbf{v}\mathbf{e}_l^\top))$ in Lemma 2.9. □

[11] A pair $(\mathbf{u}, \mathbf{v})$ of vectors of $\mathbb{R}^L$ is said to be a dual pair with respect to $\|\cdot\|$ if $\|\mathbf{v}\|_D \|\mathbf{u}\| = \mathbf{v}^\top \mathbf{u} = 1$.

Note that the optimal dual variable in (3.29) is equal to the optimal $\boldsymbol{\lambda}$ in (3.52) and (3.53). Using Lemma 2.9, we can now give analytically the optimal value and solution of (3.28) when $\mathcal{P} = \{\mathbf{p} \mid p_l \leq \bar{p} \quad l\}$.

Corollary 3.9. The optimal value and solution of (3.28) are given respectively by

$$\alpha^\star = \rho\left(\mathrm{diag}(\boldsymbol{\beta})(\mathbf{B}(\mathbf{p}^\star) + (1/\bar{p})\mathbf{v}\mathbf{e}_i^\top)\right) \tag{3.57}$$

and

$$\mathbf{p}^\star = \mathbf{x}\left(\mathrm{diag}(\boldsymbol{\beta})(\mathbf{B}(\mathbf{p}^\star) + (1/\bar{p})\mathbf{v}\mathbf{e}_i^\top)\right), \tag{3.58}$$

$$\text{where } i = \arg\max_{l=1,\ldots,L} \rho\left(\mathrm{diag}(\boldsymbol{\beta})(\mathbf{B}(\mathbf{p}^\star) + (1/\bar{p})\mathbf{v}\mathbf{e}_l^\top)\right). \tag{3.59}$$

Furthermore, $p_i^\star = \bar{p}$ for the i (not necessarily unique) in (3.59).

Remark 3.5. In general, the optimal index i in (3.59) differs from (3.44). The numerical simulations show that both are empirically the same when the CEM solution is close to $\mathbf{p}^\star$, especially so in the low-powered regime (cf. Figure 3.2). Unlike (3.59), (3.44) can be computed *a priori* from the problem parameters.

Table 3.1 summarizes the connection between the Perron-Frobenius spectrum (of the respectively different concave self-mappings) and the optimal value and solution of the optimization problems under the CEM model and the Rayleigh-fading model subject to the different power constraints (individual and total power constraints). The second and third row of Table 3.1 tabulate the CEM case for individual and total power constraints respectively. The fourth and fifth row of Table 3.1 tabulate the worst outage probability case for individual and total power constraints respectively. The sixth row of Table 3.1 tabulates the results for the max-min SINR problem with a weighted power constraint for small cell users in a single macrocell.

In summary, the nonlinear Perron-Frobenius theory approach has proved very useful in solving the max-min SINR problem and min-max outage probability problem in Rayleigh-fading channels. It is interesting to generalize the analysis and algorithm design methodologies based on

the nonlinear Perron-Frobenius theory to solve the worst outage probability problem for other practical fading channel models such as the Ricean, Weibull and Nakagami distributions. We refer the reader to [74, 85] on various extensions of the min-max outage probability problem using the nonlinear Perron-Frobenius theory. It is also interesting to consider more general nonlinear power constraints or wireless utility objectives, which is the focus in the next chapter.

Table 3.1: Characterization of max-min optimization problems reviewed in this monograph using the nonlinear Perron-Frobenius theory. The respective optimal value $\alpha^\star$ and optimal solution $\mathbf{p}^\star$ of the max-min optimization can be obtained implicitly from the Perron-Frobenius eigenvalue and right eigenvector of the specially-constructed matrix given in the middle column.

Concave Self-mapping $f_l(\mathbf{p})$	*Positive function in matrix form*	Remark
$(\mathrm{diag}(\boldsymbol{\beta})(\mathbf{F}\mathbf{p}+(1/\bar{p})\mathbf{v}))_l$, $i=\arg\max_{l=1,\ldots,L}\rho\left(\mathrm{diag}(\boldsymbol{\beta})(\mathbf{F}+(1/\bar{p})\mathbf{v}\mathbf{e}_l^\top)\right)$	$\mathrm{diag}(\boldsymbol{\beta})(\mathbf{F}+(1/\bar{p})\mathbf{v}\mathbf{e}_i^\top)$	[75]
$(\mathrm{diag}(\boldsymbol{\beta})(\mathbf{F}\mathbf{p}+(1/\bar{P})\mathbf{v}))_l$	$\mathrm{diag}(\boldsymbol{\beta})(\mathbf{F}+(1/\bar{P})\mathbf{v}\mathbf{a}^\top)$	[76]
$v_l\beta_l+\sum_{j=1}^{L}p_l\log\left(1+\frac{\beta_l F_{lj}p_j}{p_l}\right)$ $i=\arg\max_{l=1,\ldots,L}\rho\left(\mathrm{diag}(\boldsymbol{\beta})(\mathbf{B}(\mathbf{p}^\star)+(1/\bar{p})\mathbf{v}\mathbf{e}_l^\top)\right)$	$\mathrm{diag}(\boldsymbol{\beta})(\mathbf{B}(\mathbf{p}^\star)+(1/\bar{p})\mathbf{v}\mathbf{e}_i^\top)$	[72, 74], Corollary 3.9
$v_l\beta_l+\sum_{j=1}^{L}p_l\log\left(1+\frac{\beta_l F_{lj}p_j}{p_l}\right)$	$\mathrm{diag}(\boldsymbol{\beta})(\mathbf{B}(\mathbf{p}^\star)+(1/\bar{P})\mathbf{v}\mathbf{a}^\top)$	[72, 74]
$(\mathbf{F}\mathbf{p}+\mathbf{v})_l$	$\mathbf{F}+\mathbf{v}\mathbf{a}^\top$	[52], Remark 3.1

4

Max-min Wireless Utility Maximization

In this chapter, we study a unifying max-min fairness optimization framework based on a generalization of the nonlinear Perron-Frobenius theory and its application to solve wireless network optimization problems that are more general than those in the previous chapter.

4.1 Unifying Max-min Fairness Framework

The max-min or min-max fairness optimization problems in the previous chapters have simple constraint sets that can appropriately model traditional wireless cellular networks. The key is that these simple power constraints can be easily transformed into equivalent norm constraints that facilitate a direct application of Theorem 2.7 (Krause's concave Perron-Frobenius theory). However, the next-generation wireless networks will be more complex than traditional wireless cellular networks. They will be heterogeneous by design and, in general, have nonlinear constraints specific to the application scenarios. For example, there are stochastic interference temperature constraints in cognitive radio networks, and there are outage probability specification constraints in heterogeneous networks.

We now introduce a general framework in [42] that not only unifies the previous works relying on the nonlinear Perron-Frobenius theory in Theorem 2.7, but also enables a rigorous treatment of nonlinear monotonic constraints that often appear in new wireless applications. This generalized nonlinear Perron-Frobenius theory can be applied to a large class of utility fairness resource allocation problems with realistic nonlinear power constraints, interference constraints, channel fading constraints, and stochastic outage constraints that are then transformed into nonlinear fixed-point problems with monotonic constraints. It also enables a systematic framework to design algorithms (with no configuration needed) to solve these nonconvex problems in a jointly optimal and scalable manner.

We also illustrate the application of this unifying framework to a few representative case studies: the max-min SINR problem with interference temperature constraints in cognitive radio networks, the min-max MSE problem subject to SINR constraints in multiuser downlink systems and the max-min throughput problem subject to nonlinear power constraints in energy-efficient wireless networks.

4.1.1 General Max-Min Utility Optimization with Monotonic Constraints

Let us consider a wireless network with L users and let $p_1, \ldots, p_L$ be the transmit powers of the L users. In particular, p_i is the transmit power of the i-th user. We assume that the power vector $\mathbf{p} = [p_1, \ldots, p_L]^\top$ can be adjusted to optimize the overall network utility. By extending the nonlinear Perron-Frobenius theory in [49], we present in the following a unified treatment of a general class of max-min utility optimization problems under monotonic system constraints and more general utility functions. Unlike the simple constraint sets considered in Chapter 3, the constraints here involve functions that can potentially be nonlinear and nonconvex.

Problem Formulation

Specifically, let $u_i : \mathbb{R}_+^L \to \mathbb{R}_+$, for $i \quad \{1, \ldots, L\}$, be a continuous function of $\mathbf{p}$ that specifies the utility of user i and let $g_k : \mathbb{R}_+^L \to \mathbb{R}_+$,

for $k \in \{1, \ldots, K\}$, be a continuous function of $\mathbf{p}$ that is used to specify the k-th system constraint. The class of problems that we consider in this work can be formulated as follows:

$$\text{maximize} \quad \min_{i=1,\ldots,L} \; u_i(\mathbf{p}) \tag{4.1a}$$

$$\text{subject to} \quad \mathbf{g}(\mathbf{p}) \leq \bar{\mathbf{g}} \tag{4.1b}$$

$$\text{variables :} \quad \mathbf{p} \tag{4.1c}$$

where $\mathbf{g}(\mathbf{p}) = [g_1(\mathbf{p}), \ldots, g_K(\mathbf{p})]^\top$ is the vector of constraint functions and $\bar{\mathbf{g}} = [\bar{g}_1, \ldots, \bar{g}_K]^\top$ is the vector of constraint values. Due to the monotonicity of the functions $\{g_k\}_{k=1}^K$, we shall refer to (4.1b) as the set of monotonic constraints.

For arbitrarily general u_i and $\{g_k\}_{k=1}^K$, solving (4.1) is in general difficult. In the following, we present how to solve (4.1) for u_i and $\{g_k\}_{k=1}^K$ taking certain forms. Specifically, we consider a class of utility functions that satisfy the following assumptions.

Assumption 1 (Competitive Utility Functions)**.**

- *Positivity*: For all i, $u_i(\mathbf{p}) > 0$ if $\mathbf{p} > \mathbf{0}$ and, in addition, $u_i(\mathbf{p}) = 0$ if and only if $p_i = 0$.
- *Competitiveness*: For all i, u_i is strictly increasing with respect to p_i and is strictly decreasing with respect to p_j, for $j = i$, when $p_i > 0$.
- *Directional Monotonicity*: For $\lambda > 1$ and $p_i > 0$, $u_i(\lambda \mathbf{p}) > u_i(\mathbf{p})$, for all i.

Moreover, we consider a class of monotonic constraints that satisfy the following assumptions.

Assumption 2 (Monotonic Constraints)**.**

- *Strict Monotonicity*: For all k, $g_k(\mathbf{p}_1) > g_k(\mathbf{p}_2)$ if $\mathbf{p}_1 > \mathbf{p}_2$, and $g_k(\mathbf{p}_1) = g_k(\mathbf{p}_2)$ if $\mathbf{p}_1 = \mathbf{p}_2$.
- *Feasibility*: The set $\{\mathbf{p} > \mathbf{0} : \mathbf{g}(\mathbf{p}) \leq \bar{\mathbf{g}}\}$ is non-empty.

- *Validity*: For any $\mathbf{p} > \mathbf{0}$, there exists $\lambda > 0$ such that $g_k(\lambda \mathbf{p}) = \bar{g}_k$, for some k.

For the utility functions, the competitiveness assumption models the interaction between users in a wireless network and the directional monotonicity captures the increase in utility as the total power consumption increases. For the constraints, the strict monotonicity captures the increase in cost or resource consumption as $\mathbf{p}$ increases, the feasibility ensures that there exists a positive power vector in the feasible set, and the validity ensures that the set of constraints is meaningful. If the validity condition does not hold, the corresponding constraint can be simply removed without loss of generality.

The class of utility functions satisfying Assumption 1 is fairly general and includes, as special cases, many standard performance metrics in wireless networks, e.g.,

- the SINR under frequency-flat fading, i.e.,

$$u_i(\mathbf{p}) = \mathsf{SINR}_i(\mathbf{p}) \;,\; \frac{G_{ii}p_i}{\sum_{j\neq i} G_{ji}p_j + \eta_i}, \tag{4.2}$$

  where G_{ji} is the channel gain between transmitter j and receiver i, and η_i is the receiver noise variance;

- the link capacity, i.e.,

$$u_i(\mathbf{p}) = \log\left(1 + \mathsf{SINR}_i(\mathbf{p})\right), \tag{4.3}$$

  where the SINR is given by (4.2);

- the reliability function (which is the complement of the outage probability [45, 72, 74]), i.e.,

$$\begin{aligned} u_i(\mathbf{p}) \;&= \Pr\left(\mathsf{SINR}_i^R(\mathbf{p}) \geq \gamma_i\right) \\ &\;,\; e^{\frac{-\gamma_i\eta_i}{G_{ii}p_i}} \prod_{j\neq i}\left(1 + \frac{\gamma_i G_{ji}p_j}{G_{ii}p_i}\right)^{-1}, \end{aligned} \tag{4.4}$$

  where γ_i is the SINR threshold of the i-th user and $\mathsf{SINR}_i^R(\mathbf{p})$ is the SINR received at the i-th receiver under Rayleigh fading, defined as

$$\mathsf{SINR}_i^R(\mathbf{p}) \;,\; \frac{G_{ii}R_{ii}p_i}{\sum_{j\neq i} G_{ji}R_{ji}p_j + \eta_i}, \tag{4.5}$$

where $\{R_{ji}\}$ are independent and identically distributed (i.i.d.) exponential random variables with unit mean. Note that the SINR under Rayleigh fading in (4.5) is a random variable whose statistics depend on $\mathbf{p}$.

The class of monotonic constraints satisfying Assumption 2 also includes a large class of constraints that are representative in wireless networks, such as

- linear power constraints, i.e.,

$$\mathbf{g}(\mathbf{p}) = \mathbf{A}\mathbf{p} \leq \bar{\mathbf{p}}, \tag{4.6}$$

where $\bar{\mathbf{p}}$ is a $K \times 1$ positive vector of power constraint values and $\mathbf{A}$ is a $K \times L$ nonnegative weight matrix (e.g., $K = L$ and $\mathbf{A} = \mathbf{I}$ in the case of individual power constraints, and $K = 1$ and $\mathbf{A} = \mathbf{1}^\top$, i.e., an all-one row vector, in the case of sum power constraints);

- interference temperature constraints, i.e.,

$$g_k(\mathbf{p}) = \Psi_k(\mathbf{p}) \ , \ \sum_{j \neq k} \alpha_{jk} p_j \leq \bar{\Psi}_k, \tag{4.7}$$

where $\Psi_k(\mathbf{p})$ and $\bar{\Psi}_k$ are respectively the interference received at the kth receiver and the upper bound for the interference temperature, and α_{jk} is a positive parameter that models the extent of influence by the powers of the j-th users on the kth user [52, 79]. If α_{jk}'s are random variables, then $\Psi_k(\mathbf{p})$ is a random variable and $g_k(\mathbf{p})$ is a stochastic interference temperature constraint.

- nonlinear power constraints [44], i.e.,

$$\mathbf{g}(\mathbf{p}) = \mathbf{J}(\mathbf{p}) \leq \bar{\mathbf{p}}, \tag{4.8}$$

where $\mathbf{J} : R_+^L \to R_+^K$ is a nonlinear monotonic function of the power vector which can be used to model nonlinearities and distortions in the transceiver circuit, e.g., the power amplifier [65, 95].

In many cases, u_i and g_k are nonlinear and nonconvex functions in $\mathbf{p}$, making the problem difficult to solve using standard convex optimization approaches [15]. In some special cases, geometric programming (or related approximation methods) [23] can be used to obtain efficient solutions, but it cannot be used to address the general case optimally. Leveraging results from nonlinear Perron-Frobenius theory, we give an efficient iterative algorithm to solve a more general class of such problems, namely, problems satisfying Assumptions 1 and 2.

General Solution

By introducing an auxiliary variable τ, the problem in (4.1) can be reformulated as:

$$\begin{aligned} &\text{maximize } \tau && \text{(4.9a)}\\ &\text{subject to } u_i(\mathbf{p}) \geq \tau, \quad \text{for } i = 1, \ldots, L, && \text{(4.9b)}\\ &\qquad\qquad g_k(\mathbf{p}) \leq \bar{g}_k, \quad \text{for } k = 1, \ldots, K, && \text{(4.9c)}\\ &\text{variables : } \mathbf{p},\ \tau. && \text{(4.9d)} \end{aligned}$$

We shall refer to the constraints in (4.9b) as the objective constraints and those in (4.9c) as the system constraints.

Lemma 4.1. For $\{u_i\}_{i=1}^{L}$, $\{g_k\}_{k=1}^{K}$, and $\{\bar{g}_k\}_{k=1}^{K}$ that satisfy Assumptions 1 and 2, the optimal solution $(\tau^\star, \mathbf{p}^\star)$ is positive, i.e., $\tau^\star > 0$ and $\mathbf{p}^\star > \mathbf{0}$, and, at optimality, all objective constraints are tight and at least one system constraint is active. That is, $u_i(\mathbf{p}^\star) = \tau^\star$, for all i and $g_k(\mathbf{p}^\star) = \bar{g}_k$, for some k.

Proof. Suppose that $(\tau^\star, \mathbf{p}^\star)$ is an optimal solution. To show that $(\tau^\star, \mathbf{p}^\star)$ is positive, we first suppose that there exists i such that $p_i^\star = 0$. Then, $u_i(\mathbf{p}^\star) = 0$ and $\tau^\star = \min_i u_i(\mathbf{p}^\star) = 0$. However, by the feasibility assumption (cf. Assumption 2), there must exist a vector $\mathbf{p}' > \mathbf{0}$ that is feasible and, by the positivity assumption (cf. Assumption 1), we can find τ , $\min_i u_i(\mathbf{p}') > 0 = \tau^\star$, which contradicts the assumption that $(\tau^\star, \mathbf{p}^\star)$ is optimal. Hence, $(\tau^\star, \mathbf{p}^\star)$ is positive.

Next, we show that all the utility constraints are tight at optimality. Suppose that there exists i such that $u_i(\mathbf{p}^\star) > \tau^\star$. Then, by the fact

that $\mathbf{p}^\star > \mathbf{0}$, as shown above, we can choose $\hat{\mathbf{p}}$ such that $0 < \hat{p}_i < p_i^\star$ and $\hat{p}_j = p_j^\star$, for all $j = i$, and such that $\tau^\star < u_i(\hat{\mathbf{p}}) < u_i(\mathbf{p}^\star)$, due to the competitiveness of the utility functions (cf. Assumption 1). However, this yields $u_j(\hat{\mathbf{p}}) > u_j(\mathbf{p}^\star)$, for all $j = i$. In this case, we can choose τ such that $\tau \ , \ \min_i u_i(\hat{\mathbf{p}}) > \min_i u_i(\mathbf{p}^\star) = \tau^\star$, which contradicts the assumption that $\tau^\star$ is optimal. Hence, all the objective constraints must be tight at optimality.

Finally, we show that at least one system constraint is tight at optimality. Suppose that $g_k(\mathbf{p}^\star) < \bar{g}_k$, for all k. Since $\mathbf{p}^\star > \mathbf{0}$, there exists $\lambda > 1$ and $\mathbf{p}' \ , \ \lambda\mathbf{p}^\star$ such that $g_k(\mathbf{p}^\star) < g_k(\mathbf{p}') \leq \bar{g}_k$, for all k. Then, by the fact that $\mathbf{p}^\star > \mathbf{0}$ and the directional monotonicity of the utility functions (cf. Assumption 1), it follows that $u_i(\mathbf{p}') > u_i(\mathbf{p}^\star)$, for all i. This contradicts the assumption that $\mathbf{p}^\star$ is optimal. Hence, at least one of the system constraints must be tight at optimality. □

By Lemma 4.1, it follows that

$$\frac{1}{\tau^\star} p_i^\star = \frac{1}{u_i(\mathbf{p}^\star)} p_i^\star \ , \ T_i(\mathbf{p}^\star). \tag{4.10}$$

This means that the optimal power vector $\mathbf{p}^\star$ is a solution to the fixed point equation

$$\frac{1}{\tau^\star}\mathbf{p}^\star = [T_1(\mathbf{p}^\star), \ldots, T_L(\mathbf{p}^\star)]^\top \ , \ \mathbf{T}(\mathbf{p}^\star). \tag{4.11}$$

Definition 4.1. The function $\beta : R_+^L \to R_+$ of $\mathbf{p}$ (called the *scale* of $\mathbf{p}$) is defined as

$$\beta(\mathbf{p}) \ , \ \min\{\beta' = 0 : g_k(\mathbf{p}/\beta') \leq \bar{g}_k, \ \ k\}. \tag{4.12}$$

Lemma 4.2. The scale $\beta : R_+^L \to R_+$ defined in Definition 4.1 satisfies the following properties:

1. β is not identically zero and, in fact, $\beta(\mathbf{p}) > 0$, for all $\mathbf{p} > \mathbf{0}$;
2. $\beta(\lambda\mathbf{p}) = \lambda\beta(\mathbf{p})$ for $\mathbf{p} = \mathbf{0}$ and $\lambda = 0$ (i.e., positively homogeneous);

3. $\mathbf{0} \leq \mathbf{p} \leq \mathbf{q}$ implies $\beta(\mathbf{p}) \leq \beta(\mathbf{q})$ (i.e., monotonic).

Proof. The properties of β are shown as follows.

1) Suppose that statement 1) in Lemma 4.2 is not true. Then, there exists $\mathbf{p}' > \mathbf{0}$ such that $\beta(\mathbf{p}') = 0$. This implies that $g_k(\mathbf{p}'/\beta') < \bar{g}_k$ for all k and for all $\beta' > 0$. This contradicts the validity assumption in Assumption 2. Hence, it follows that $\beta(\mathbf{p}) > 0$, for all $\mathbf{p} > \mathbf{0}$.

2) The property follows trivially for $\lambda = 0$ since $\beta(0\mathbf{p}) = \beta(\mathbf{0}) = 0 = 0\beta(\mathbf{p})$. To prove the property for $\lambda > 0$, let us recall, from the definition of β, that $g_k(\mathbf{p}/\beta(\mathbf{p})) \leq \bar{g}_k$, for all k. Thus, for $\lambda > 0$, it follows that $g_k(\lambda\mathbf{p}/\lambda\beta(\mathbf{p})) \leq \bar{g}_k$, for all k. This implies that $\lambda\beta(\mathbf{p}) \geq \beta(\lambda\mathbf{p})$, $\min\{\beta' : g_k(\lambda\mathbf{p}/\beta') \leq \bar{g}_k, \ k\}$. Suppose that $\lambda\beta(\mathbf{p}) > \beta(\lambda\mathbf{p})$. Then, we can choose $\hat{\beta}$, $\beta(\lambda\mathbf{p})/\lambda < \beta(\mathbf{p})$ such that $g_k(\mathbf{p}/\hat{\beta}) = g_k(\lambda\mathbf{p}/\beta(\lambda\mathbf{p})) \leq \bar{g}_k$, for all k, which contradicts the definition that $\beta(\mathbf{p})$, $\min\{\beta' : g_k(\mathbf{p}/\beta') \leq \bar{g}_k, \ k\}$. Hence, $\lambda\beta(\mathbf{p}) = \beta(\lambda\mathbf{p})$.

3) The property is trivially satisfied for $\beta(\mathbf{p}) = 0$. Now, let us consider the case where $\beta(\mathbf{p}) > 0$. By the monotonicity of g_k, we know that $g_k(\mathbf{p}) \leq g_k(\mathbf{q})$, for any $\mathbf{p} \leq \mathbf{q}$. Therefore, for $\beta' > 0$, it follows that $g_k(\mathbf{p}/\beta') \leq g_k(\mathbf{q}/\beta')$, for any $\mathbf{p} \leq \mathbf{q}$. Hence, $\{\beta' : g_k(\mathbf{p}/\beta') \leq \bar{g}_k, \ k\}$ $\{\beta' : g_k(\mathbf{q}/\beta') \leq \bar{g}_k, \ k\}$ and, thus, $\beta(\mathbf{p})$, $\min\{\beta' : g_k(\mathbf{p}/\beta') \leq \bar{g}_k, \ k\} \leq \{\beta' : g_k(\mathbf{q}/\beta') \leq \bar{g}_k, \ k\}$, $\beta(\mathbf{q})$. □

Notice that, when $\mathbf{p} > 0$, the scale $\beta(\mathbf{p}) > 0$ (cf. Lemma 4.2) is chosen such that, after normalization, the power vector $\tilde{\mathbf{p}} = \mathbf{p}/\beta(\mathbf{p})$ yields the largest feasible solution in the direction of $\mathbf{p}$. In this case, at least one of the system constraints must be satisfied with equality, i.e., $g_k(\mathbf{p}/\beta(\mathbf{p})) = \bar{g}_k$ for some k. Therefore, the set of feasible solutions of $\mathbf{p}$ must include, as a subset, the set of $\mathbf{p}$ that has scale equal to 1, i.e., $\{\mathbf{p} = \mathbf{0} : g_k(\mathbf{p}) \leq \bar{g}_k, \ k\}$ $\{\mathbf{p} = \mathbf{0} : \beta(\mathbf{p}) = 1\}$, U.

Lemma 4.3. The optimal solution of (4.1) is included in U.

Proof. Let $\mathbf{p}^\star$ be an optimal solution of (4.1). We first show that $\beta(\mathbf{p}^\star) \leq 1$. Suppose that $\beta(\mathbf{p}^\star) > 1$ and recall, from Lemma 4.1, that $\mathbf{p}^\star$ must be nonzero in all components. It then follows by the strict monotonicity and validity of the constraints that $g_k(\mathbf{p}^\star) > g_k(\mathbf{p}^\star/\beta(\mathbf{p}^\star)) = \bar{g}_k$ for some k. Therefore, $\mathbf{p}^\star$ is infeasible and contradicts the assumption that $\mathbf{p}^\star$ is optimal.

Moreover, by Lemma 4.1, we know that $g_k(\mathbf{p}^\star)$ 5 $\bar{g}_k$, for all k, and there exists k' such that $g_{k'}(\mathbf{p}^\star) = \bar{g}_{k'}$. Suppose that $\beta(\mathbf{p}^\star) < 1$, then the power vector $\tilde{\mathbf{p}} = \mathbf{p}^\star/\beta(\mathbf{p}^\star)$ is also feasible. By the fact that $\mathbf{p}^\star > \mathbf{0}$ (cf. Lemma 4.1) and by the directional monotonicity of the utility functions, it follows that $u_i(\tilde{\mathbf{p}}) > u_i(\mathbf{p}^\star)$, for all i. This implies that $\min_i u_i(\tilde{\mathbf{p}}) > \min_i u_i(\mathbf{p}^\star)$, which contradicts the assumption that $\mathbf{p}^\star$ is optimal. Hence, $\beta(\mathbf{p}^\star) = 1$ and, thus, $\mathbf{p}^\star$ U. □

By Lemma 4.3, it follows that the solution of the optimization problem in (4.9) (and, thus, (4.1)) is a solution of the conditional eigenvalue problem [49], where the objective is to find $(\tau^\star, \mathbf{p}^\star)$ such that

$$\frac{1}{\tau^\star}\mathbf{p}^\star = \mathbf{T}(\mathbf{p}^\star),\ \tau^\star \quad R,\ \mathbf{p}^\star \quad U. \tag{4.13}$$

Hence, by exploiting the connection with nonlinear Perron-Frobenius theory [49], the authors in [42] proposed in Algorithm 4 an efficient iterative procedure for the computation of $\mathbf{p}^\star$. Here, we use $\mathbf{p}(t)$ to represent the power vector obtained in the t-th iteration of the algorithm.

Algorithm 4 Max-Min Utility Optimization under Monotonic Constraints

1. Update power vector $\mathbf{p}(t+1)$:

$$p_i(t+1) = \frac{p_i(t)}{u_i(\mathbf{p}(t))}\Big(\ ,\ T_i(\mathbf{p}(t))\Big), \quad i. \tag{4.14}$$

2. Scale power vector $\mathbf{p}(t+1)$:

$$\mathbf{p}(t+1) \leftarrow \frac{\mathbf{p}(t+1)}{\beta(\mathbf{p}(t+1))}. \tag{4.15}$$

The following theorem establishes the existence and the uniqueness of the solution of the conditional eigenvalue problem in (4.13) as well as the convergence of Algorithm 4.

Theorem 4.4. Suppose that $\mathbf{T} : R_+^L \to R_+^L$, defined as $\mathbf{T}(\mathbf{p}) = [T_1(\mathbf{p}), \ldots, T_L(\mathbf{p})]^\top$, where $T_i(\mathbf{p}) = p_i/u_i(\mathbf{p})$, satisfies the following conditions: (i) there exist numbers $a > 0$, $b > 0$, and a vector $\mathbf{e} > \mathbf{0}$ such that $a\mathbf{e} \leq \mathbf{T}(\mathbf{p}) \leq b\mathbf{e}$, for all $\mathbf{p} \in U$; (ii) for any $\mathbf{p}$, $\mathbf{q} \in U$ and $0 \leq \lambda \leq 1$: If $\lambda\mathbf{p} \leq \mathbf{q}$, then $\lambda\mathbf{T}(\mathbf{p}) \leq \mathbf{T}(\mathbf{q})$; and, if $\lambda\mathbf{p} \leq \mathbf{q}$ with $\lambda < 1$, then $\lambda\mathbf{T}(\mathbf{p}) < \mathbf{T}(\mathbf{q})$. Then, the following properties hold:

(a) The conditional eigenvalue problem in (4.13) has a unique solution $\mathbf{p}^\star \in U$ and $\tau^\star > 0$.

(b) The power vector $\mathbf{p}(t)$ in Algorithm 4 converges to $\mathbf{p}^\star$ (i.e., the solution of (4.13) and, thus, (4.1)) for any initial point $\mathbf{p}(0) = \mathbf{0}$ with $\beta(\mathbf{T}(\mathbf{p}(0))) > 0$.

Proof. Let us invoke the following theorem from [49] regarding the solution of the conditional eigenvalue problem.

Theorem 4.5 ([49]). Suppose that $\beta : R_+^L \to R_+$ is not identically 0, positively homogeneous (i.e., $\beta(\lambda\mathbf{p}) = \lambda\beta(\mathbf{p})$ for $\mathbf{p} = \mathbf{0}$ and $\lambda = 0$), and monotonic (i.e., $\mathbf{0} \leq \mathbf{p} \leq \mathbf{q}$ implies $\beta(\mathbf{p}) \leq \beta(\mathbf{q})$), and that the function $\mathbf{T} : R_+^L \to R_+^L$ satisfies the following conditions: (i) there exists numbers $a > 0$, $b > 0$, and a vector $\mathbf{e} > \mathbf{0}$ such that $a\mathbf{e} \leq \mathbf{T}(\mathbf{p}) \leq b\mathbf{e}$, for all $\mathbf{p} \in U$; (ii) for any $\mathbf{p}$, $\mathbf{q} \in U$ and $0 \leq \lambda \leq 1$:: If $\lambda\mathbf{p} \leq \mathbf{q}$, then $\lambda\mathbf{T}(\mathbf{p}) \leq \mathbf{T}(\mathbf{q})$; and, if $\lambda\mathbf{p} \leq \mathbf{q}$ with $\lambda < 1$, then $\lambda\mathbf{T}(\mathbf{p}) < \mathbf{T}(\mathbf{q})$. Then, the following properties hold:

(a) $\frac{1}{\tau}\mathbf{p} = \mathbf{T}(\mathbf{p})$ has a unique solution $\mathbf{p}^\star \in U$ and $\tau^\star > 0$.

(b) $\mathbf{p}^\star = \lim_{n\to\infty} \tilde{\mathbf{T}}^n(\mathbf{p})$, where $\tilde{\mathbf{T}}(\mathbf{p}) = \mathbf{T}(\mathbf{p})/\beta(\mathbf{p})$, for any $\mathbf{p} = \mathbf{0}$ with $\beta(\mathbf{T}(\mathbf{p})) > 0$.

By Lemma 4.2, we know that β is indeed not identically zero, positively homogeneous, and monotonic. Condition (a) in Theorem 4.5 above leads directly to condition (a) in Theorem 4.4 and condition (b) in Theorem 4.5 leads to the iterative max-min utility optimization algorithm given in Algorithm 4 and, thus, its convergence. □

The proof of the theorem utilizes a generalized result in nonlinear Perron-Frobenius theory presented in [49]. We refer the reader to [42] for the details of the proof. The following corollary, which follows directly from the results in [49], gives an immediate consequence of the conditions in Theorem 4.4.

Corollary 4.6. For $\beta(\mathbf{p})$ that is zero only when $\mathbf{p} = \mathbf{0}$, the properties in Theorem 4.4 hold for $\mathbf{T}$ that is positive and concave, i.e., $\mathbf{T}(\mathbf{p}) > \mathbf{0}$ for $\mathbf{p} \geq \mathbf{0}$ and

$$\mathbf{T}(\lambda\mathbf{p} + (1 - \lambda)\mathbf{q}) \geq \lambda\mathbf{T}(\mathbf{p}) + (1 - \lambda)\mathbf{T}(\mathbf{q}), \tag{4.16}$$

for all $\mathbf{p} \neq \mathbf{0}$, $\mathbf{q} \neq \mathbf{0}$, and $0 \leq \lambda \leq 1$.

Even though conditions (i) and (ii) in Theorem 4.4 are more general, the conditions in Corollary 4.6 are easier to verify and are, in fact, sufficient for most applications. The requirement that $\beta(\mathbf{p})$ is zero only when $\mathbf{p} = \mathbf{0}$ is satisfied when the power of all users are constrained, i.e., no user's transmit power can go to infinity, which is the case in most practical applications.

Remark 4.1. The computation of (4.14) in Algorithm 4 can be distributed since the respective power and utility are attainable at each user. The scaling step in (4.15), however, should be computed centrally. We discuss the efficient computation of $\beta(\mathbf{p})$ in the following section, which can be geometrically fast.

Efficient Computation of $\beta(\mathbf{p})$

In Algorithm 4, it is necessary to compute the scale $\beta(\mathbf{p}(t))$ for $\mathbf{p}(t)$ obtained in each iteration t. In particular, for given $\mathbf{p} > \mathbf{0}$ (which is the case in each iteration when Algorithm 4 is initialized with a positive power vector, i.e., $\mathbf{p}(0) > \mathbf{0}$), the scale $\beta(\mathbf{p})$ is chosen such that the normalized power vector $\tilde{\mathbf{p}} \ , \ \mathbf{p}/\beta(\mathbf{p})$ guarantees that at least one system constraint in (4.1) is tight. In general, this scale can be found via a bisection search as described in Algorithm 5 in which the upper bound of $\beta(\mathbf{p})$ is first established in the initialization phase and

Algorithm 5 Computation of β via Bisection Search

Initialization:

i) Set $i \leftarrow 0$, $L \leftarrow 0$, and $U \leftarrow 2^i$.

ii) If there exists k such that $g_k(\mathbf{p}/U) > \bar{g}_k$, then increment $i \leftarrow i+1$ and set $U \leftarrow 2^i$.

iii) Repeat (ii) until $g_k(\mathbf{p}/U) \leq \bar{g}_k$ for all k.

Bisection Search

1. Set $\beta \leftarrow (U+L)/2$. If $g_k(\mathbf{p}/\beta) > \bar{g}_k$ for some k, then set $L \leftarrow \beta$. Otherwise, set $U \leftarrow \beta$.

2. Repeat until $|U - L| < \epsilon$.

the actual value of $\beta(\mathbf{p})$ is then obtained by decreasing the interval between the upper and lower bounds geometrically.

Alternatively, notice that, for $\mathbf{p} > \mathbf{0}$, finding $\beta(\mathbf{p})$ by (4.12) is equivalent to choosing the minimum value of $\beta' > 0$ such that

$$I_k(\beta') \ , \ \beta' g_k(\mathbf{p}/\beta')/\bar{g}_k \leq \beta', \tag{4.17}$$

for $k = 1, \ldots, K$. Based on this observation, an efficient iterative algorithm can be proposed for the computation of $\beta(\mathbf{p})$ by generalizing the results from [92]. Following [92], let us define the following class of standard functions.

Definition 4.2 ([92]). A function $I : R_+ \rightarrow R_+$ is *standard* if the following conditions[1] are satisfied for all $\beta > 0$:

1. Monotonicity: If $\beta^{(a)} \leq \beta^{(b)}$, then $I(\beta^{(a)}) \leq I(\beta^{(b)})$.

[1] Notice that, even though $\beta \geq 0$ was required in [92], the results hold equally for just $\beta > 0$. Moreover, notice that positivity (i.e., $I(\beta) > 0$) was required explicitly in [92], but can actually be implied by monotonicity and scalability since the latter two yield $tI(\beta) > I(t\beta) \geq I(\beta)$, for $t > 1$.

2. Scalability: For $\lambda > 1$, $\lambda I(\beta) > I(\lambda\beta)$.

For $\{I_k\}_{k=1}^K$ that are standard, the authors in [42] proposed the following algorithm for the computation of $\beta(\mathbf{p})$. With a slight abuse of notation, we denote $\beta(t)$ in the following as the value of β in the t-th iteration.

Algorithm 6 Computation of β via Fixed-Point Iteration

1. Set initial value $\beta(0) > 0$.
2. Set $\beta(t+1) \leftarrow \max_k I_k(\beta(t))$.
3. Repeat Step 2 until convergence.

The following theorem shows the convergence and the validity of the above algorithm.

Theorem 4.7. For given $\mathbf{p} > 0$ and for $\{g_k\}_{k=1}^K$ such that $I_k(\beta)$, $\beta g_k(\mathbf{p}/\beta)$ is standard, for all k, the following properties hold:

1. Algorithm 6 converges to a unique fixed point $\beta^\star$.
2. The fixed point $\beta^\star$ is equal to $\beta(\mathbf{p})$ defined in (4.12).

The above theorem is proved following similar procedures as in [92] and is omitted for brevity. However, it is worthwhile to note that, in [92], the properties in Definition 4.2 are required to hold for $\beta = 0$ as well. However, by initializing Algorithm 6 with $\beta(0) > 0$, the value of $\beta(t)$ will always be positive for all t and, thus, the convergence proof presented in [92] holds in the case here as well. In the following, we present a sufficient condition on g_k for efficient evaluation of whether I_k is standard.

Corollary 4.8. The properties in Theorem 4.7 hold for $\mathbf{p} > \mathbf{0}$ and for $\{g_k\}_{k=1}^K$ that are concave and satisfy Assumption 2.

Proof. This proof relies on showing that $I_k \ , \ \beta g_k(\mathbf{p}/\beta)$ is standard by Definition 4.2 for all k. In particular, to show the monotonicity of I_k, let us first take the derivative of $I_k(\beta)$ with respect to β, which yields

$$I_k'(\beta) = g_k(\mathbf{p}/\beta) - \frac{1}{\beta}\mathbf{p}^T \quad {}_{\mathbf{p}} g_k(\mathbf{p}/\beta), \tag{4.18}$$

where $\quad_{\mathbf{p}}$ represents the gradient operator with respect to $\mathbf{p}$. By the change of variable $x = 1/\beta$, we have

$$f(x) \ , \ I_k'(1/x) = g_k(x\mathbf{p}) - x\mathbf{p}^T \quad {}_{\mathbf{p}} g_k(x\mathbf{p}). \tag{4.19}$$

Notice that $f(0) = g_k(0) = 0$ and

$$f'(x) = -x\mathbf{p}^T \quad {}^2_{\mathbf{p}} g_k(x\mathbf{p})\mathbf{p} = 0, \tag{4.20}$$

for all $x > 0$, due to the concavity of g_k, where $\quad^2_{\mathbf{p}}$ represents the Hessian operator with respect to $\mathbf{p}$. Therefore, $f(x) = I_k'(1/x) = 0$, for all $x = 0$ and, thus, $I'(\beta) = 0$, for all $\beta > 0$. Hence, we can conclude that I_k is nondecreasing for $\beta > 0$, i.e., monotonicity holds for I_k. Moreover, notice that, for $\lambda > 1$ and $\mathbf{p} > \mathbf{0}$, we have $\lambda I_k(\beta) = \lambda\beta g_k(\mathbf{p}/\beta) > \lambda\beta g_k(\mathbf{p}/(\lambda\beta)) = I_k(\lambda\beta)$ since $\mathbf{p}/\beta > \mathbf{p}/(\lambda\beta)$. Hence, scalability holds for I_k. Since I_k satisfies monotonicity and scalability, it is standard by Definition 4.2 and, thus, properties of Theorem 4.7 hold for this case as well. □

The proof relies on showing that I_k is standard if g_k is concave and monotone.

In the following sections, we utilize the mathematical tool developed above to solve representative problems in cognitive radio networks, multiuser downlink networks and energy-efficient wireless networks and also illustrate the performance of Algorithm 4.

4.2 Case Studies

In this section, we present three case studies to illustrate the application of the above unifying max-min fairness framework.

Case Study I: Cognitive Radio Networks with Stochastic Interference Temperature Constraints

Let us consider a cognitive radio network with M primary receivers and L secondary transmitter-receiver pairs. Here, we consider a representative example where the power vector $\mathbf{p} = [p_1, \ldots, p_L]^\top$ associated with the L secondary transmitters is adjusted to maximize the minimum SINR among secondary receivers subject to interference temperature constraints at primary receivers and individual power constraints at secondary transmitters. This problem was previously investigated in [52, 97] for the case where the interference temperature constraints are deterministic. In [25], stochastic interference temperature constraints were considered but only approximate solutions could be obtained. Here, using the tool developed in Section 4.1.1, we show that the problem with stochastic interference temperature constraints can also be solved exactly.

Specifically, let us consider the case where the instantaneous channels between all secondary transmitters and secondary receivers and those between all secondary transmitters and primary receivers $1, \ldots, M$ are perfectly known. The SINR at secondary receiver i is given by (4.2) and the interference temperature at primary receiver m is given by (4.7). The representative problem that we consider in this subsection can thus be formulated as follows:

$$\text{maximize} \quad \min_{i=1,\ldots,L} \mathsf{SINR}_i(\mathbf{p}) \tag{4.21a}$$

$$\text{subject to} \quad \Pr\left(\Psi_m(\mathbf{p}) \geq \bar{\Psi}_m\right) \leq \epsilon, \quad m = 1, \ldots, M, \tag{4.21b}$$

$$p_i \leq \bar{p}_i, \quad i = 1, \ldots, L, \tag{4.21c}$$

$$\text{variables :} \quad \mathbf{p}, \tag{4.21d}$$

where (4.21b) represents the stochastic interference temperature constraints with ϵ being a small given constant, and (4.21c) represents the individual power constraints. It is easy to verify that all the constraints mentioned above satisfy Assumption 2.

Moreover, to justify the use of Algorithm 4, it is necessary to verify that the utility functions satisfy Assumption 1 and the conditions in Theorem 4.4 (or those in Corollary 4.6). The former is straightforward

to show and, thus, we focus only on the latter.

Using the notations in (1.3) and (1.4), let us express the objective functions as

$$u_i(\mathbf{p}) = \mathsf{SINR}_i(\mathbf{p}) = \frac{p_i}{(\mathbf{F}\mathbf{p} + \mathbf{v})_i}, \tag{4.22}$$

for $i = 1, \ldots, L$. Notice that $\mathbf{T}(\mathbf{p}) = [T_1(\mathbf{p}), \ldots, T_L(\mathbf{p})]^\top = \mathbf{F}\mathbf{p} + \mathbf{v}$ is affine and, thus, is concave as we have shown earlier in Chapter 3. Moreover, since $\mathbf{F}$ is a nonnegative matrix and $\mathbf{v}$ has elements that are strictly positive, $\mathbf{T}$ is a positive mapping, i.e., $\mathbf{T}(\mathbf{p}) > \mathbf{0}$, for all $\mathbf{p} \geq \mathbf{0}$. Hence, the conditions in Corollary 4.6 are satisfied and, thus, the optimal solution can be obtained iteratively with guaranteed convergence using Algorithm 4. The value of $\beta(\mathbf{p}(t))$ in each iteration t is computed using the bisection search described in Algorithm 5.

Case Study II: Reliable Multiuser Downlink System with SINR Requirement Constraints

In this subsection, we consider a single cell multiuser downlink system, where the base station (the transmitter) is equipped with an antenna array and each user (the receiver) has a single receive antenna, transmitting simultaneously on a shared spectrum. Assume that L users operate over a common frequency-flat channel. Channel state information (CSI) is available at both the receiver and transmitter sides. Under this system setting, the antenna array forms a multiple-input-single-output (MISO) channel to obtain transmit diversity, which provides the extra degree of freedom. The accuracy and computational complexity of decoding depends on the mean-square error (MSE), thereby optimization of MSE is required for the reliable transmission [76, 71]. In addition, SINR requirements are imposed on all the users. Thus, we seek to minimize the maximum weighted MSE between the transmitted and estimated symbols subject to SINR constraints.

Let the vector $\mathbf{p} = [p_1, \ldots, p_L]^\top$ denote the transmit power vector. The SINR of the i-th user is given similarly as in (4.22) with the nonnegative matrix $\mathbf{F}$ and the vector $\mathbf{v}$ defined in (1.3) and (1.4) respectively. Suppose that the linear minimum mean-square error (LMMSE)

estimator is used to estimate the received symbol at each user. In this case, we can express the MSE of the i-th user as

$$\mathsf{MSE}_i(\mathbf{p}) = \frac{1}{1+\mathsf{SINR}_i(\mathbf{p})}. \tag{4.23}$$

The objective is to minimize the maximum weighted MSE, i.e., $\min_{\mathbf{p}} \max_{i=1,\ldots,L} w_i \mathsf{MSE}_i(\mathbf{p})$, where $\mathbf{w}$ is a positive vector with the entry w_i assigned to the i-th link to reflect some priority. A larger w_i denotes a higher priority. Notice that solving $\min_{\mathbf{p}} \max_{i=1,\ldots,L} w_i \mathsf{MSE}_i(\mathbf{p})$ is equivalent to solving $\max_{\mathbf{p}} \min_{i=1,\ldots,L} u_i(\mathbf{p})$, where

$$u_i(\mathbf{p}) = \frac{1+\mathsf{SINR}_i(\mathbf{p})}{w_i} = \frac{(\mathbf{F}\mathbf{p}+\mathbf{v})_i + p_i}{w_i(\mathbf{F}\mathbf{p}+\mathbf{v})_i}. \tag{4.24}$$

Hence, the problem can be formulated as

$$\begin{aligned} \text{maximize} \quad & \min_{i=1,\ldots,L} \; u_i(\mathbf{p}) && \text{(4.25a)} \\ \text{subject to} \quad & \mathsf{SINR}_i(\mathbf{p}) \geq \gamma_i, \quad i=1,\ldots,L && \text{(4.25b)} \\ \text{variables}: \quad & \mathbf{p}, && \text{(4.25c)} \end{aligned}$$

where γ_i is the SINR threshold of user i, i.e., the received SINR at user i must be higher than γ_i. Let $\boldsymbol{\gamma} = [\gamma_1, \ldots, \gamma_L]^\top$ be the SINR threshold vector. In this case, the SINR constraints can be shown to satisfy Assumption 2 by rewriting the constraints in the equivalent matrix form given by $(\mathbf{I} - \mathrm{diag}(\boldsymbol{\gamma})\mathbf{F})\mathbf{p} \geq \mathrm{diag}(\boldsymbol{\gamma})\mathbf{v}$. Notably, $g_i(\mathbf{p}) = (\mathrm{diag}(\boldsymbol{\gamma})\mathbf{F} - \mathbf{I})\mathbf{p}$ is affine, and thus, is concave. Therefore, Corollary 4.8 holds and Algorithm 6 can be adopted to compute $\beta(\mathbf{p})$.

To show that $\{u_i\}_{i=1}^L$ satisfies Assumption 1, we first observe that the function in (4.24) is positive and monotonically increases with respect to p_i. Furthermore, the first order derivative of $u_i(\mathbf{p})$ at p_j, for $j=i$, is given by $\partial u_i(\mathbf{p})/\partial p_j = -w_i^{-1} p_i F_{ij} (\mathbf{F}\mathbf{p}+\mathbf{v})^{-2} < 0$, and thus the competitiveness of (4.24) follows. For $\lambda > 1$, we have

$$u_i(\lambda\mathbf{p}) = \frac{1}{w_i}\left(1 + \frac{p_i}{(\mathbf{F}\mathbf{p} + \frac{1}{\lambda}\mathbf{v})_i}\right) < u_i(\mathbf{p}),$$

for all i, which implies the directional monotonicity.

Next, we verify that $\{u_i\}_{i=1}^L$ satisfies the conditions in Theorem 4.4 (or equivalently, Corollary 4.6). Let us define $\mathbf{T}(\mathbf{p}) =$

$[T_1(\mathbf{p}), \ldots, T_L(\mathbf{p})]^\top$, where

$$T_i(\mathbf{p}) = \frac{w_i p_i}{1 + \mathsf{SINR}_i(\mathbf{p})} = w_i(\mathbf{F}\mathbf{p} + \mathbf{v})_i \frac{\mathsf{SINR}_i(\mathbf{p})}{1 + \mathsf{SINR}_i(\mathbf{p})}. \tag{4.26}$$

It is easy to see that $\mathbf{T}$ is positive. Moreover, to show that $\mathbf{T}$ is concave in $\mathbf{p}$, let us invoke the following lemma from [18].

Lemma 4.9 ([18]). If $h : R^m \to R$ is concave, and $\mathbf{A} \quad R^{m\times n}$, $\mathbf{b} \quad R^m$, $\mathbf{c} \quad R^n$, and $d \quad R$, then

$$g(\mathbf{x}) = (\mathbf{c}^\top \mathbf{x} + d)h((\mathbf{A}\mathbf{x} + \mathbf{b})/(\mathbf{c}^\top \mathbf{x} + d)) \tag{4.27}$$

is concave on $\{\mathbf{x} | \mathbf{c}^\top \mathbf{x} + d > 0, (\mathbf{A}\mathbf{x} + \mathbf{b})/(\mathbf{c}^\top \mathbf{x} + d) \quad \mathbf{dom}(h)\}$, where $\mathbf{dom}(h)$ denotes the domain of function h.

Since $h(s) = \frac{s}{1+s}$ is concave and by letting $m = 1$, $\mathbf{A} = \mathbf{e}_i^\top$, $\mathbf{b} = 0$, $\mathbf{c}^\top$ be the i-th row of $\mathbf{F}$, $\mathbf{x} = \mathbf{p}$, $d = \eta_i/G_{ii}$ in Lemma 4.9, we have that T_i (and, thus, $\mathbf{T}$) is concave. Hence, it follows from Corollary 4.6 that the optimal solution to this problem can be obtained iteratively with guaranteed convergence using Algorithm 4.

Case Study III: Energy-Efficient Wireless Networks with Nonlinear Power Constraints

Most works in the literature on wireless communications make the idealized assumption that the transmit power is linear to the power consumption in the user devices. However, this is not the case in practice due to circuit nonlinearities. For example, under the Rapp model [65], the input and output power relations of a nonlinear power amplifier can be written as

$$p_i = \alpha p_{i,\text{in}} \left[1 + \left(\frac{\alpha p_{i,\text{in}}}{b_{\text{sat}}}\right)^q\right]^{-1/q}, \tag{4.28}$$

where p_i is the output power, $p_{i,\text{in}}$ is the input power, α is the linear gain of the power amplifier, and b_{sat} is the saturation power as $p_{i,\text{in}} \to \infty$. Such nonlinearities may have a significant impact on the system performance [44]. Moreover, the cost of emitting a certain amount of

power may also be nonlinear due to various factors such as incremental pricing on the energy usage or distortions in transceiver design [95].

Let us consider a wireless network with L transmit-receive pairs and we want to maximize (through adjustment of $\mathbf{p}$) the minimum throughput among the L transmission links subject to nonlinear constraints on power and cost. Using previous developments of the nonlinear Perron-Frobenius theory, a similar max-min throughput optimization problem was examined in [18] under linear power constraints. However, the tools developed in [18] are not sufficient to address the nonlinear power and cost constraints considered here.

Specifically, by assuming that the input-output power relations can be modeled by the strictly monotonic function h_i, i.e., $p_i = h_i(p_{i,\text{in}})$ (e.g., (4.28)), the power constraints at the transmitters can be generally expressed as

$$\mathbf{A}\tilde{\mathbf{h}}(\mathbf{p}) \leq \bar{\mathbf{p}}, \tag{4.29}$$

where $\tilde{\mathbf{h}}(\mathbf{p}) = [h_1^{-1}(p_1), \ldots, h_L^{-1}(p_L)]^T$ is the vector of the actual powers that are consumed, and $\bar{\mathbf{p}}$ is a $K \times 1$ positive vector of constraint values. Here, $\mathbf{A}$ is a $K \times L$ nonnegative weight matrix, where no column or row is identically zero. For example, we have $K = L$ and $\mathbf{A} = \mathbf{I}$ in the case of individual power constraints, and $K = 1$ and $\mathbf{A} = \mathbf{1}^T$ (i.e., an all-one row vector) in the case of sum power constraints.

Moreover, the power consumed by each user, say user i, may also be subject to a (nonlinear) strictly monotonic cost function $c_i : R_+ \to R_+$. The transmission may thus also be subject to a linear constraint on the cost, i.e.,

$$\mathbf{B}\mathbf{c}(\mathbf{p}) \leq \bar{\mathbf{c}}, \tag{4.30}$$

where $\mathbf{c}(\mathbf{p}) = [c_1(p_1), \ldots, c_L(p_L)]^T$, $\bar{\mathbf{c}}$ is an $S \times 1$ positive vector of constraint values, and $\mathbf{B}$ is an $S \times L$ nonnegative matrix with no row or column that is identically zero.

Let us consider the representative example where the goal is to maximize the minimum throughput among L users subject to the nonlinear power and cost constraints given above. By the Shannon capacity formula (e.g., see [24]), we model the throughput of user i as $u_i(\mathbf{p}) = \log(1 + \mathsf{SINR}_i(\mathbf{p}))$, where $\mathsf{SINR}_i(\mathbf{p})$ is defined as in (4.2). Simi-

lar to (4.22), we can also write u_i as

$$u_i(\mathbf{p}) = \log\left(1 + \frac{p_i}{(\mathbf{F}\mathbf{p} + \mathbf{v})_i}\right). \tag{4.31}$$

The problem can thus be formulated as

$$\begin{aligned} \text{maximize} \quad & \min_{i=1,\ldots,L} u_i(\mathbf{p}) && \text{(4.32a)} \\ \text{subject to} \quad & \mathbf{A}\tilde{\mathbf{h}}(\mathbf{p}) \leq \bar{\mathbf{p}} && \text{(4.32b)} \\ & \mathbf{B}\mathbf{c}(\mathbf{p}) \leq \bar{\mathbf{c}} && \text{(4.32c)} \\ \text{variables :} \quad & \mathbf{p}. && \text{(4.32d)} \end{aligned}$$

By properties of $\mathbf{A}$, $\mathbf{B}$, $\tilde{\mathbf{h}}$ and $\mathbf{c}$, strict monotonicity of the constraints is trivially satisfied; and, through appropriate choices of $\bar{\mathbf{p}}$ and $\bar{\mathbf{c}}$, feasibility and validity can be guaranteed as well. Therefore, Assumption 2 is satisfied. Furthermore, since $u_i(\mathbf{p})$ is a monotonic function of $\mathsf{SINR}_i(\mathbf{p})$, it inherits the competitiveness and directional monotonicity from $\mathsf{SINR}_i(\mathbf{p})$. Also, by definition of u_i, we have $u_i(\mathbf{p}) = 0$ when $p_i = 0$. Hence, Assumption 1 is satisfied as well.

Next, it is necessary to verify that $\{u_i\}_{i=1}^{L}$ satisfy the conditions in Theorem 4.4 or Corollary 4.6. Let us define

$$T_i(\mathbf{p}) = \frac{p_i}{\log(1 + \mathsf{SINR}_i(\mathbf{p}))}. \tag{4.33}$$

By taking the derivative of $T_i(\mathbf{p})$ with respect to p_j, we have

$$\frac{\partial T_i(\mathbf{p})}{\partial p_j} = \begin{cases} \frac{1}{(\log(x))^2}\left[\log(x) - (1 - \frac{1}{x})\right], & \text{for } i = j, \\ \frac{1}{(\log(x))^2}\frac{1}{x}(x-1)^2\frac{G_{ji}R_{ji}}{G_{ii}R_{ii}}, & \text{otherwise,} \end{cases} \tag{4.34}$$

where $x = 1 + \mathsf{SINR}_i(\mathbf{p}) > 1$ for all $p_i > 0$. We can see that $\partial T_i(\mathbf{p})/\partial p_j > 0$, for all $p_i > 0$, when $j = i$. To show that $\partial T_i(\mathbf{p})/\partial p_i > 0$, let us consider the function $J(x) \;,\; \log(x) - (1 - \frac{1}{x})$. Notice that $J(1) = 0$ and that, for $x > 1$, its first derivative is $J'(x) = \frac{1}{x^2}(x - 1) > 0$. This indicates that $J(x)$ is positive for all $x > 1$ and, thus, $\partial T_i(\mathbf{p})/\partial p_i > 0$ for $p_i > 0$. Therefore, all the entries of $\mathsf{O}T_i(\mathbf{p})$ are positive for $p_i > 0$ and, thus, $T_i(\mathbf{p})$ increases monotonically in $\mathbf{p}$. Since $\mathbf{T}(\mathbf{0}) = \mathbf{0}$, it follows that $\mathbf{T}$ is positive for $\mathbf{p} \geq \mathbf{0}$.

Similar to the proof of concavity in Section 4.2, by the fact that $h(s) = \frac{s}{\log(1+s)}$ is a concave function and by taking $m = 1$, $\mathbf{A} = \mathbf{e}_i^T$, $\mathbf{b} = 0$, $\mathbf{c}^T$ the i-th row of $\mathbf{F}$, $\mathbf{x} = \mathbf{p}$, $d = \eta_i/G_{ii}$ in Lemma 4.9, we know that T_i (and, thus, $\mathbf{T}$) is concave. Hence, it follows from Corollary 4.6 that power control for this problem can be performed iteratively with guaranteed convergence by Algorithm 4.

4.3 Numerical Examples

In this section, we provide numerical examples to demonstrate the effectiveness of Algorithm 4 for solving the max-min utility optimization problems described in Section 4.2. We refer the reader to [42] for more details on validating the convergence and more experiments.

4.3.1 Experiment I (Cognitive Radio Networks with Deterministic and Stochastic Interference Temperature Constraints)

Let us consider a cognitive radio network with $M = 2$ PRs and $L = 3$ ST-SR pairs. Following [25], the long-term path gain is given by $G_{ji} = d_{ji}^{-\nu} s_{ji}$, where d_{ji} and s_{ji} are the distance and the shadowing effect between ST j and SR i, respectively, and $\nu = 3.5$ is the path-loss exponent. s_{ji} is defined as $10^{X/10}$ with X being a Gaussian random variable with mean 0 and standard deviation 10 (in dB). Moreover, the short-term fading gain R_{ji} is assumed to be Nakagami-m with $m = 10$. Assume that the STs have instantaneous knowledge of their channels to PR 1, which are set as $[G_{11}^{\mathrm{PU}}, G_{21}^{\mathrm{PU}}, G_{31}^{\mathrm{PU}}]^T = [303^{-3.5} \cdot 0.02, 284^{-3.5} \cdot 143.45, 218^{-3.5} \cdot 3.04]^T$ and $[R_{11}^{\mathrm{PU}}, R_{21}^{\mathrm{PU}}, R_{31}^{\mathrm{PU}}]^T = [0.87, 1.14, 0.99]^T$, but the STs have only the distance information between themselves and PR 2, i.e., $[d_{11}^{\mathrm{PU}}, d_{21}^{\mathrm{PU}}, d_{31}^{\mathrm{PU}}]^T = [219, 209, 191]^T$, as well as the channel statistics. The instantaneous channels between STs and SRs are assumed to be known and are given by

$$\mathbf{G} = \begin{bmatrix} 71^{-3.5} \times 0.60 & 61^{-3.5} \times 0.74 & 253^{-3.5} \times 3.13 \\ 83^{-3.5} \times 44.98 & 65^{-3.5} \times 2.37 & 199^{-3.5} \times 0.22 \\ 222^{-3.5} \times 0.32 & 204^{-3.5} \times 0.39 & 84^{-3.5} \times 1.96 \end{bmatrix}$$

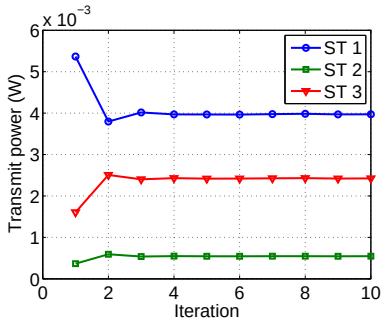

Figure 4.1: Evolution of the transmit powers at 3 STs.

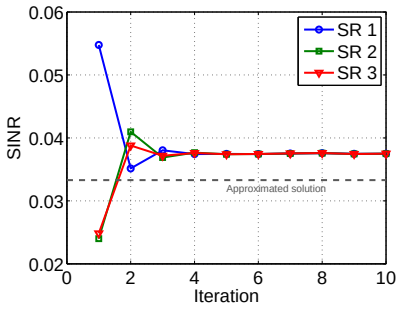

Figure 4.2: Evolution of the SINRs at 3 SRs.

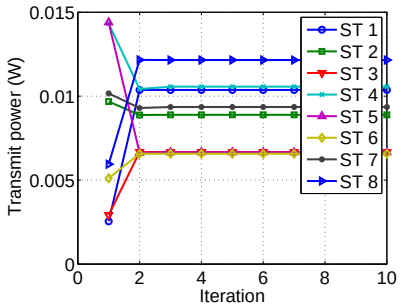

Figure 4.3: Evolution of the transmit powers at 8 out of the 100 STs.

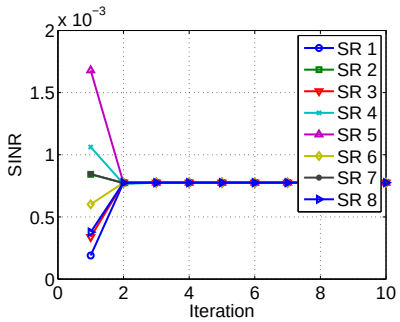

Figure 4.4: Evolution of the SINRs at 8 out of the 100 SRs.

and

$$\mathbf{R} = \begin{bmatrix} 1.13 & 1.25 & 1.18 \\ 1.15 & 0.90 & 1.11 \\ 0.99 & 0.97 & 0.93 \end{bmatrix}.$$

The interference thresholds for both PRs are set to -80 dBW (i.e., $t_1 = t_2 = 10^{-8}$), and the IT outage probability threshold for PR 2 is set to 0.01 (i.e., $\varepsilon_2 = 0.01$) [25]. The maximum transmit power for all STs is 5 W (i.e., $\bar{p}_1 = \bar{p}_2 = \bar{p}_3 = 5$).

In Fig. 4.1-4.4, we can see that both the ST transmit powers and the SINR at the SRs converge rapidly, with the latter reaching a common value for all SRs, within 5 iterations using Algorithm 4. The IT outage probability is evaluated in each iteration of the bisection search for $\beta(\mathbf{p})$ using sample average approximations (averaged over 10^7 realizations).

The terminating parameter in Algorithm 5 is set as $\epsilon = 5 \cdot 10^{-5}$. The "approximated solution" indicated in Fig. 4.2 represents the converged SINR value obtained with the approximate IT outage probability expression adopted in [25], which yields only a suboptimal solution. In Figs. 4.3 and 4.4, we consider the case with $M = 60$ PRs and $L = 100$ ST-SR pairs. The instantaneous channels to all PRs are assumed to be known in this case. Here, we show the evolution of the transmit powers of 8 out of the 100 STs and the SINR at their corresponding SRs, demonstrating the scalability of Algorithm 4.

4.3.2 Experiment II (Reliable Multiuser Downlink System with SINR Requirement Constraints)

Let us consider a single-cell multiuser downlink system with a single BS serving $L = 3$ users, i.e., users 1, 2 and 3. The downlink transmit powers are p_1, p_2 and p_3. In the channel gain matrix $\mathbf{G} = [G_{ij}]_{i,j=1}^{L} > \mathbf{0}_{L\times L}$, the diagonal entries G_{ii}, for all i, represents the effective channel gain from the transmitter to user i and G_{ji}, for $j = i$, represents the effective cross-channel interference coefficient between the signal intended for user j and the reception at user i (i.e., the inner product between the channel vector at user i and the beamforming vector used for user j's signal). We let

$$\mathbf{G} = \begin{bmatrix} 0.65 & 0.22 & 0.14 \\ 0.15 & 0.78 & 0.26 \\ 0.19 & 0.13 & 0.72 \end{bmatrix}, \tag{4.35}$$

and consider the weights $\mathbf{w} = [0.42\ 0.45\ 0.5]^{\top}$ for the weighted MSE objective. The noise power of each user is 1 W, and the SINR threshold vector is $\boldsymbol{\gamma} = [0.52\ 0.77\ 0.65]^{\top}$.

Figs. 4.5 and 4.6 plot the evolution of the base station transmit powers and the resulting weighted MSE at the 3 users using Algorithm 4. In this numerical example, $\beta(\mathbf{p}(t))$ is evaluated using Algorithm 6. We can observe from these figures that both the transmit powers and the weighted MSE values converge rapidly (within 9 iterations) to the optimal solution (verifying Theorem 4.4). Moreover, for a large network with $L = 100$ users, we show in Figs. 4.7 and 4.8 the evolution of the

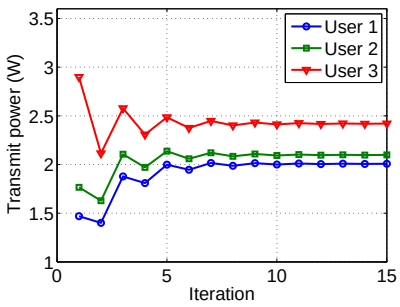

Figure 4.5: Evolution of the transmit powers intended for the 3 users.

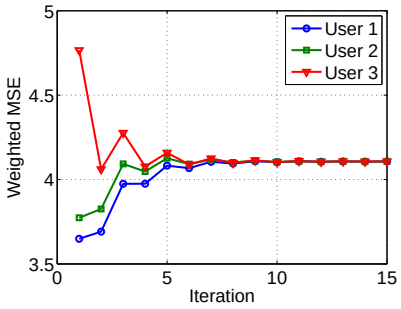

Figure 4.6: Evolution of the weighted MSE at 3 users.

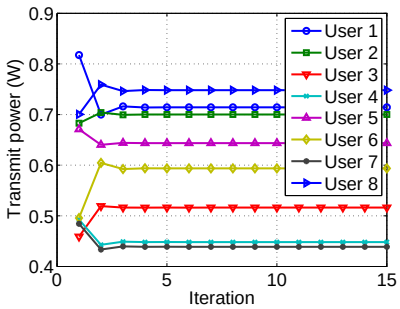

Figure 4.7: Evolution of the transmit powers intended for 8 out of the 100 users.

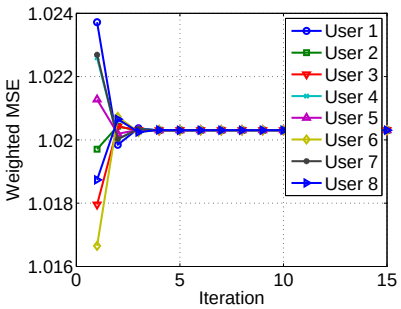

Figure 4.8: Evolution of the weighted MSE at 8 out of the 100 users.

base station transmit powers for 8 of the 100 users as well as their weighted MSE. These figures again demonstrate the scalability of Algorithm 4.

4.3.3 Experiment III (Energy-Efficient Wireless Networks with Nonlinear Power Constraints)

Let there be $L = 3$ transmit-receive pairs and consider the power amplifier (PA SM1720-50) whose input-output power relation fits into the Rapp model with parameters $b_{\text{sat}} = 10$ W, $\alpha = 316.2278$ and $q = 4$ [44]. Moreover, let us set the maximum input power as $\bar{p} = 0.01$ W, the noise variance as 1 pW, and the nonnegative weight matrix as

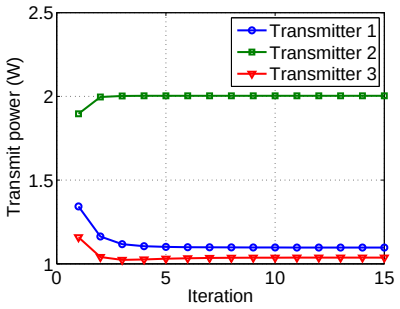

Figure 4.9: Evolution of the transmit powers in a wireless network with 3 transmit-receive pairs.

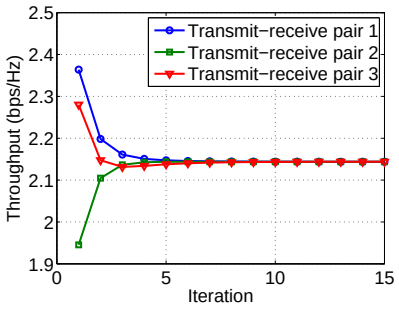

Figure 4.10: Evolution of the throughput of 3 transmit-receive pairs in a wireless network.

$$\mathbf{A} = \begin{bmatrix} 0.9134 & 0.2785 & 0.9649 \\ 0.6324 & 0.5469 & 0.1576 \\ 0.0975 & 0.9575 & 0.9706 \end{bmatrix}. \tag{4.36}$$

Let us consider the following nonlinear pricing: the cost is \$1/Wm when the power consumption is under 70 Watt-minute (Wm), \$5/Wm between 70 Wm and 110 Wm, and \$10/Wm when over 110 Wm. The transmit powers are updated every minute. The total cost of the three transmit-receive pairs should be less than \$500 per minute, i.e., $\mathbf{B} = \mathbf{1}^T$ and $\bar{c} = 500$. The following channel gain matrix $\mathbf{G}$ is used:

$$\mathbf{G} = \begin{bmatrix} 80^{-4} & 103^{-4} & 208^{-4} \\ 227^{-4} & 98^{-4} & 94^{-4} \\ 305^{-4} & 207^{-4} & 23^{-4} \end{bmatrix}. \tag{4.37}$$

In Figs. 4.9 and 4.10, we again show that both the transmit powers and the throughput converge rapidly (within 10 iterations) using Algorithm 4. The value of $\beta(\mathbf{p}(t)$ is again computed using Algorithm 5 with $\epsilon = 5 \cdot 10^{-5}$.

4.4 Open Issues

There are several issues worth exploring further. First, the Perron-Frobenius theory shows that the solution to the fixed-point problems

can be viewed as a meaningful equilibrium point that coincides with the optimal solution of the wireless max-min fairness optimization problem. This suggests that sensitivity analysis can be used to study the utility-cost tradeoff curves at the equilibrium. Next, it is an open issue to solve (4.1) for more general utility functions and constraints, i.e., beyond the competitive utility functions in Assumption 1 and the monotonic constraints in Assumption 2. One potential approach is to consider some form of convex relaxations or convex approximations to tackle the more general version of (4.1) using the mathematical tools studied in this chapter.

It is also interesting to study the Lagrange duality of (4.1), which can be useful for extensions involving MIMO transmit beamforming. This can lead to new characterizations of the *uplink-downlink duality* in wireless networks that can jointly optimize the beamformers and powers in a distributed manner [80]. Recent efforts in this direction include the cognitive radio network duality in [97] and the MISO-SIMO duality for sum-rate maximization in [99, 53]. These new forms of network duality can lead to further insights on global optimality. They can also significantly expand the scope of distributed algorithm design for problems involving MIMO beamforming, stochastic fading channel models, realistic nontrivial power and interference constraints etc. A potential approach is to consider a joint primal and dual algorithm design by applying the nonlinear Perron-Frobenius theory to the Lagrange primal and dual space of the wireless network optimization problems [86, 76, 16, 17, 100].

5

General Wireless Utility Maximization

In the previous chapters, we have studied specific wireless max-min utility optimization problems that are amenable to a direct analysis and characterization of its optimality by the nonlinear Perron-Frobenius theory. There are also other kinds of more general wireless utility optimization problems that are practically important in wireless networks. In this chapter, we consider the static transmission system model in Section 3.1 to model the achievable data rate of the lth user by

$$r_l = \log(1 + \mathsf{SINR}_l(\mathbf{p})) \quad \text{nats/symbol} \tag{5.1}$$

and study a general utility maximization problem with the total data rates as the key utility metric. In other words, we are interested to maximize the total throughput in the wireless network. In addition, a weight w_l is given to the lth user to indicate a priority status in comparison to other users. A user with a higher priority has a bigger weight. The objective function of the utility maximization problem is then a weighted sum of all the data rates (i.e., $\sum_l w_l r_l$). This sum rate maximization problem is notoriously hard to solve optimally in the wireless networking literature. We explain in this chapter how mathematical tools from the nonnegative matrix theory and the nonlinear Perron-Frobenius theory can be used to tackle this problem.

5.1 Sum Rate Maximization

Suppose that there are L users in the wireless network. The sum rate maximization problem is given by:

$$\begin{array}{ll} \text{maximize} & \displaystyle\sum_{l=1}^{L} w_l \log(1+\mathsf{SINR}_l(\mathbf{p})) \\ \text{subject to} & \mathbf{g}(\mathbf{p}) \ \mathsf{5} \ \bar{\mathbf{g}} \\ \text{variables:} & p_l \quad l, \end{array} \tag{5.2}$$

where $\mathsf{SINR}_l(\mathbf{p})$ is given in (1.5), and w_l is some given positive weight.

Let us denote the optimal solution of (5.2) by $\mathbf{p}^\star = (p_1^\star, \ldots, p_L^\star)^\top$. For any feasible $\mathbf{p}$ in (5.2), we call $\mathbf{r} = [r_1, \ldots, r_L]$, evaluated at $\mathbf{p}$, a feasible rate vector that lies in the achievable rate region, which is the set of all feasible rate vectors. Then, the data rate evaluated at $\mathbf{p}^\star$ is given by $r_l^\star = \log(1+\mathsf{SINR}_l(\mathbf{p}^\star))$. For the two user case, i.e., $L = 2$, Figure 5.1 gives the geometrical illustration of the weighted sum rate maximization problem in the rate region, i.e., finding $\mathbf{r}^\star$ for a given $\mathbf{w}$.

Now, (5.2) is in general hard to solve, and there are few nontrivial analytical characterizations of the optimality of (5.2) in the literature. In fact, the authors in [57] showed that, when there are individual power constraints (i.e., $\mathbf{g}(\mathbf{p}) \ \mathsf{5} \ \bar{\mathbf{g}}$ specializes as $\mathbf{p} \leq \bar{\mathbf{P}}$), (5.2) is NP-hard and there is a positive Lagrange duality gap in general. There have also been work that use the Lagrange dual decomposition to design algorithms for solving (5.2) (see, for example, [57]), but the Lagrange dual algorithms cannot guarantee global optimality in general.

Despite the known NP-hardness characterization, it is interesting to ask the following questions:

- Can we identify special cases of (5.2), if any, that can be solved optimally and efficiently in polynomial time? If yes, can they even be characterized analytically and a polynomial-time algorithm be given?
- Are there efficient convex relaxation to (5.2)?

Answering the above two questions is nontrivial in general for any nonconvex problem from a standard optimization-theoretic viewpoint.

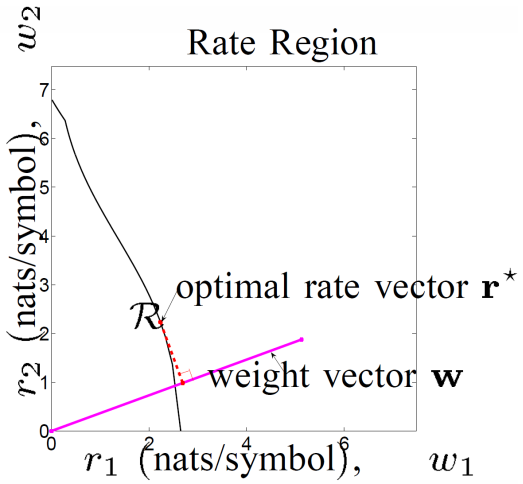

Figure 5.1: An illustration of sum rate maximization in an achievable rate region R for a 2-user Gaussian interference channel. The positive weight vector $\mathbf{w}$ is superimposed on the rate region. Given this $\mathbf{w}$, the optimal rate vector $\mathbf{r}^\star = [r_1^\star, r_2^\star]$ is chosen on the boundary of the achievable rate region, where a perpendicular line from $\mathbf{w}$ (shown as the red dotted line) intersects with the rate region.

In this chapter, we describe how the Perron-Frobenius theory can be useful to overcome this nonconvexity hurdle in (5.2) by providing partial answers to the above two questions.

We briefly summarize the related work development before going into the details of this Perron-Frobenius theory approach. In [76], the authors studied (5.2) for the single total power constraint (applicable to a cellular downlink system), and identified polynomial-time solvable special cases (such as under low interference scenarios, i.e., when the cross-channel gains in (1.5) are sufficiently small). By using the Friedland-Karlin inequalities in Chapter 2, [76] showed that Algorithm 3 can solve (5.2) (optimally under special cases when $\mathbf{w}$ takes certain form). In [77], the authors studied (5.2) for the individual power constraints (applicable to a cellular uplink system), and provided polynomial-time algorithms (including Algorithm 3) with performance bounds on the suboptimality as compared to the global optimal value.

These works present an interesting relationship between the max-min fairness problems (e.g., (3.1) studied in Chapter 3 and are readily solved optimally) and the seemingly unrelated general utility maximization problems (such as (5.2)) that are harder to solve.

In [79, 78], by using reformulation and the Friedland-Karlin inequalities in Chapter 2, the authors proposed global optimization algorithms to solve (5.2) for the individual power constraints. In [99], the authors studied (5.2) for general affine power and interference temperature constraints (applicable to cognitive radio networks [40, 96, 70]), and leverages nonnegative matrix theory to first obtain a convex relaxation of (5.2) by solving a convex optimization problem over a closed bounded convex set. It also enables the sum-rate optimality to be quantified analytically through the spectrum of specially-crafted nonnegative matrices. Furthermore, polynomial-time verifiable sufficient conditions have been obtained that can identify polynomial-time solvable problem instances. In the general case, the authors in [99] propose a global optimization algorithm by utilizing this convex relaxation and branch-and-bound to compute an ϵ-optimal solution. Extensions to tackle the joint MIMO beamforming and power control of the sum rate maximization problem can be found in [53].

In the following, we describe in details the general idea of using the nonlinear Perron-Frobenius theory and the quasi-invertibility in nonnegative matrix theory (cf. Definition 2.1) to solve (5.2) when there are affine power constraints. In particular, we consider two different sets of power constraints. The first one is a general weighted power constraint to model resource budget. The second one is a constraint on the *interference temperature*:

$$\mathbf{q} = \mathbf{F}\mathbf{p} + \mathbf{v},$$

where we have introduced a new variable $\mathbf{q}$ to capture the interference. In essence, this is still a particular form of power constraints, but its expression in terms of $\mathbf{q}$ can explicitly model interference management requirements such as preventing the interference of some users (e.g., secondary users) from overwhelming the other users (e.g., primary users) in a wireless cognitive radio network.

These weighted power constraint set P and the weighted interfer-

ence temperature constraint set Q are respectively given by:

$$P = \{\mathbf{p} \,|\, \mathbf{a}_k^\top \mathbf{p} \le \bar{p}_k,\ k = 1, \ldots, K\}, \tag{5.3}$$

and

$$Q = \{\mathbf{q} \,|\, \mathbf{b}_m^\top \mathbf{q} \le \bar{q}_m,\ m = 1, \ldots, M\}, \tag{5.4}$$

where $\bar{\mathbf{p}} \quad R^K$ and $\mathbf{a}_k \quad R^L$ $k = 1, \ldots, K$ are respectively the upper bound and positive weight vectors for the weighted power constraints, and $\bar{\mathbf{q}} \quad R^M$ and $\mathbf{b}_m \quad R^L$ $m = 1, \ldots, M$ are respectively the upper bound and positive weight vectors for the weighted interference temperature constraints. Note that we must have $\bar{q}_m \ge \mathbf{b}_m^\top \mathbf{v}$ for a nonempty constraint set. As special cases, when $\mathbf{a}_k = \mathbf{e}_k$, we have the individual power constraints $p_k \le \bar{p}_k$ for all k, and when $\mathbf{a}_k = \mathbf{1}$ and $K = 1$, we have a single total power constraint. Thus, the vectors $\mathbf{a}_k$ and $\mathbf{b}_m$ are general enough to model the power constraints and interference temperature constraints in many wireless network optimization problems.

By considering the above affine constraints, the weighted sum rate maximization problem can be written as:

$$\begin{array}{rl} \text{maximize} & \displaystyle\sum_{l=1}^{L} w_l \log\left(1 + \mathsf{SINR}_l(\mathbf{p})\right) \\ \text{subject to} & \mathbf{p} \quad P, \\ & \mathbf{q} \quad Q, \\ \text{variable:} & \mathbf{p}, \mathbf{q}, \end{array} \tag{5.5}$$

where $\mathbf{w} = [w_1, \ldots, w_L]^\top > \mathbf{0}$ is a given probability vector, i.e. $\mathbf{1}^\top \mathbf{w} = 1$, and w_l is a weight assigned to the lth link to reflect priority (a larger weight reflects a higher priority). We denote the optimal solution of (5.5) by $\mathbf{p}^\star = (p_1^\star, \ldots, p_L^\star)^\top$ and $\mathbf{q}^\star = (q_1^\star, \ldots, q_L^\star)^\top$. In general, (5.5) is nonconvex (due to the nonconvex objective function) and thus is generally hard to solve.

We next study a reparameterization of (5.5) from the power $\mathbf{p}$ and $\mathbf{q}$ to an equivalent optimization problem that only has the achievable rate $\mathbf{r}$ and $\mathbf{q}$ as the explicit optimization variables. The advantage of the reformulation is an efficient technique to bound the nonconvex pareto rate region using convex relaxation. The convex relaxation is then used to develop algorithms to solve (5.5). In addition, the reformulation is

particularly suitable for cognitive radio network optimization as both the interference temperature and achievable rate are jointly optimized.

Let us first define the following set of nonnegative matrices:

$$\mathbf{B}_k = \mathbf{F} + \frac{1}{\bar{p}_k}\mathbf{v}\mathbf{a}_k^\top, \quad k = 1, \ldots, K, \tag{5.6}$$

$$\mathbf{D}_m = \left(\mathbf{I} + \frac{1}{\bar{q}_m - \mathbf{b}_m^\top \mathbf{v}}\mathbf{v}\mathbf{b}_m^\top\right)\mathbf{F}, \quad m = 1, \ldots, M. \tag{5.7}$$

Note that $\mathbf{B}_k$ and $\mathbf{D}_m$ contain the problem parameters associated with the kth power budget constraint in P and the mth interference temperature constraint in Q respectively. We now introduce a reformulation of (5.5) in the following.

Theorem 5.1. The optimal value in (5.5) is equal to the optimal value of the following problem:

$$\begin{array}{ll} \text{maximize} & \displaystyle\sum_{l=1}^{L} w_l r_l \\ \text{subject to} & \mathbf{B}_k \mathrm{diag}(e^{\mathbf{r}})\mathbf{q} \leq (\mathbf{I} + \mathbf{B}_k)\mathbf{q}, \quad k = 1, \ldots, K, \\ & \mathbf{D}_m \mathrm{diag}(e^{\mathbf{r}})\mathbf{q} \leq (\mathbf{I} + \mathbf{D}_m)\mathbf{q}, \quad m = 1, \ldots, M, \\ \text{variables:} & \mathbf{r}, \mathbf{q}. \end{array} \tag{5.8}$$

Denote the optimal $\mathbf{r}$ and $\mathbf{q}$ in (5.8) by $\mathbf{r}^\star$ and $\mathbf{q}^\star$ respectively. We also have $\mathbf{p}^\star$ in (5.5) given by $\mathbf{p}^\star = \mathrm{diag}(e^{\mathbf{r}^\star} - \mathbf{1})\mathbf{q}^\star$.

Though (5.8) has a linear objective function, (5.8) is still nonconvex due to the nonconvex constraint set. However, the transformation from (5.5) to (5.8) plays an instrumental role that facilitates the use of the quasi-invertibility (cf. Definition 2.1) for convex relaxation and algorithm design. In Section 5.2, we examine a polynomial-time algorithm proposed in [99] to solve (5.8) when the convex relaxation is exact. We refer the reader to [99], where a global optimization algorithm that uses both this convex relaxation and a branch-and-bound method to compute an ϵ-optimal solution for (5.5).

5.2 Convex Relaxation and Polynomial-time Algorithms

In this section, we first show that the constraints in (5.8) can in fact be equivalently rewritten as convex Perron-Frobenius eigenvalue con-

straints for those special cases in Section 5.2.1 that can be solved in polynomial time. Then, for the general case, we examine a convex relaxation of (5.8) proposed in [99] in Section 5.2.2, equivalently that of (5.5). All the analytical approach and algorithm design are based on exploiting the problem structure of (5.8).

5.2.1 Polynomial-time Solvable Special Cases

The reformulation introduced in Theorem 5.1 allows us to decompose the weighted sum rate maximization problem in (5.5) into first optimizing $\mathbf{r}$ and $\mathbf{q}$ and then projecting the solution (through a one-to-one mapping) back to $\mathbf{p}$. Although (5.8) is nonconvex, the Perron-Frobenius theorem (Theorem 2.1) enables us to rewrite (5.8) into one that has the rates characterized by a set of Perron-Frobenius eigenvalue constraints (i.e., $\mathbf{r}$ is the only variable) when the following assumption is satisfied. Essentially, this assumption is based on the quasi-invertibility of nonnegative matrices (cf. Definition 2.1) crafted in terms of the given problem parameters.

Assumption 3. Let $\mathbf{B}_k$ and $\mathbf{D}_m$ be given in (5.6) and (5.7) respectively. The following is satisfied:

$$\widetilde{\mathbf{B}}_k = (\mathbf{I} + \mathbf{B}_k)^{-1}\mathbf{B}_k \succeq \mathbf{0}, \quad k = 1, \ldots, K, \tag{5.9}$$

$$\widetilde{\mathbf{D}}_m = (\mathbf{I} + \mathbf{D}_m)^{-1}\mathbf{D}_m \succeq \mathbf{0}, \quad m = 1, \ldots, M, \tag{5.10}$$

i.e., $\widetilde{\mathbf{B}}_k$ and $\widetilde{\mathbf{D}}_m$ are irreducible nonnegative matrices for all k and m.

When there is no interference, i.e., $G_{lj} = 0,\ l = j$ and $\mathbf{F}$ in (1.3) is an all-zero matrix, we have $\mathbf{B}_k = \frac{1}{\bar{p}_k}\mathbf{v}\mathbf{a}_k^\top$, which implies that $\widetilde{\mathbf{B}}_k = \frac{1}{\bar{p}_k + \mathbf{a}_k^\top \mathbf{v}}\mathbf{v}\mathbf{a}_k^\top$ for all k. Thus, Assumption 3 can be satisfied under certain SNR and interference conditions.

Corollary 5.2. If Assumption 3 is satisfied, then (5.5) can be solved by

the following convex optimization problem:

$$\begin{array}{ll} \text{maximize} & \displaystyle\sum_{l=1}^{L} w_l r_l \\ \text{subject to} & \log\rho(\widetilde{\mathbf{B}}_k \operatorname{diag}(e^{\mathbf{r}})) \le 0, \quad k=1,\ldots,K, \\ & \log\rho(\widetilde{\mathbf{D}}_m \operatorname{diag}(e^{\mathbf{r}})) \le 0, \quad m=1,\ldots,M, \\ \text{variables:} & \mathbf{r}, \end{array} \tag{5.11}$$

where $\widetilde{\mathbf{B}}_k$ and $\widetilde{\mathbf{D}}_m$ are given in (5.9) and (5.10) respectively.

Due to the log-convexity property of the Perron-Frobenius eigenvalue [15], $\log\rho(\widetilde{\mathbf{B}}_l \operatorname{diag}(e^{\mathbf{r}}))$ and $\log\rho(\widetilde{\mathbf{D}}_m \operatorname{diag}(e^{\mathbf{r}}))$ are convex functions in $\mathbf{r}$ for the irreducible nonnegative matrices $\widetilde{\mathbf{B}}_k$ and $\widetilde{\mathbf{D}}_m$ respectively. Hence, (5.11) is a convex optimization problem (implying that (5.5) can be solved in polynomial time). In the appendix, we have presented the details on how such an convex optimization problem with a linear objective function and Perron-Frobenius eigenvalue constraint set can be numerically solved.

In fact, we can obtain a closed form solution to (5.5) whenever Assumption 3 holds.

Lemma 5.3. If Assumption 3 is satisfied, then we have

$$\rho(\widetilde{\mathbf{B}}_i \operatorname{diag}(e^{\mathbf{r}^\star})) = 1, \;\; \mathbf{p}^\star = \operatorname{diag}(e^{\mathbf{r}^\star} - \mathbf{1})\mathbf{x}(\widetilde{\mathbf{B}}_i \operatorname{diag}(e^{\mathbf{r}^\star})),$$
$$\text{and } \mathbf{q}^\star = \mathbf{x}(\widetilde{\mathbf{B}}_i \operatorname{diag}(e^{\mathbf{r}^\star})),$$

$$\text{where} \quad i = \arg\max_{k=1,\ldots,K} \rho(\widetilde{\mathbf{B}}_k \operatorname{diag}(e^{\mathbf{r}^\star})), \tag{5.12}$$

or

$$\rho(\widetilde{\mathbf{D}}_\iota \operatorname{diag}(e^{\mathbf{r}^\star})) = 1, \;\; \mathbf{p}^\star = \operatorname{diag}(e^{\mathbf{r}^\star} - \mathbf{1})\mathbf{x}(\widetilde{\mathbf{D}}_\iota \operatorname{diag}(e^{\mathbf{r}^\star})),$$
$$\text{and } \mathbf{q}^\star = \mathbf{x}(\widetilde{\mathbf{D}}_\iota \operatorname{diag}(e^{\mathbf{r}^\star})),$$

$$\text{where} \quad \iota = \arg\max_{m=1,\ldots,M} \rho(\widetilde{\mathbf{D}}_m \operatorname{diag}(e^{\mathbf{r}^\star})). \tag{5.13}$$

Next, we study the weighted max-min rate fairness problem whose solution is to provision rate fairness. How to adapt the weights in the

weighted max-min rate fairness problem (cf. Case Study 3 of Chapter 4 that is solvable in polynomial-time) to solve the sum rate maximization (a nonconvex problem in general)? This interesting and important connection between these two problems will be made precise in the following. Next, instead of solving (5.11) directly, let us consider the following weighted max-min rate problem with the same constraint set in (5.11):

$$\begin{array}{ll} \text{maximize} & \min\limits_{l=1,\ldots,L} \dfrac{r_l}{\beta_l} \\ \text{subject to} & \log \rho(\widetilde{\mathbf{B}}_k \operatorname{diag}(e^{\mathbf{r}})) \leq 0, \quad k = 1, \ldots, K, \\ & \log \rho(\widetilde{\mathbf{D}}_m \operatorname{diag}(e^{\mathbf{r}})) \leq 0, \quad m = 1, \ldots, M. \\ \text{variables:} & \mathbf{r}, \end{array} \tag{5.14}$$

where $\boldsymbol{\beta} \quad \mathbf{R}_+^L$ are weights assigned to reflect priority among users. This means that a user requiring a higher quality-of-service has a larger weight, i.e., β_l is larger. In the following, we apply nonnegative matrix theory, particularly the Perron-Frobenius theorem (Theorem 2.1), to characterize the optimal solution and the optimal value of (5.14).

Lemma 5.4. The optimal solution of (5.14) denoted by $\mathbf{r}^\star$ is a vector with $r_l^\star/\beta_l$ equal to a common value $\delta^\star$, i.e., $\mathbf{r}^\star = \delta^\star \boldsymbol{\beta}$, where $\delta^\star$ is the optimal value of (5.14).

Remark 5.1. We remark that this weighted max-min rate problem in (5.14) can be solved by different approaches. One approach has been illustrated in Case Study 3 of Chapter 4. Another approach that uses a generalized version of the Perron-Frobenius theorem for matrix pencil, i.e., Lemma 2.6 in Chapter 2, can be found in [98].

We now explain how solving (5.14) can lead to a polynomial-time algorithm to compute the optimal solution of (5.11) that requires solving (5.14) as an intermediate step. In particular, with $\boldsymbol{\beta}$ appropriately chosen in (5.14), both (5.11) and (5.14) can have the same optimal solution.

Lemma 5.5. Both (5.11) and (5.14) have the same optimal solution with $\boldsymbol{\beta} = (\boldsymbol{\xi}^\star - (\log \varrho^\star)\mathbf{1})/(\mathbf{1}^\top \boldsymbol{\xi}^\star - L \log \varrho^\star)$, where $\boldsymbol{\xi}^\star$ and $\log \varrho^\star$ are

respectively the optimal solution and the optimal value of the following optimization problem:

$$\begin{aligned} \text{minimize} \quad & \max\Big\{ \max_{k=1,\ldots,K} \Big\{\rho(\widetilde{\mathbf{B}}_k \operatorname{diag}(e^{\boldsymbol{\xi}}))\Big\}, \\ & \qquad \max_{m=1,\ldots,M} \Big\{\rho(\widetilde{\mathbf{D}}_m \operatorname{diag}(e^{\boldsymbol{\xi}}))\Big\}\Big\} \\ \text{subject to} \quad & \sum_{l=1}^{L} w_l \xi_l \geq 1, \\ \text{variables:} \quad & \boldsymbol{\xi}. \end{aligned} \tag{5.15}$$

Remark 5.2. Using Lemma 5.5, an important special case will now be explained. Solving (5.14) with $\boldsymbol{\beta} = \mathbf{1}$ is equivalent to solving (5.11) with $\mathbf{w}$ given by $\mathbf{w} = \mathbf{x}(\boldsymbol{\Omega}) \circ \mathbf{y}(\boldsymbol{\Omega})$, where $\boldsymbol{\Omega} = \arg_{\boldsymbol{\Omega}\in\{\widetilde{\mathbf{B}}_k,\widetilde{\mathbf{D}}_m\}} \max\big\{ \max_{k=1,\ldots,K}\{\rho(\widetilde{\mathbf{B}}_k)\}, \max_{m=1,\ldots,M}\{\rho(\widetilde{\mathbf{D}}_m)\}\big\}$. This interesting connection between (5.11) (a generally hard problem) and (5.14) (a polynomial-time solvable problem) is obtained using the Friedland-Karlin inequality (Theorem 2.3 in Chapter 2). In addition, this connection will be used in the convergence proofs of Algorithm 7 given below.

Suppose Assumption 3 holds, then the following two-time scale algorithm computes the optimal solution $\mathbf{r}^\star$ of (5.8): the outer loop iterates to solve (5.15) and to update the weight $\boldsymbol{\beta}(t)$ used in (5.14), which is solved by the inner loop.

Algorithm 7 Polynomial-time Algorithm

Initialize $\boldsymbol{\xi}(0)$.

1: Update $\boldsymbol{\xi}(t+1)$ as follows:

if $\rho(\widetilde{\mathbf{B}}_{i_t} \operatorname{diag}(e^{\boldsymbol{\xi}(t)})) \geq \rho(\widetilde{\mathbf{D}}_{\iota_{t+1}} \operatorname{diag}(e^{\boldsymbol{\xi}(t)}))$

$$\xi_l(t+1) = \max\Big\{\xi_l(t) + w_l - \Big(\mathbf{x}(\widetilde{\mathbf{B}}_{i_t} \operatorname{diag}(e^{\boldsymbol{\xi}(t)})) \circ \mathbf{y}(\widetilde{\mathbf{B}}_{i_t} \operatorname{diag}(e^{\boldsymbol{\xi}(t)}))\Big)_l, 0\Big\},$$

else

$$\xi_l(t+1) = \max\Big\{\xi_l(t) + w_l - \Big(\mathbf{x}(\widetilde{\mathbf{D}}_{\iota_t} \operatorname{diag}(e^{\boldsymbol{\xi}(t)})) \circ \mathbf{y}(\widetilde{\mathbf{D}}_{\iota_t} \operatorname{diag}(e^{\boldsymbol{\xi}(t)}))\Big)_l, 0\Big\}.$$

Algorithm 7 Polynomial-time Algorithm (Cont)

2: Normalize $\boldsymbol{\xi}(t+1)$:
Compute $i_{t+1} = \arg\max_{k=1,\ldots,K} \rho(\widetilde{\mathbf{B}}_k \operatorname{diag}(e^{\boldsymbol{\xi}(t+1)}))$ and $\iota_{t+1} = \arg\max_{m=1,\ldots,M} \rho(\widetilde{\mathbf{D}}_m \operatorname{diag}(e^{\boldsymbol{\xi}(t+1)}))$.

if $\rho(\widetilde{\mathbf{B}}_{i_{t+1}} \operatorname{diag}(e^{\boldsymbol{\xi}(t+1)})) \geq \rho(\widetilde{\mathbf{D}}_{\iota_{t+1}} \operatorname{diag}(e^{\boldsymbol{\xi}(t+1)}))$

$\boldsymbol{\xi}(t+1) \leftarrow \log\Big(e^{\boldsymbol{\xi}(t+1)} / \rho(\widetilde{\mathbf{B}}_{i_{t+1}} \operatorname{diag}(e^{\boldsymbol{\xi}(t+1)}))\Big)$,

else

$\boldsymbol{\xi}(t+1) \leftarrow \log\Big(e^{\boldsymbol{\xi}(t+1)} / \rho(\widetilde{\mathbf{D}}_{\iota_{t+1}} \operatorname{diag}(e^{\boldsymbol{\xi}(t+1)}))\Big)$.

3: Update $\boldsymbol{\beta}(t+1)$ as follows:

$$\varrho(k+1) = \max\{\rho(\widetilde{\mathbf{B}}_{i_{t+1}} \operatorname{diag}(e^{\boldsymbol{\xi}(t+1)})), \rho(\widetilde{\mathbf{D}}_{\iota_{t+1}} \operatorname{diag}(e^{\boldsymbol{\xi}(t+1)}))\},$$

$$\boldsymbol{\beta}(k+1) = \Big(\boldsymbol{\xi}(t+1) - \big(\log \varrho(t+1)\big)\mathbf{1}\Big) \Big/ \Big(\mathbf{1}^\top \boldsymbol{\xi}(k+1) - L \log \varrho(t+1)\Big).$$

4: Compute $\mathbf{p}(t+1)$ and $\mathbf{q}(t+1)$ by solving (5.14) with the weight replaced by $\boldsymbol{\beta}(t+1)$:

while $\mathbf{p}(\tau) - \mathbf{p}(\tau-1) \geq \epsilon$

$$p_l(\tau+1) = \Big(\frac{\beta_l(t+1)}{\log(1+\mathsf{SINR}_l(\mathbf{p}(\tau)))}\Big) p_l(\tau),$$

$$\mathbf{p}(\tau+1) \leftarrow \frac{\mathbf{p}(\tau+1)}{\max\Big\{\max_{k=1,\ldots,K}\{\frac{\mathbf{a}_k^\top \mathbf{p}(\tau+1)}{\bar{p}_k}\}, \max_{m=1,\ldots,M}\{\frac{\mathbf{b}_m^\top \mathbf{F}\mathbf{p}(\tau+1)}{(\bar{q}_m - \mathbf{b}_m^\top \mathbf{v})}\}\Big\}},$$

$$r_l(\tau+1) = \log(1+\mathsf{SINR}_l(\mathbf{p}(\tau+1))),$$

$$q_l(\tau+1) = p_l(\tau+1)/(e^{r_l} - 1).$$

$\mathbf{p}(t+1) = \mathbf{p}(\tau)$, $\mathbf{q}(t+1) = \mathbf{q}(\tau)$, and $\mathbf{r}(t+1) = \mathbf{r}(\tau)$.

when $\mathbf{p}(\tau)$ converges in the inner loop, and go to Step 1.

Lemma 5.6. Suppose Assumption 3 holds, starting from any initial point $\boldsymbol{\xi}(0)$, $\boldsymbol{\xi}(t)$ converges to the optimal solution of (5.15) and $\boldsymbol{\beta}(t)$ calculated in terms of $\boldsymbol{\xi}(t)$ is of the same scaling of the optimal solution $\mathbf{r}^\star$ of (5.11). In addition, $\mathbf{r}(t)$ converges to the optimal solution of (5.11) with $\mathbf{p}(t)$ and $\mathbf{q}(t)$ being the corresponding optimal power and interference temperature.

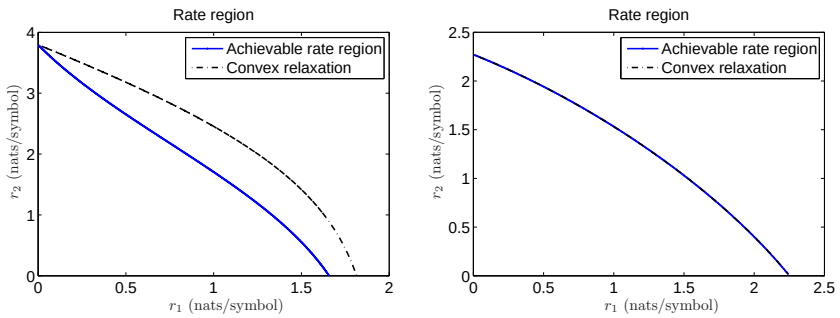

Figure 5.2: Achievable rate region and relaxed rate region for a 2-user case. The channel gains are given by $G_{11} = 0.85$, $G_{12} = 0.13$, $G_{21} = 0.14$ and $G_{22} = 0.87$. The noise power for both users are 0.1W. The other parameters are: (a) $\bar{\mathbf{p}} = (5, 5)^\top$, $\mathbf{a}_1 = (10, 1)^\top$, $\mathbf{a}_2 = (1, 1)^\top$; (b) $\bar{\mathbf{p}} = (1, 100)^\top$, $\mathbf{a}_1 = (1, 1)^\top$, $\mathbf{a}_2 = (1, 1)^\top$.

5.2.2 Convex Relaxation

In this section, we study a convex relaxation proposed in [99] to yield useful upper bounds to (5.5). This convex relaxation in [99] exploits the quasi-invertibility introduced in Section 5.2.1. Whenever the quasi-inverse condition holds, the convex relaxation is in fact tight, otherwise the convex relaxation provides a useful bound to the global optimal value. In particular, we exploit the spectrum of specially-constructed nonnegative matrices ($\widehat{\mathbf{B}}_k$ and $\widehat{\mathbf{D}}_m$ introduced below) that are obtained from $\mathbf{B}_k$ and $\mathbf{D}_m$, thereby leveraging the techniques in Section 5.2.1.

First, for notation purpose, let us introduce the Frobenius norm denoted by $\|\mathbf{A}\|_F$, which is defined as the square root of the sum of the absolute squares of the elements of a matrix $\mathbf{A}$. Thus, the Frobenius norm is a matrix norm that is convex in $\mathbf{A}$ [15].

Now, let us consider the following set of nonnegative matrices (without making Assumption 3):

$$\widehat{\mathbf{B}}_k = \left(\mathbf{I} + \mathbf{B}_k + \mathrm{diag}(\boldsymbol{\varepsilon})\right)^{-1}(\mathbf{B}_k - \widetilde{\mathbf{X}}_k^{\star}), \quad k = 1, \ldots, K, \tag{5.16}$$

where $\widetilde{\mathbf{X}}_k^{\star}$ is obtained by solving

$$\begin{array}{ll} \text{minimize} & \widetilde{\mathbf{X}}_k \ _F \\ \text{subject to} & \left(\mathbf{I} + \mathbf{B}_k + \mathrm{diag}(\boldsymbol{\varepsilon})\right)^{-1}(\mathbf{B}_k - \widetilde{\mathbf{X}}_k) \succeq 0, \\ & \widetilde{\mathbf{X}}_k \succeq 0, \\ \text{variables:} & \widetilde{\mathbf{X}}_k, \end{array} \tag{5.17}$$

and

$$\widehat{\mathbf{D}}_m = \left(\mathbf{I} + \mathbf{D}_m + \mathrm{diag}(\boldsymbol{\varepsilon})\right)^{-1}(\mathbf{D}_m - \widetilde{\mathbf{Y}}_m^{\star}), \quad m = 1, \ldots, M, \tag{5.18}$$

where $\widetilde{\mathbf{Y}}_m^{\star}$ is obtained by solving

$$\begin{array}{ll} \text{minimize} & \widetilde{\mathbf{Y}}_m \ _F \\ \text{subject to} & \left(\mathbf{I} + \mathbf{D}_m + \mathrm{diag}(\boldsymbol{\varepsilon})\right)^{-1}(\mathbf{D}_m - \widetilde{\mathbf{Y}}_m) \succeq 0, \\ & \widetilde{\mathbf{Y}}_m \succeq 0, \\ \text{variables:} & \widetilde{\mathbf{Y}}_m. \end{array} \tag{5.19}$$

Note that $\boldsymbol{\varepsilon}$ is a vector with each entry being a given small positive scalar (which is required in case $(\mathbf{I}+\mathbf{B}_k)$ or $(\mathbf{I}+\mathbf{D}_m)$ is not invertible); otherwise, $\boldsymbol{\varepsilon}$ can be an all-zero vector. Notably, (5.17) and (5.19) are convex optimization problems that can be solved numerically using the interior-point method. An example of such a numerical interior-point method solver is the `cvx` software package [38]. Furthermore, $\widetilde{\mathbf{X}}_k^{\star}$ or $\widetilde{\mathbf{Y}}_m^{\star}$ are all-zero matrices whenever $\widetilde{\mathbf{B}}_k$ or $\widetilde{\mathbf{D}}_m$ are nonnegative, i.e., the quasi-inverse of $\widetilde{\mathbf{B}}_k$ or $\widetilde{\mathbf{D}}_m$ exists ($\widehat{\mathbf{B}}_k = \widetilde{\mathbf{B}}_k$ and $\widehat{\mathbf{D}}_m = \widetilde{\mathbf{D}}_m$); otherwise $\widetilde{\mathbf{X}}_k^{\star}$ and $\widetilde{\mathbf{Y}}_m^{\star}$ are relatively small matrices (as compared to $\widetilde{\mathbf{B}}_k$ and $\widetilde{\mathbf{D}}_m$) with most of their entries being zeros.

After solving the convex relaxation in (5.17) and (5.19), the next step is to replace $\mathbf{B}_k$ and $\mathbf{D}_m$ on the righthand-side of the constraints in (5.8) such that we have, respectively, $(\mathbf{B}_k - \widetilde{\mathbf{X}}_k^{\star})\,\mathrm{diag}(e^{\mathbf{r}})\mathbf{q} \preceq (\mathbf{I}+\mathbf{B}_k)\mathbf{q}$ and $(\mathbf{D}_m - \widetilde{\mathbf{Y}}_m^{\star})\,\mathrm{diag}(e^{\mathbf{r}})\mathbf{q} \preceq (\mathbf{I}+\mathbf{D}_m)\mathbf{q}$. We can then compute the nonnegative $\widehat{\mathbf{B}}_k$ and $\widehat{\mathbf{D}}_m$, and rewrite the constraints as $\widehat{\mathbf{B}}_k\,\mathrm{diag}(e^{\mathbf{r}})\mathbf{q} \preceq \mathbf{q}$ and $\widehat{\mathbf{D}}_m\,\mathrm{diag}(e^{\mathbf{r}})\mathbf{q} \preceq \mathbf{q}$.

By using the Perron-Frobenius theorem (and also the Subinvariance Theorem in Chapter 2), we consider the following convex optimization:

$$\begin{array}{rl} \text{maximize} & \displaystyle\sum_{l=1}^{L} w_l r_l \\ \text{subject to} & \log\rho(\widehat{\mathbf{B}}_k \operatorname{diag}(e^{\mathbf{r}})) \preceq 0, \quad k=1,\ldots,K, \\ & \log\rho(\widehat{\mathbf{D}}_m \operatorname{diag}(e^{\mathbf{r}})) \preceq 0, \quad m=1,\ldots,M, \\ \text{variables:} & \mathbf{r}. \end{array} \tag{5.20}$$

This relaxation given by (5.20) convexifies the nonconvex feasible region in (5.8) to one that is convex. Fig. 5.2 illustrates how the convex relaxation obtained by (5.20) produces a convex set for two different sets of parameter setting. The blue curves are the boundaries of the original pareto rate regions, while the dashed convex curves are the boundaries of the relaxed convex sets. As observed, Fig. 5.2(a) illustrates that the relaxation gap between the original rate region and the relaxed rate region can be remarkably small. Furthermore, when the (in general nonconvex) original rate region turns out to be convex in shape, the relaxed rate region coincides exactly with the original rate region, as illustrated in Fig. 5.2(b).

Observe that (5.20) has a problem structure (linear objective and Perron-Frobenius eigenvalue constraint set) similar to that of (5.11). This allows us to leverage Algorithm 7 to solve (5.20). This is given in Algorithm 8. Please refer to the appendix on solving (5.20) numerically by the interior-point method (a centralized algorithm), whose solution can be verified with the output of Algorithm 7. Although an upper bound of the optimal value of (5.5) can be computed by Algorithm 8 (which solves (5.20)), it is desirable that this bound can be further tightened and, more importantly, eventually yields the global optimal solution to (5.5). We refer the reader to [99] for details on combining the convex relaxation described in this chapter with a branch-and-bound method to solve (5.5) optimally.

5.3 Special Case with Individual Power Constraints

In the previous sections, we examine a reformulation technique that cast the optimization variables from the power domain to the achievable

Algorithm 8 Convex Relaxation Algorithm

1. Solve (5.17) and (5.19) to obtain $\widetilde{\mathbf{X}}_k$ and $\widetilde{\mathbf{Y}}_m$ respectively. Then compute $\widehat{\mathbf{B}}_k$ and $\widehat{\mathbf{D}}_m$ by (5.16) and (5.18) respectively.
2. Run Algorithm 7 with $\widetilde{\mathbf{B}}_k$ and $\widetilde{\mathbf{D}}_m$ replaced by $\widehat{\mathbf{B}}_k$ and $\widehat{\mathbf{D}}_m$ respectively.

data rate domain. For the special case of individual power constraints (i.e., $\mathbf{g}(\mathbf{p}) \leq \bar{\mathbf{g}}$ specializes to $\mathbf{p} \leq \bar{\mathbf{p}}$), we examine another reformulation technique in [79, 78] in the following that casts the optimization variables from the power domain to the achievable SINR domain. These reformulations thus offer different algorithm design possibilities, each with its distinct advantages, to solving the same nonconvex problem.

Let us denote a vector containing the achievable SINR value of all the users by $\boldsymbol{\gamma}(\mathbf{p})$ with its lth entry $\gamma_l(\mathbf{p})$ that is defined by (1.1). Then $\rho(\mathrm{diag}(\boldsymbol{\gamma}(\mathbf{p}))\mathbf{F}) < 1$. Hence, for $\boldsymbol{\gamma} = \boldsymbol{\gamma}(\mathbf{p})$,

$$\mathbf{p} = P(\boldsymbol{\gamma}) := (\mathbf{I} - \mathrm{diag}(\boldsymbol{\gamma})\mathbf{F})^{-1}\mathrm{diag}(\boldsymbol{\gamma})\mathbf{v}. \tag{5.21}$$

Vice versa, if $\boldsymbol{\gamma}$ is in the set

$$\Gamma := \{\boldsymbol{\gamma} \geq \mathbf{0},\ \rho(\mathrm{diag}(\boldsymbol{\gamma})\mathbf{F}) < 1\}, \tag{5.22}$$

then $\mathbf{p}$ given in (5.21) is nonnegative. Furthermore, $\boldsymbol{\gamma}(P(\mathbf{p})) = \boldsymbol{\gamma}$. That is, $\boldsymbol{\gamma} : \mathbf{R}_+^L \to \Gamma$, and $P : \Gamma \to \mathbf{R}_+^L$ are inverse mappings. In particular, we have the following result given in [79, 78].

Theorem 5.7. When there are individual power constraints, i.e., $\mathbf{p} \leq \bar{\mathbf{p}}$, the optimal value in (5.2) (in the power domain) is equal to the optimal value of the problem (in the achievable SINR domain):

$$\begin{array}{ll} \text{maximize} & \displaystyle\sum_{l=1}^{L} w_l \log(1+\gamma_l) \\ \text{subject to} & \rho(\mathrm{diag}(\boldsymbol{\gamma})(\mathbf{F} + (1/\bar{p}_l)\mathbf{v}\mathbf{e}_l^\top)) \leq 1 \quad l, \\ \text{variables:} & \gamma_l, \quad l. \end{array} \tag{5.23}$$

Now, $\boldsymbol{\gamma}^\star$ is an optimal solution to (5.23) if and only if $P(\boldsymbol{\gamma}^\star)$ is an optimal solution to (5.2). In particular, $\boldsymbol{\gamma}^\star$ satisfies

$$\rho\left(\mathrm{diag}(\boldsymbol{\gamma}^\star)\left(\mathbf{F} + (1/\bar{p}_i)\mathbf{v}\mathbf{e}_i^\top\right)\right) = 1 \tag{5.24}$$

for some integer i.

Observe that, after a logarithmic change-of-variable transformation, (5.23) in Theorem 5.7 resembles solving an inverse eigenvalue problem in (2.8) of Chapter 2 with a differently-chosen objective function (the similarities lie in the Perron-Frobenius eigenvalue constraint sets). Even then, the transformed problem is still not a convex optimization (which is unlike solving (2.8)) and hence cannot be solved efficiently. The authors in [79, 78] have exploited these similarities with the inverse eigenvalue problem to propose several approximation as well as global optimization algorithms to solve (5.23), equivalently solving (5.2).

Of particular interests is the global optimization algorithm design proposed in [79]. Specifically, after a logarithmic change-of-variable transformation of $\boldsymbol{\gamma}$ (i.e., let $\gamma_l = e^{\tilde{\gamma}_l}$ for all l) in (5.23), we obtain a convex maximization problem in $\tilde{\gamma}_l$ for all l:

$$\begin{array}{ll} \text{maximize} & f(\tilde{\boldsymbol{\gamma}}) = \sum_l w_l \log(1 + e^{\tilde{\gamma}_l}) \\ \text{subject to} & \log \rho(\text{diag}(e^{\tilde{\gamma}})(\mathbf{F} + (1/\bar{p}_l)\mathbf{v}\mathbf{e}_l^{\top})) \leq 0 \quad l, \\ \text{variables:} & \tilde{\gamma} = (\tilde{\gamma}_1, \ldots, \tilde{\gamma}_n)^{\top} \quad \mathbf{R}^L. \end{array} \tag{5.25}$$

Observe that the objective function and the Perron-Frobenius eigenvalue constraint set in (5.25) become strictly convex in $\tilde{\boldsymbol{\gamma}}$. This means that the global optimal solution $\tilde{\boldsymbol{\gamma}}$ occurs at an extreme point of the convex region formed by the constraint set of (5.25). Therefore, one can employ an outer approximation method to yield this extreme point by first enclosing this convex region in a convex polyhedron (yielding a relaxation problem), and thereafter to iteratively remove the infeasible part (shrinking the initial polyhedron to improve the relaxation). At each iteration, the solution to the relaxation problem occurs at a vertex of the (shrinking) polyhedron. As a result, this outer approximation algorithm can yield the global optimal solution to (5.25) asymptotically.

Obviously, the choice of the initial polyhedron in this outer approximation method is critical. The idea in [79] is to leverage the Friedland-Karlin inequalities in Theorem 2.3 to obtain this initial polyhedron. Notice that this yields a polyhedron in $\tilde{\boldsymbol{\gamma}}$, thereby effectively providing a good initial point to kickstart the outer approximation method. The outer approximation algorithm that computes the optimal solution of (5.2) is summarized in the following.

Algorithm 9 Sum Rate Outer Approximation Algorithm

1: Compute the vertices of the enclosing linear polyhedron $D^{(0)}$, described by the set of constraints:

$$\begin{aligned}&\sum_j (\mathbf{x}(\mathbf{F}+(1/\bar{p}_l)\mathbf{v}\mathbf{e}_l^\top)\circ \mathbf{y}(\mathbf{F}+(1/\bar{p}_l)\mathbf{v}\mathbf{e}_l^\top))_j\tilde{\gamma}_j + \\ &\log\rho(\mathbf{F}+(1/\bar{p}_l)\mathbf{v}\mathbf{e}_l^\top) \leq 0,\end{aligned} \tag{5.26}$$

and $\tilde{\gamma}_l \geq -K$ for all l. Let $V^{(0)}$ be the set of vertices of $D^{(0)}$. Set $k=1$ and go to Step 2.

2: Iteration k: Solve the problem:

$$\begin{array}{ll}\text{maximize} & \sum_l w_l \log(1+e^{\tilde{\gamma}_l}) \\ \text{subject to} & \tilde{\gamma}_l \quad D^{(k-1)}\end{array} \tag{5.27}$$

by selecting $\max\left\{\sum_l w_l \log(1+e^{\tilde{\gamma}_l}) : v \quad V^{(k-1)}\right\}$. Let $\tilde{\boldsymbol{\gamma}}^k$ be the optimizer to (5.27).

3: Compute

$$\mathbf{p}^k = \left(\mathbf{I} - \text{diag}(\exp(\tilde{\boldsymbol{\gamma}}^k))\mathbf{F}\right)^{-1}\text{diag}(\exp(\tilde{\boldsymbol{\gamma}}^k))\mathbf{v}. \tag{5.28}$$

4: If $\mathbf{p}^k \leq \bar{\mathbf{p}}$, stop: $\tilde{\boldsymbol{\gamma}}^k$ is the solution to (5.25) and $\mathbf{p}^k$ is the solution to (5.2). Otherwise, let

$$\begin{aligned}J^k = \{&l : \log\rho(\text{diag}(\exp(\tilde{\boldsymbol{\gamma}}^k))(\mathbf{F}+(1/\bar{p}_l)\mathbf{v}\mathbf{e}_l^\top)) \\ &= \max_{1\leq j\leq L}\log\rho(\text{diag}(\exp(\tilde{\boldsymbol{\gamma}}^k))(\mathbf{F}+(1/\bar{p}_j)\mathbf{v}\mathbf{e}_j^\top))\}\end{aligned}$$

and choose any $j^k \quad J^k$.

5: Compute the Perron-Frobenius left eigenvector $\mathbf{y}_{j^k}$ and Perron-Frobenius right eigenvector $\mathbf{x}_{j^k}$ of $\text{diag}(\exp(\tilde{\boldsymbol{\gamma}}^k))(\mathbf{F}+(1/\bar{p}_{j^k})\mathbf{v}\mathbf{e}_{j^k}^\top)$. Set

$$\begin{aligned}G_{j^k}^k(\tilde{\boldsymbol{\gamma}}) = &\log\rho(\text{diag}(\exp(\tilde{\boldsymbol{\gamma}}^k))(\mathbf{F}+(1/\bar{p}_{j^k})\mathbf{v}\mathbf{e}_{j^k}^\top)) + \\ &\frac{[\exp(\tilde{\boldsymbol{\gamma}}^k)\circ\mathbf{x}_{j^k}\circ\mathbf{y}_{j^k}]^\top(\tilde{\boldsymbol{\gamma}}-\tilde{\boldsymbol{\gamma}}^k)}{\rho(\text{diag}(\exp(\tilde{\boldsymbol{\gamma}}^k))(\mathbf{F}+(1/\bar{p}_{j^k})\mathbf{v}\mathbf{e}_{j^k}^\top))}.\end{aligned} \tag{5.29}$$

6: Set $D^{(k)} = D^{(k-1)} \cap \{\tilde{\boldsymbol{\gamma}} : G_{j^k}^k(\tilde{\boldsymbol{\gamma}}) \leq 0\}$, $V^{(k)} = \{\text{extreme points of } D^{(k)}\}$.

7: Set $k \leftarrow k+1$. Go to Step 2.

The following result establishes the convergence of $\mathbf{p}^k$ in Algorithm 9 to the global optimal solution of (5.2).

Theorem 5.8. Every limit point of the sequence $\mathbf{p}^k = \left(\mathbf{I} - \text{diag}(\exp(\tilde{\boldsymbol{\gamma}}^k))\mathbf{F}\right)^{-1} \text{diag}(\exp(\tilde{\boldsymbol{\gamma}}^k))\mathbf{v}$ in Algorithm 9 solves (5.2).

Several remarks are in order concerning the implementation and optimality of Algorithm 9. At Step 5, the gradient of $\log \rho(\text{diag}(\exp(\tilde{\boldsymbol{\gamma}}))(\mathbf{F} + (1/\bar{p}_{j^k})\mathbf{v}\mathbf{e}_{j^k}^\top))$ (given by $[\exp(\tilde{\boldsymbol{\gamma}}) \circ \mathbf{x}_{j^k} \circ \mathbf{y}_{j^k}]/\rho(\text{diag}(\exp(\tilde{\boldsymbol{\gamma}}))(\mathbf{F} + (1/\bar{p}_{j^k})\mathbf{v}\mathbf{e}_{j^k}^\top))$) at $\tilde{\boldsymbol{\gamma}}^k$ is used to construct the inequality cut given by (5.29) that separates $\tilde{\boldsymbol{\gamma}}^k$ (infeasible with respect to (5.25)) from the feasible constraint set of (5.25). In fact, notice that every limit point of the sequence $\mathbf{x}_{j^k}$ for any $j^k \quad J^k$ converges to the limit point of the sequence $\mathbf{p}^k$ in Algorithm 9. Also, a finite number of iterations can be obtained by replacing the stopping rule at Step 4 with stop if $\max_l p_l^k - \bar{p}_l \leq \epsilon$ or stop if $\log \rho(\text{diag}(\exp(\tilde{\boldsymbol{\gamma}}^k))(\mathbf{F} + (1/\bar{p}_{j^k})\mathbf{v}\mathbf{e}_{j^k}^\top)) \leq \epsilon$, where ϵ is a positive error tolerance number. Lastly, at Step 6, an online vertex enumeration procedure (for example, see [81]) can be used to speed up the computation of the new vertex set $V^{(k)}$.

5.3.1 Equivalence via Max-min SINR Optimization

The following result demonstrates a special case in which the optimal solution to (5.2) is given analytically.

Corollary 5.9. If $\tilde{\gamma}_l^\star$ is equal for all l, then $\mathbf{w} = \mathbf{x}(\mathbf{F} + (1/\bar{p}_i)\mathbf{v}\mathbf{e}_i^\top) \circ \mathbf{y}(\mathbf{F} + (1/\bar{p}_i)\mathbf{v}\mathbf{e}_i^\top)$, where $i = \arg\max_l \rho(\mathbf{F} + (1/\bar{p}_l)\,\mathbf{v}\mathbf{e}_l^\top)$.

Proof. Suppose that $\tilde{\gamma}_l^\star$ is equal (to a value $\tilde{\gamma}^\star$) for all l. At optimality, the constraint set of (5.25) reduces to $\tilde{\gamma}^\star + \log \rho(\mathbf{F} + (1/\bar{p}_l)\mathbf{v}\mathbf{e}_l^\top) \leq 0$ for all l, and since at least one of the spectral radius constraints in (5.25) is tight, $\tilde{\gamma}^\star = -\log \rho(\mathbf{F} + (1/\bar{p}_i)\mathbf{v}\mathbf{e}_i^\top)$, where $i = \arg\max_l \rho(\mathbf{F} + (1/\bar{p}_l)\,\mathbf{v}\mathbf{e}_l^\top)$. Now, from Corollary 2.5 in Chapter 2, we also have the optimality condition:

$$\begin{aligned} &\mathbf{x}(\text{diag}(e^{\tilde{\gamma}^\star})(\mathbf{F} + (1/\bar{p}_i)\mathbf{v}\mathbf{e}_i^\top)) \circ \mathbf{y}(\text{diag}(e^{\tilde{\gamma}^\star})(\mathbf{F} + (1/\bar{p}_i)\mathbf{v}\mathbf{e}_i^\top)) \\ &= \quad \Phi_{\mathbf{w}}(e^{\tilde{\gamma}^\star}) \circ e^{\tilde{\gamma}^\star}/\mathbf{1}^\top(\quad \Phi_{\mathbf{w}}(e^{\tilde{\gamma}^\star}) \circ e^{\tilde{\gamma}^\star}). \end{aligned} \tag{5.30}$$

Using the fact that $\tilde{\gamma}_l^\star$ is equal for all l, (5.30) reduces to

$$\mathbf{x}(\mathbf{F} + (1/\bar{p}_i)\mathbf{v}\mathbf{e}_i^\top) \circ \mathbf{y}(\mathbf{F} + (1/\bar{p}_i)\mathbf{v}\mathbf{e}_i^\top) = \mathbf{w}.$$

Hence, $\mathbf{w} = \mathbf{x}(\mathbf{F} + (1/\bar{p}_i)\mathbf{v}\mathbf{e}_i^\top) \circ \mathbf{y}(\mathbf{F} + (1/\bar{p}_i)\mathbf{v}\mathbf{e}_i^\top)$ only if $\tilde{\gamma}_l^\star$ is equal for all l. □

Figure 5.3 gives the geometrical illustration of the weighted sum rate maximization problem in the rate region, i.e., finding $\mathbf{r}^\star$ for $\mathbf{w} = \mathbf{x} \circ \mathbf{y}$. Observe that the max-min SINR solution (depicted in dotted red lines within the rate region) coincides with that of the sum rate maximization problem for this particular choice of $\mathbf{w}$.

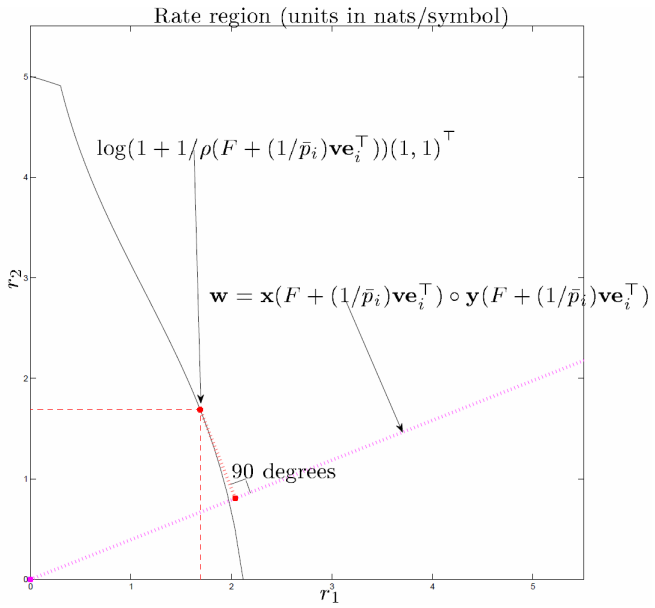

Figure 5.3: An illustration of sum rate maximization in an achievable rate region R for a 2-user Gaussian interference-limited channel. The positive weight vector $\mathbf{w} = \mathbf{x} \circ \mathbf{y}$ is superimposed on the rate region. Given this $\mathbf{w}$, the optimal rate vector $\mathbf{r}^\star = [r_1^\star, r_2^\star]$ is chosen on the boundary of the achievable rate region, where a perpendicular line from $\mathbf{w}$ intersects with the rate region. This illustrates how the max-min SINR solution (that can always be solved optimally) coincides with that of the sum rate maximization problem (a truly nonconvex problem).

5.3.2 Numerical Simulation

We provide a numerical example to illustrate the performance of Algorithm 9 that can be used to solve (5.2) for two users, i.e., $L = 2$. Consider the channel gain matrix given by

$$\mathbf{G} = \begin{bmatrix} 0.73 & 0.04 \\ 0.03 & 0.89 \end{bmatrix}. \tag{5.31}$$

Let the maximum power constraint vector be $\bar{\mathbf{p}} = [1.8 \ 100.5]^\top$ mW and the noise power of each user be 0.1mW. The weight vector is given by $\mathbf{w} = \mathbf{x}(\mathbf{F} + (1/\bar{p}_i)\mathbf{v}\mathbf{e}_i^\top) \circ \mathbf{y}(\mathbf{F} + (1/\bar{p}_i)\mathbf{v}\mathbf{e}_i^\top)$, where $i = \arg\max_l \rho(\mathbf{F} + (1/\bar{p}_l)\mathbf{v}\mathbf{e}_l^\top)$. We set $\epsilon = 1 \times 10^{-8}$ and $K = 100$ in Algorithm 9. Now, the optimal solution is achieved at the equal SINR allocation for the two users (equivalent to maximizing the minimum SINR problem), where $\mathbf{p}^\star = \mathbf{x}(\mathbf{F} + (1/\bar{p}_i)\mathbf{v}\mathbf{e}_i^\top) = [1.8000 \ 1.442]^\top$ mW. Thus, the optimal sum rate is 2.2336 nats/symbol.

At the first iteration, the vertices of $V^{(0)}$ are $(-100.0, \ -100.0)$, $(-100.0, \ 103.6279)$, $(39.4757, \ -100.0)$, $(0.9959, \ 5.1941)$. The vertex of $V^{(0)}$ having the maximum objective function value is $\tilde{\boldsymbol{\gamma}}^1 = (39.4757 \ -100.0)$ and $\mathbf{p}^1 = [1.909 \times 10^{19} \ 0]^\top$. At Step 4, evaluating each constraint function at $\tilde{\boldsymbol{\gamma}}^1 = (39.4757 \ -100.0)$, we have $\log(\mathrm{diag}(\tilde{\boldsymbol{\gamma}}^1)(\mathbf{F} + (1/\bar{p}_1)\mathbf{v}\mathbf{e}_1^\top)) = 36.9$ and $\log(\mathrm{diag}(\tilde{\boldsymbol{\gamma}}^1)(\mathbf{F} + (1/\bar{p}_2)\mathbf{v}\mathbf{e}_2^\top)) = -33.4$. We thus choose $j^1 = 1$, and a new constraint is obtained at Step 5 as $\tilde{\gamma}_1 \leq 2.5757$.

Therefore, we have $D^1 = D^0 \cap \{\tilde{\boldsymbol{\gamma}} : \ \tilde{\gamma}_1 \leq 2.5757\}$ at Step 6. The vertices of D^1 are $(-100.0, \ -100.0)$, $(-100.0, \ 103.6279)$, $(2.5757, \ -100.0)$, $(2.5757, \ 0.8754)$, $(0.9959, \ 5.1941)$. We then proceed to Step 2 to find the optimal vertex of D^1.

After twenty nine more iterations, we arrive at the power vector $\mathbf{p}^{29} = [1.8000 \ 1.442]^\top$ mW, and $\max_l p_l^{29} - \bar{p}_l = 5.5485 \times 10^{-9}$, whereupon Algorithm 9 terminates. Figure 5.5 illustrates the evolution of the approximating polyhedron, where Figure 5.5(a) and (b) show the initial enclosing polyhedron $D^{(0)}$ and the polyhedron $D^{(14)}$ at the fourteen iteration, respectively. We observe that, by the fourteen iteration, $D^{(14)}$ provides a relatively good approximation to the feasible region $D(\{\mathbf{F}\}, K)$. Figure 5.4 illustrates the convergence of the rate vectors generated by $[\log(1 + \gamma_1(\mathbf{p}^k)) \ \ \log(1 + \gamma_2(\mathbf{p}^k))]^\top$. As shown, the rate

vector converges close to the optimal rate vector by the tenth iteration. Figure 5.4 also illustrates the optimal rate vector.

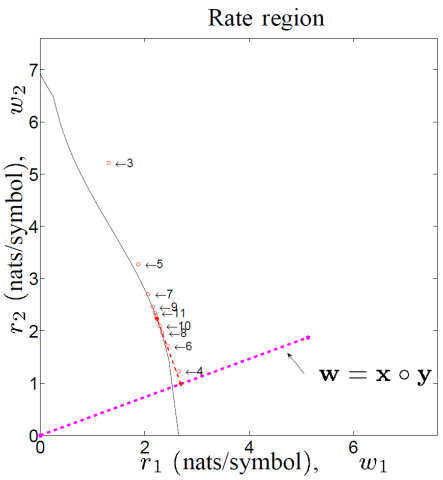

Figure 5.4: Illustration of the convergence of Algorithm 9 yielding the rate vector generated. Only the rate vectors obtained up to the eleventh iteration are shown.

The above two-user numerical example illustrates the convergence performance. As shown, the choice of the initial relaxation (via the Friedland-Karlin inequalities and the Perron-Frobenius theorem in Chapter 2) dramatically speeds up the convergence of the global optimization algorithm and thus the algorithm converges typically in a modest number of iterations for a medium-sized problem instances. We refer the reader to [79, 78] for details of other relaxation techniques (that utilizes Theorem 5.7 with nonnegative matrix theory and the Perron-Frobenius theorem) as well as more extensive numerical simulation.

5.4 Open Issues

In this chapter, we have introduced several recent work to solve (5.2) for affine constraints. There are a number of interesting extensions and remaining open issues to solving (5.2). It is possible to extend the analysis

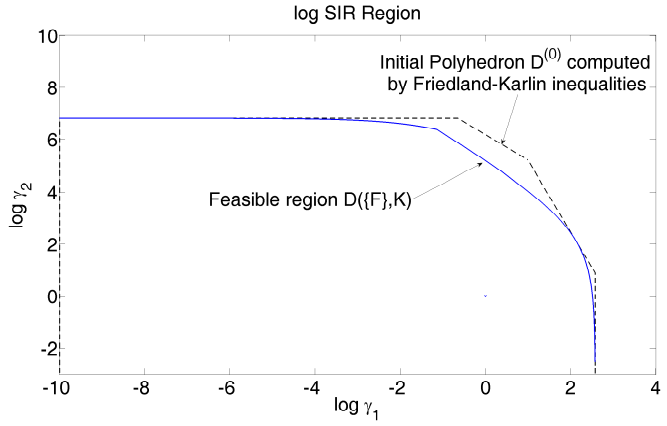

(a)

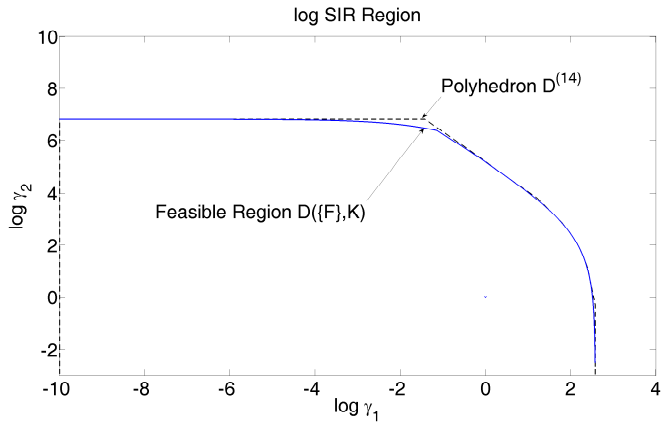

(b)

Figure 5.5: Illustration of the convergence of the global optimization algorithm in the logarithmic variable $\tilde{\gamma}$ region in [79] with (a) the initial polyhedron given by $D^{(0)}$ and (b) the polyhedron $D^{(14)}$ at the fourteen iteration.

in this chapter to consider the set of monotonic constraints in Chapter 4. However, it is still challenging to solve (5.2) when there are more general power constraints and to find convex relaxations that are more efficient than those studied in this chapter. It is interesting to study how the nonlinear Perron-Frobenius theory, e.g., in [49, 50], might be related to some form of nonnegative matrix inequalities (such as the Friedland-Karlin inequalities in [34, 32]), and whether such mathematical relationships can be useful for the purpose of convex relaxation and convex approximation. In fact, there can be fruitful potential in connecting several wireless network optimization problems (such as connecting an easily solved one to a general difficult one, cf. [76, 77, 97, 99, 100]) as we have shown in tackling the sum rate maximization problem in this chapter.

In summary, by combining mathematical tools in nonnegative matrix theory with optimization techniques such as reformulations, convex relaxations and convex approximations, there are several promising methodologies that can be used to overcome the nonconvexity barrier in the general wireless utility maximization problems. First, it can identify special cases that can be optimally solved in polynomial-time (whenever that is possible). Second, tight convex relaxations can be systematically generated to bound the global optimal value from different equivalent reformulations. Third, it offers a value for suboptimal algorithm design showing how computationally efficient fixed-point algorithms can yield an optimal value with a bounded suboptimality. This can provide new perspectives to solving wireless network optimization problems in the large-scale setting as well as designing distributed algorithms with low complexity.

6

Conclusion

We have presented an advanced suite of mathematical tools and algorithms based on the nonlinear Perron-Frobenius theory to solve a broad class of max-min fairness optimization problems and nonconvex utility maximization problems for optimal resource allocation and interference management in wireless networks. For the class of max-min fairness problems, the nonlinear Perron-Frobenius theory characterizes the global optimality analytically through the solution of positive monotonic fixed-point problems. It also enables a systematic way to design distributed iterative algorithms with low complexity and good convergence behavior for power and data rate control, antenna beamforming and cross-layer optimization. For truly nonconvex utility maximization problems such as the sum rate maximization, mathematical tools in nonegative matrix theory and the nonlinear Perron-Frobenius theory provide promising ways to enable convex relaxation and approximations to overcome the nonconvexity barriers, and can even identify polynomial-time solvable instances of these nonconvex problems. The Perron-Frobenius theory suggests that the unique equilibrium that results from resource competition in these wireless network optimization problems is a meaningful one.

Acknowledgements

The author gratefully acknowledges the collaborations and interactions on this topic with many colleagues, including Desmond W. H. Cai, Mung Chiang, Shmuel Friedland, Peter Yao-Win Hong, Yichao Huang, C.-L. Hsieh, K. R. Krishnan, I-Wei Lai, Chia-Han Lee, Steven H. Low, Tony Q. Quek, Bhaskar D. Rao, R. Srikant, Ao Tang, Wenyi Zhang and Liang Zheng. The research was supported in part by grants from The Research Grants Council of Hong Kong Project No. RGC 125212, 122013 and 11212114, the Science, Technology and Innovation Commission of Shenzhen Municipality Project No. JCYJ20120829161727318 and JCYJ20130401145617277, a NRF Fellowship, Qualcomm Inc., and the American Institute of Mathematics that fostered initial ideas and collaboration at the "Nonnegative Matrix Theory: Generalizations and Applications" workshop.

Appendices

A

Modeling the Perron-Frobenius Eigenvalue by Optimization Software

In this appendix, we introduce a software implementation for modeling the Perron-Frobenius eigenvalue function encountered in the specific optimization problems studied in this monograph. The software is useful for the numerical evaluation of the Perron-Frobenius eigenvalue function as well as for the rapid prototyping of the formulation and solution of various wireless network optimization problems.

A.0.1 A software implementation

The software implementation of a Perron-Frobenius eigenvalue function Matlab routine is created using the widely-used `cvx` optimization software package in [38]. The `cvx` software is an optimization parser-solver that runs in Matlab and is freely available for download from the World Wide Web. The parser in the `cvx` software can automatically identify optimization problems that are appropriately modeled using a set of libraries known as the *atom library* in `cvx`. The *atom library* contains implementation of convex functions that are commonly encountered in practice. In this way, the modularity of the *atom library* software makes it easy to model and solve specific optimization problems by adding new `cvx` atoms in the atom library.

In particular, the cvx atoms that implement the mathematical functions use a software paradigm known as the *disciplined convex programming* ruleset (or DCP ruleset for short). These are rules that are drawn from basic principles of convex optimization (cf. [15]), and a violation of these modeling rules can lead to a parsing error. As such, creating new cvx atom has to follow the DCP ruleset.

Let us examine the following convex function encountered in (2.6) and also in (2.8) given by:

$$f(\boldsymbol{\eta}) = \rho(\,\mathrm{diag}(e^{\boldsymbol{\eta}})\mathbf{B}). \tag{A.1}$$

As discussed in Chapter 2, this function is log-convex [46, 61]. Furthermore, Corollary 2.5 characterizes the solution to an inverse eigenvalue problem in nonnegative matrix theory, and this solution can in fact be efficiently obtained by solving a convex optimization problem involving (A.1) (cf. (2.8) in Chapter 2 and also [78]). In the following, we describe how to model and solve this convex optimization problem numerically using the cvx software.

To model this function in cvx and to follow the DCP ruleset in cvx, we proceed to evaluate (A.1) by leveraging the linear Perron-Frobenius theorem (Theorem 2.1) to rewrite (A.1) as a function:

$$f : R^L \rightarrow R_+, \quad f(\boldsymbol{\eta}) \;,\; \inf\{\lambda \,|\, \mathrm{diag}(e^{\boldsymbol{\eta}})\mathbf{B}\mathbf{z} \leq \lambda\mathbf{z}\},$$

where $\mathbf{z} \quad R^L$ is an (auxiliary) optimization variable.

Notably, (A.1) can be evaluated numerically by solving a geometric program (i.e., a class of convex optimization problems [27, 15, 14]) that the cvx software can handle. Using the cvx software modeling format, we list down the Matlab routine code of the Perron-Frobenius eigenvalue function as follows:

```
function cvx_optval = spectral_radius( eta, B )
s = size( B, 1 );
cvx_begin gp
    variables rho z( s )
    minimize( rho );
    subject to
        diag( exp(eta) ) * B * z <= rho * z;
cvx_end
```

After putting the above function cvx_optval code into a subdi-

rectory folder `@cvx` (i.e., the atom library) located in the `cvx` software installation directory on the computer, the `cvx` software automatically recognizes a function call of `spectral_radius` whenever it is found in the constraints or the objective function of a convex optimization problem that conforms to the DCP ruleset.

Let us give an illustrate example using the `cvx` Matlab code to solve the following convex optimization problem:

$$\begin{array}{rl} \text{maximize} & \boldsymbol{\omega}^{\top}\tilde{\boldsymbol{\gamma}} \\ \text{subject to} & \log\rho(\,\mathrm{diag}(e^{\tilde{\gamma}})\mathbf{B}_l) \le 0, \quad l = 1,\ldots,3 \\ \text{variables:} & \tilde{\boldsymbol{\gamma}}. \end{array} \tag{A.2}$$

Using the `cvx` atom function `spectral_radius` given in the above, the `cvx` Matlab code to solve (A.2) is given by:

```
cvx_begin
    variables gamma_tilde(3)
    maximize( w' * gamma_tilde );
    subject to
        log( spectral_radius( gamma_tilde, B1 ) ) <= 0;
        log( spectral_radius( gamma_tilde, B2 ) ) <= 0;
        log( spectral_radius( gamma_tilde, B3 ) ) <= 0;
cvx_end
```

Note that, in the above, `w` is a given constant positive vector, and `B1`, `B2` and `B3` are all constant nonnegative matrices with entries given in terms of the problem parameters. The optimal primal solution of (A.2) is numerically stored in the vector `gamma_tilde`. Exploring the use of the `dual variable` software option in the `cvx` Matlab code to access the optimal Lagrange dual solution of (A.2) and to compare that numerically with the Schur product of the Perron-Frobenius eigenvectors of some nonnegative matrix (say, to verify Collorary 2.5) is left as an exercise for the reader.

References

[1] J. M. Aein. Power balancing in systems employing frequency reuse. *COMSAT Technical Review*, 3(2):277–299, September 1973.

[2] H. Alavi and R. W. Nettleton. Downstream power control for a spread-spectrum cellular mobile radio system. *Proceedings of the IEEE Global Communications Conference (GLOBECOM)*, 3:84–88, November 1982.

[3] C. Avin, M. Borokhovich, Y. Haddad, E. Kantor, Z. Lotker, M. Parter, and D. Peleg. Generalized Perron–Frobenius theorem for multiple choice matrices, and applications. *Proceedings of the 24th Annual ACM-SIAM Symposium on Discrete Algorithms (SODA13)*, 2013.

[4] R. B. Bapat, D. D. Olesky, and P. van den Driessche. Perron-Frobenius theory for a generalizaed eigenproblem. *Linear and Multilinear Algebra*, 40:141–152, 1995.

[5] R. Bellman. *Introduction to Matrix Analysis*. McGraw-Hill Book Co., 1960.

[6] A. Berman. Nonnegative matrices: Old problems, new applications. *Lecture Notes in Control and Information Sciences*, 341:1–9, 2006.

[7] A. Berman and R. J. Plemmons. *Nonnegative Matrices in the Mathematical Sciences*. Academic Press, USA, 1st edition, 1979.

[8] D. P. Bertsekas and J. N. Tsitsiklis. *Parallel and Distributed Computation: Numerical Methods*. Prentice Hall, Englewood Cliffs, NJ, 1989.

[9] V. D. Blondel, L. Ninove, and P. Van Dooren. An affine eigenvalue problem on the nonnegative orthant. *Linear Algebra and its Applications*, 404:69–84, 2005.

[10] H. Boche and M. Schubert. Solution of the multiuser downlink beamforming problem with individual SINR constraints. *IEEE Transactions on Vehicular Technology*, 53(1):18–28, 2004.

[11] H. Boche and M. Schubert. Resource allocation in multiantenna systems–achieving max-min fairness by optimizing a sum of inverse SIR. *IEEE Transactions on Signal Processing*, 54(6):1990–1997, 2006.

[12] S. C. Borst, M. G. Markakis, and I. Saniee. Nonconcave utility maximization in locally coupled systems, with applications to wireless and wireline networks. *IEEE/ACM Transactions on Networking*, 22(2):674–687, 2013.

[13] S. Boyd, A. Ghosh, B. Prabhakar, and D. Shah. Randomized gossip algorithms. *IEEE Transactions on Information Theory*, 52(6):2508–2530, 2006.

[14] S. Boyd, S. J. Kim, L. Vandenberghe, and A. Hassibi. A tutorial on geometric programming. *Optimization and Engineering*, 8(1):67–127, 2007.

[15] S. Boyd and L. Vanderberghe. *Convex Optimization*. Cambridge University Press, 2004.

[16] D. W. Cai, T. Q. Quek, and C. W. Tan. A unified analysis of max-min weighted SINR for MIMO downlink system. *IEEE Transactions on Signal Processing*, 59(8):3850–3862, 2011.

[17] D. W. Cai, T. Q. Quek, C. W. Tan, and S. H. Low. Max-min SINR coordinated multipoint downlink transmission - duality and algorithms. *IEEE Transactions on Signal Processing*, 60(10):5384–5396, 2012.

[18] D. W. Cai, C. W. Tan, and S. H. Low. Optimal max-min fairness rate control in wireless networks: Perron-Frobenius characterization and algorithms. *Proceedings of IEEE INFOCOM*, 2012.

[19] M. Chiang. Balancing transport and physical layers in wireless multihop networks: Jointly optimal congestion control and power control. *IEEE Journal on Selected Areas in Communications*, 23(1):104–116, 2005.

[20] M. Chiang. Geometric programming for communication systems. *Foundations and Trends in Communications and Information Theory*, 2(1-2):1–156, 2005.

[21] M. Chiang and J. Bell. Balancing supply and demand of bandwidth in wireless cellular networks: Utility maximization over powers and rates. *Proceedings of IEEE INFOCOM*, 2004.

[22] M. Chiang, P. Hande, T. Lan, and C. W. Tan. Power control in wireless cellular networks. *Foundations and Trends in Networking*, 2(4):381–533, 2008.

[23] M. Chiang, C. W. Tan, D. P. Palomar, D. O'Neill, and D. Julian. Power control by geometric programming. *IEEE Transactions on Wireless Communications*, 6(7):2640–2651, July 2007.

[24] T. M. Cover and J. A. Thomas. *Elements of Information Theory*. John Wiley and Sons, New York, USA, 1991.

[25] E. Dall'Anese, S.-J. Kim, G. B. Giannakis, and S. Pupolin. Power control for cognitive radio networks under channel uncertainty. *IEEE Transactions on Wireless Communications*, 10(10):3541–3551, 2011.

[26] G. Dartmann, X. Gong, W. Afzal, and G. Ascheid. On the duality of the max-min beamforming problem with per-antenna and per-antenna-array power constraints. *IEEE Transactions on Vehicular Technology*, 62(2):606–619, 2012.

[27] R. J. Duffin, E. L. Peterson, and C. M. Zener. *Geometric Programming: Theory and Application*. John Wiley and Sons, New York, USA, 1967.

[28] T. ElBatt and A. Ephremides. Joint scheduling and power control for wireless ad hoc networks. *IEEE Transactions on Wireless Communications*, 3(1):74–85, 2004.

[29] L. Elsner. Characterizations of spectral radius of positive operators. *Linear Algebra and its Applications*, 61:31–35, 1984.

[30] J. A. Fax and R. M. Murray. Information flow and cooperative control of vehicle formations. *IEEE Transactions on Automatic Control*, 49(9):1465–1476, 2004.

[31] G. J. Foschini and Z. Miljanic. A simple distributed autonomous power control algorithm and its convergence. *IEEE Transactions on Vehicular Technology*, 42(4):641–646, 1993.

[32] S. Friedland. Convex spectral functions. *Linear and Multilinear Algebra*, 9(4):299–316, 1981.

[33] S. Friedland. Characterizations of spectral radius of positive operators. *Linear Algebra and its Applications*, 134:93–105, 1990.

[34] S. Friedland and S. Karlin. Some inequalities for the spectral radius of non-negative matrices and applications. *Duke Mathematical Journal*, 42(3):459–490, 1975.

[35] G. Frobenius. über Matrizen aus nicht negativen Elementen. *Sitzungsber. Kon Preuss. Akad. Wiss. Berlin*, pages 456–457, 1912.

[36] L. Georgiadis, M. J. Neely, and L. Tassiulas. Resource allocation and cross-layer control in wireless networks. *Foundations and Trends in Networking*, 1(1):1–144, 2006.

[37] S. A. Grandhi, R. Vijayan, and D. Goodman. Distributed power control in cellular radio systems. *IEEE Transactions on Communications*, 42(2):226–228, 1994.

[38] M. Grant and S. Boyd. CVX: Matlab software for disciplined convex programming, version 1.21. http://cvxr.com/cvx/, April 2011.

[39] P. Hande, S. Rangan, M. Chiang, and X. Wu. Distributed uplink power control for optimal SIR assignment in cellular data networks. *IEEE/ACM Transactions on Networking*, 16(6):1420–1433, 2008.

[40] S. Haykin. Cognitive radio: brain-empowered wireless communications. *IEEE Journal on Selected Areas in Communications*, 23(2):201–220, 2005.

[41] S. He, Y. Huang, L. Yang, A. Nallanathan, and P. Liu. A multi-cell beamforming design by uplink-downlink max-min SINR duality. *IEEE Transactions on Wireless Communications*, 11(8):2858–2867, 2012.

[42] Y.-W. Hong, C. W. Tan, L. Zheng, C.-L. Hsieh, and C.-H. Lee. A unified framework for wireless max-min utility optimization with general monotonic constraints. *Proceedings of IEEE INFOCOM*, 2014.

[43] Y. Huang, C. W. Tan, and B. D. Rao. Joint beamforming and power control in coordinated multicell: Max-min duality, effective network and large system transition. *IEEE Transactions on Wireless Communications*, 12(6):2730–2742, 2013.

[44] J. Joung, C. Ho, and S. Sun. Spectral efficiency and energy efficiency of OFDM systems: Impact of power amplifiers and countermeasures. *IEEE Journal on Selected Areas in Communications*, 32(2):208–220, 2013.

[45] S. Kandukuri and S. Boyd. Optimal power control in interference-limited fading wireless channels with outage-probability specifications. *IEEE Transactions on Wireless Communications*, 1(1):46–55, Jan 2002.

[46] J. F. C. Kingman. A convexity property of positive matrices. *The Quarterly Journals of Mathematics, Oxford*, 12(2):283–284, 1961.

[47] H. Kobayashi, B. L. Mark, and W. Turin. *Probability, Random Processes, and Statistical Analysis*. Cambridge University Press, 2012.

[48] S. Koskie and Z. Gajic. Signal-to-interference-based power control for wireless networks: A survey, 1992–2005. *Dynamics of Continuous, Discrete and Impulsive Systems B: Applications and Algorithms*, 13(2):187–220, 2006.

[49] U. Krause. Perron's stability theorem for nonlinear mappings. *Journal of Mathematical Economics*, 15:275–282, 1986.

[50] U. Krause. Concave Perron-Frobenius theory and applications. *Nonlinear analysis*, 47(2001):1457–1466, 2001.

[51] U. Krause. A local−global stability principle for discrete systems and difference equations. *Proceedings of the 6th International Conference on Di erence Equations 2001*, CRC Press:167–180, 2004.

[52] K. R. Krishnan and H. Luss. Power selection for maximizing SINR in femtocells for specified SINR in macrocell. *Proceedings of the IEEE Wireless Communications and Networking Conference (WCNC)*, 2011.

[53] I.-W. Lai, L. Zheng, C.-H. Lee, and C. W. Tan. Beamforming duality and algorithms for weighted sum rate maximization in cognitive radio networks. *IEEE Journal on Selected Areas in Communications*, 33(5):832–847, 2015.

[54] J.-W. Lee, R. R. Mazumdar, and N. B. Shroff. Joint opportunistic power scheduling and end-to-end rate control for wireless ad hoc networks. *IEEE Transactions on Vehicular Technology*, 56(2):801–809, 2007.

[55] B. Lemmens and R. Nussbaum. *Nonlinear Perron–Frobenius Theory*. Cambridge University Press, 2012.

[56] X. Lin, N. B. Shroff, and R. Srikant. A tutorial on cross-layer optimization in wireless networks. *IEEE Journal on Selected Areas in Communications*, 24(8):1452–1463, 2006.

[57] Z.-Q. Luo and S. Zhang. Dynamic spectrum management: Complexity and duality. *IEEE Journal on Selected Areas in Signal Processing*, 2(1):57–73, 2008.

[58] H. Mahdavi-Doost, M. Ebrahimi, and A. K. Khandani. Characterization of SINR region for interfering links with constrained power. *IEEE Transactions on Information Theory*, 56(6):2816–2828, 2010.

[59] V. Mehrmann, D. D. Olesky, T. X. T. Phan, and P. van den Driessche. Relations between Perron-Frobenius results for matrix pencils. *Linear Algebra and its Applications*, 287:257–269, 1999.

[60] H. J. Meyerhoff. Method for computing the optimum power balance in multibeam satellites. *COMSAT Technical Review*, 4(1):139–146, 1974.

[61] R. D. Nussbaum. Convexity and log convexity for the spectral radius. *Linear Algebra and its Applications*, 73:59–122, 1986.

[62] H. Park, S.-H. Park, J.-S. Kim, and I. Lee. SINR balancing techniques in coordinated multi-cell downlink systems. *IEEE Transactions on Wireless Communications*, 12(2):626–635, 2013.

[63] O. Perron. Zur Theorie der über Matrizen. *Math. Ann*, 64:248–263, 1907.

[64] S. U. Pillai, T. Suel, and S. Cha. The Perron-Frobenius theorem: some of its applications. *IEEE Signal Processing Magazine*, 22(2):62–75, 2005.

[65] C. Rapp. Effects of HPA-nonlinearity on a 4-DPSK/OFDM signal for a digital sound broadcasting system. *Proceedings of the European Conference on Satellite Communications*, 1991.

[66] F. Rashid-Farrokhi, K. J. R. Liu, and L. Tassiulas. Transmit beamforming and power control for cellular wireless systems. *IEEE Journal on Selected Areas in Communications*, 16(8):1437–1450, 1998.

[67] M. Schwartz. *Mobile Wireless Communications*. Cambridge University Press, 2004.

[68] E. Seneta. *Non-negative Matrices and Markov Chains*. Springer, 2nd edition, 2006.

[69] S. Shakkottai and R. Srikant. Network optimization and control. *Foundations and Trends in Networking*, 2(3):271–379, 2007.

[70] S. J. Shellhammer, A. K. Sadek, and W. Zhang. Technical challenges for cognitive radio in the TV white space spectrum. *Proceedings of the Information Theory and Applications Workshop*, pages 323–333, 2009.

[71] Q. Shi, M. Razaviyayn, Z. Q. Luo, and C. He. An iteratively weighted MMSE approach to distributed sum-utility maximization for a MIMO interfering broadcast channel. *IEEE Transactions on Signal Processing*, 59(9):4331–4340, 2011.

[72] C. W. Tan. Optimal power control in Rayleigh-fading heterogeneous networks. *Proceedings of IEEE INFOCOM*, 2011.

[73] C. W. Tan. Wireless network optimization by Perron-Frobenius theory. *Proceedings of the 50th Annual Conference on Information Systems and Sciences (CISS)*, 2014.

[74] C. W. Tan. Optimal power control in Rayleigh-fading heterogeneous wireless networks. *IEEE/ACM Transactions on Networking*, forthcoming 2015.

[75] C. W. Tan, M. Chiang, and R. Srikant. Fast algorithms and performance bounds for sum rate maximization in wireless networks. *Proceedings of IEEE INFOCOM*, 2009.

[76] C. W. Tan, M. Chiang, and R. Srikant. Maximizing sum rate and minimizing MSE on multiuser downlink: optimality, fast algorithms and equivalence via max-min SINR. *IEEE Transactions on Signal Processing*, 59(12):6127–6143, 2011.

[77] C. W. Tan, M. Chiang, and R. Srikant. Fast algorithms and performance bounds for sum rate maximization in wireless networks. *IEEE/ACM Transactions on Networking*, 21(3):706–719, 2013.

[78] C. W. Tan, S. Friedland, and S. H. Low. Nonnegative matrix inequalities and their application to nonconvex power control optimization. *SIAM Journal on Matrix Analysis and Applications*, 32(3):1030–1055, 2011.

[79] C. W. Tan, S. Friedland, and S. H. Low. Spectrum management in multiuser cognitive wireless networks: Optimality and algorithm. *IEEE Journal on Selected Areas in Communications*, 29(2):421–430, 2011.

[80] D. N. C. Tse and P. Viswanath. *Fundamentals of Wireless Communication*. Cambridge University Press, 1st edition, 2005.

[81] H. Tuy. *Convex analysis and global optimization*. Kluwer Academic Publishers, 1998.

[82] R. S. Varga. *Matrix iterative analysis*. Prentice Hall, 1963.

[83] P. Viswanath, V. Anantharam, and D. N. C. Tse. Optimal sequences, power control, and user capacity of synchronous CDMA systems with linear MMSE multiuser receivers. *IEEE Transactions on Information Theory*, 45(6):1968–1983, 1999.

[84] R. von Mises and H. Pollaczek-Geiringer. Praktische Verfahren der Gleichungsauflösung. *Zeitschrift für Angewandte Mathematik und Mechanik*, 9:152–164, 1929.

[85] H. Wang and Z. Ding. Power control and resource allocation for outage balancing in femtocell networks. *IEEE Transactions on Wireless Communications*, 14(4):2043–2057, 2015.

[86] A. Wiesel, Y. C. Eldar, and S. Shamai. Linear precoding via conic optimization for fixed MIMO receivers. *IEEE Transactions on Signal Processing*, 54(1):161– 176, 2006.

[87] W. S. Wong. Control and estimation problems in mobile communication systems. *Proceedings of IEEE 34th Conference on Decision and Control*, 1995.

[88] Y. K. Wong. Some mathematical concepts for linear economic models. *Chapter in Economic Activity Analysis*, Edited by O. Morgenstern, John Wiley & Sons, Inc.:283–339, 1954.

[89] Q. Xu, Y. Chen, and K. Liu. Combating strong-weak focusing effect in time-reversal uplinks. *IEEE Transactions on Wireless Communications*, forthcoming 2015.

[90] W. Yang and G. Xu. Optimal downlink power assignment for smart antenna systems. *Proceedings of the IEEE International Conference on Acoustics, Speech and Signal Processing (ICASSP)*, pages 3337–3340, 1998.

[91] Y. D. Yao and A. Sheikh. Investigations into cochannel interference in microcellular mobile radio systems. *IEEE Transactions on Vehicular Technology*, 41(2):114–123, May 1992.

[92] R. D. Yates. A framework for uplink power control in cellular radio systems. *IEEE Journal on Selected Areas in Communications*, 13(7):1341–1348, 1995.

[93] M. Yavuz, F. Meshkati, S. Nanda, A. Pokhariyal, N. Johnson, B. Raghothaman, and A. Richardson. Interference management and performance analysis of UMTS-HSPA+ femtocells. *IEEE Communications Magazine*, 47(9):102–109, 2009.

[94] J. Zander. Distributed cochannel interference control in cellular radio systems. *IEEE Transactions on Vehicular Technology*, 41:57–62, 1992.

[95] W. Zhang. A general framework for transmission with transceiver distortion and some applications. *IEEE Transactions on Communications*, 60(2):384–399, 2012.

[96] Q. Zhao and B. M. Sadler. A survey of dynamic spectrum access. *IEEE Signal Processing Magazine*, 24(3):79–89, 2007.

[97] L. Zheng and C. W. Tan. Cognitive radio network duality and algorithms for utility maximization. *IEEE Journal on Selected Areas in Communications*, 31(3):500–513, 2013.

[98] L. Zheng and C. W. Tan. Egalitarian fairness framework for joint rate and power optimization in wireless networks. *ACM SIGMETRICS Performance Evaluation Review*, 42(2):58–60, 2014.

[99] L. Zheng and C. W. Tan. Maximizing sum rates in cognitive radio networks: Convex relaxation and global optimization algorithms. *IEEE Journal on Selected Areas in Communications*, 32(3):667–680, 2014.

[100] L. Zheng and C. W. Tan. Optimal algorithms in wireless utility maximization: Proportional fairness decomposition and nonlinear Perron–Frobenius theory framework. *IEEE Transactions on Wireless Communications*, 13(4):2086–2095, 2014.